A METHOD FOR THE ANALYSIS OF MODULATED NEUTRON EXPERIMENTS

A THESIS

Presented to

The Faculty of the Graduate Division

by

Robert Neill Macdonald

In Partial Fulfillment

of the Requirements for the Degree

Doctor of Philosophy

in the School of Nuclear Engineering

Georgia Institute of Technology

June, 1966

In presenting the dissertation as a partial fulfillment of the requirements for an advanced degree from the Georgia Institute of Technology, I agree that the Library of the Institute shall make it available for inspection and circulation in accordance with its regulations governing materials of this type. I agree that permission to copy from, or to publish from, this dissertation may be granted by the professor under whose direction it was written, or, in his absence, by the Dean of the Graduate Division when such copying or publication is solely for scholarly purposes and does not involve potential financial gain. It is understood that any copying from, or publication of, this dissertation which involves potential financial gain will not be allowed without written permission.

_____

3/17/65
b

GEORGIA INSTITUTE OF TECHNOLOGY LIBRARY

Regulations for the Use of Theses

Unpublished theses submitted for the Master's and Doctor's degrees and deposited in the Georgia Institute of Technology Library are open for inspection and consultation, but must be used with due regard for the rights of the authors. Passages may be copied only with permission of the authors, and proper credit must be given in subsequent written or published work. Extensive copying or publication of the thesis in whole or in part requires the consent of the Dean of the Graduate Division of the Georgia Institute of Technology.

This thesis by ROBERT NEILL MACDONALD has been used by the following persons, whose signatures attest their acceptance of the above restrictions.

A library which borrows this thesis for use by its patrons is expected to secure the signature of each user.

NAME AND ADDRESS OF USER	BORROWING LIBRARY	DATE

A METHOD FOR THE ANALYSIS OF MODULATED NEUTRON EXPERIMENTS

Approved:

_____

Chairman

_____

Date approved by Chairman: June 3, 1966

ACKNOWLEDGMENTS

The initial idea for this thesis was suggested by Dr. C. E. Cohn of Argonne National Laboratory. Dr. Cohn has continued to serve as a special consultant throughout the course of this work and I wish to express my appreciation for his many helpful comments and for the great sacrifice of his time. I am grateful to my thesis advisor, Dr. L. J. Gallaher, for his encouragement and valuable discussions concerning the numerical techniques used in solution of the equations. My reading committee, Dr. Nathan W. Snyder and Dr. J. D. Clement, have been exceptionally helpful in assessing the progress of this work and in offering many excellent suggestions during the preparation of this manuscript.

I am also grateful to Dr. C. J. Roberts, Dr. W. B. Harrison, and to the School of Nuclear Engineering for financial support and for its assistance in obtaining computer time and the assembly of the noise analysis equipment. Finally, I want to thank the many people who have endured my alternating tales of woe and bursts of enthusiasm while this work was in progress.

TABLE OF CONTENTS

TABLE OF CONTENTS (Concluded)

LIST OF TABLES

LIST OF ILLUSTRATIONS

LIST OF ILLUSTRATIONS (Continued)

LIST OF ILLUSTRATIONS (Concluded)

SUMMARY

A method is developed by which the class of kinetics experiments, known as modulated neutron experiments, may be analyzed by means of the well-developed algorithms commonly used for obtaining static flux distributions. Currently these experiments are analyzed by modal methods, in which the response of a system to a disturbance is resolved in terms of flux eigenfunctions, or by nodal methods, in which the system is treated as a number of intercoupled regions, or by a series expansion of the Laplace transformed neutron balance equations. The method described herein and referred to as the complex source model is perfectly general for computing the effects of source perturbations, and, since it does not require the truncation of a series, it is limited in accuracy only by the statics model chosen and by the numerical techniques used to obtain a solution. It also has the possible advantage of being extended to multidimensional, heterogeneous systems with linear feedback for which either eigenfunctions or coupling coefficients are not available.

The method is developed in terms of the one-dimensional (cylindrical), two-group, telegrapher's equations. These equations are then applied to the analysis of three types of modulated neutron experiments. These are:

1. Pile oscillator experiments in the NORA and Georgia Tech Research Reactors.

2. Wave propagation in graphite and heavy water.

3. Noise measurements in the Georgia Tech Research Reactor.

Comparison of the calculations with experimental data obtained at the Institutt for Atomenergi, Kjeller, Norway, the University of Florida, and at the Georgia Institute of Technology shows excellent agreement and lends support to the validity of the model.

Derivation of the equations proceeds in the following manner: the starting point can be considered the telegrapher's equation representing the time and space dependence of the neutron flux. The equation includes source terms representing the contributions of the prompt, delayed, and externally supplied neutrons. The external source is the input to the system. It is now assumed that each of the time dependent quantities can be resolved into the sum of a steady component dependent upon position only and a fluctuating component dependent upon position and time. On substitution into the original equation it is found that the equation is satisfied by the fluctuating parts alone. (If the mean flux is not steady, e.g., if the reactor is on a period, a similar decomposition can still be made.) Since any disturbance to the system can be Fourier analyzed into its frequency components, we can transform the time dependent equation into a frequency dependent equation by representing each of the fluctuating components (flux, source, etc.) by a complex amplitude dependent upon position times exp ($i\omega t$). This substitution yields a complex equation dependent on position and frequency but independent of time. A complete solution now consists of finding, for each frequency, the complex amplitude of the flux response.

To find these solutions, the complex equations are separated into their real and imaginary components yielding coupled, inhomogeneous differential equations (two for each energy group) which have real coefficients.

These coefficients are combinations of the usual macroscopic cross sections with the frequency and neutron velocity. On examining the form of the equations it is seen that each of the "frequency dependent cross sections" fits exactly into the slots reserved for the macroscopic cross sections in statics codes, e.g., CRAM and EXTERMINATOR. Thus we might expect that, with proper interpretation, statics codes may be used to solve dynamics problems.

At this point the question of convergence of the iterative methods used in the codes becomes important. In the normal statics problem the iteration matrix is nonnegative and convergence to the correct answer is assured. However in the complex source problem the frequency dependent cross sections are of both signs and the iteration matrix is no longer nonnegative. No theorems are known which guarantee convergence of this type problem. In order to determine whether or not solutions to the mathematical model existed and if they were representative of the physics involved, a computer program was written to solve the two-group telegrapher's equations in one dimension. The methods used to find the solution are noniterative, that is, Choleski inversion of the coefficient matrix or the method of conjugate gradients. Both techniques are found to give identical results and also agree with the physical problem. Subsequently it was shown that both CRAM and EXTERMINATOR reproduce the results although the rate of convergence is slow. The majority of the calculations in this thesis are done with the Choleski method.

Application of the model to the various modulated neutron experiments requires a slightly different interpretation for each experiment. The pile oscillator case is the easiest to visualize. Here the external source term is made to represent the varying absorption of the oscillator and is placed

in the spatial regions and energy groups in which the oscillator operates. Small changes in the absorption are assumed. The complex amplitude of the flux now represents the time varying response a detector would have if it were placed at each location within the reactor. Calculated response amplitudes and phase shifts are compared with experimental data for the NORA reactor and the GTRR taken over a wide range of frequencies.

The wave experiment is similar to the pile oscillator except that the source is now truly an extraneous source and is usually located at the boundary of a system. The complex flux represents the amplitude and phase of a wave propagating through the system. A dispersion law for the medium may be defined which relates the real and imaginary parts of the complex amplitude as a function of frequency. This dispersion law is calculated and compared with theory and experiment for both graphite and heavy water.

Noise experiments are somewhat more complicated. The source in this case is a statistical variation in the reaction rates of various neutron processes such as absorption, fission, or leakage and is distributed throughout the reactor. Since these sources are in general independent and thus have a random phase relationship, it is necessary to sum the square magnitude of the response due to each source taken separately. When the summation is properly made the results may be presented in terms of the noise power spectral density from a single detector or as cross power spectra and transfer functions between two detectors. These three quantities are calculated for the GTRR and the results are plotted for selected locations in the reactor. In addition a proposed experiment to measure these quantities is discussed in detail.

The conclusions of the author are that the work discussed demon-

strates the validity of the complex source method. However work remains to be done in improving the convergence rate of the codes and in verifying the noise calculations experimentally. Extension of the method to multi-dimensional systems and to higher order transport approximations is straightforward and should be of great value in the study of thermalization kernels and effects at the interface between two media. It should also be pointed out that the inclusion of linear feedback equations in the model is possible and thus the stability of large power reactors may be studied. Finally it can be seen from this application that the reactor statics codes in use today are of sufficient flexibility to be considered an algorithm for the solution of general sets of differential equations. This means that the codes will be of great value when applied to problems in fields other than nuclear engineering.

CHAPTER I

INTRODUCTION

The field of reactor dynamics is based on the excitation of the neutron field in some manner and observing the subsequent variations of the field throughout the reactor. By observing the input-output relationship, one extracts information about the system which can be compared to theoretical models. The classic approach has been to study the reactor's response with the zero-power point-reactor kinetics model. In recent years however, it has become evident that with the advent of large power reactors, a space-time analysis would be necessary. This chapter will review briefly the status of space-time analysis and touch lightly on some of the experiments that are being performed today. The final section is a description of the thesis problem which is to develop a simple method for the analysis of modulated neutron experiments which may be routinely used by the nuclear engineer to study spatial effects in realistic systems and which may be readily extended to include linear feedback effects.

Review of Space-Time Analysis

The status of space-time analysis has recently been reviewed by Kerlin (1). Four basic techniques are in use. The simplest is known as the adiabatic method (2), or the instantaneous-tilt method (3). This approximation assumes that a reactor in changing from a steady-state condition A to steady-state condition B does so instantaneously. Kerlin states,

The procedure for the adiabatic method is as follows:

1. Solve the stationary spatial problem for various combinations of system parameters expected to change during the transient.
2. Express the spatial distributions as a function of reactor conditions.
3. Develop feedback equations to give the reactor parameters for the new flux conditions.
4. Solve the point kinetics equations with feedback determined by 2 and 3.

This method has been tried (4,5) with considerable improvement over the point reactor modal, but with less accuracy than the synthesis method discussed below.

Nodal analysis treats the reactor by dividing it into sections or nodes. Each node is treated as a point and the space independent equations are written at each node. The points are interconnected by allowing neutron diffusion, heat, or mass transfer from node to node. In principle the inclusion of nonlinear feedback is a straightforward extention of the zero power problem. However, in practical problems such a large amount of computer time is required that the existing codes (6,7) are limited to one dimension.

Modal analysis is currently the most popular theoretical technique, probably because it allows the analyst to use some very elegant mathematics. The starting point of the various modal methods is usually the same. A general linear operator $A(E,\vec{r},t)$ is defined which is dependent on energy, position, and time and includes not only the neutron distribution but also feedback effects. This operator relates the neutron field $\psi(E,\vec{r},t)$ and an arbitrary source term $f(E,\vec{r},t)$ by the equation

$$A\psi = f \ . \qquad (1)$$

The procedure is then to assume the solution vector Ψ is a linear combination of space functions Φ_j and time coefficients C_j

$$\Psi(E,\vec{r},t) = \sum_{j=1}^{N} C_j(t)\ \Phi_j(E,\vec{r}) \ . \qquad (2)$$

Equation 2 is substituted into 1 and a solution for $C_j(t)$ is obtained. This type of analysis is particularly suited to neutron waves or noise and has been discussed in great detail by Moore (15,16,17).

Once the form of Φ_j has been chosen, the difficulties lie in actually calculating the values of Φ_j and C_j for a given case and in deciding how many modes are necessary for a good solution. Depending on the space function chosen, the technique is given different names. Among these are Helmholtz modes (8), omega modes (9,10,11), lambda modes (9, 12) or Green's function modes (13). With the exception of the Green's function modes, these methods are restricted to simple geometries for which orthogonal eigenfunctions may be determined. For anything other than simple cases the amount of computer time required becomes very large.

One approach which avoids orthogonal eigenfunctions is the flux synthesis method (14). The idea here is that the reactor behavior during a transient can be expressed as a linear combination of the initial solution, the asymptotic solution, and possible intermediate solutions. These solutions are multiplied by weighting coefficients which have the advantage of being easily obtained and fitted to each particular problem. Another method (42) is to expand the Laplace transformed neutron balance equations in a Taylor series of the transform variable. For practical appli-

cation this technique suffers the disadvantage of terminating the series after relatively few terms.

Kerlin's conclusions of space-time analysis are quoted below.

> It is clear that space-time dynamics theory has been actively studied in recent years and that significant progress is being made. However, it is also clear that sufficient experience has not been achieved with practical problems to permit a judgment of the relative merits of the various methods. Most space-time work has considered only one space dimension and no feedback. The necessary extensions to the two- and three-dimensional cases and the inclusion of feedback both linear and nonlinear, are the next steps as the need expands; the knowledge of space-time effects increases; and computers get larger and larger.

Review of Modulated Neutron Experiments

The use of modulated sources dates back to the original papers of Weinberg and Schweinler (18) for the pile oscillator technique and of Raievski and Horowitz (19) for wave propagation. Noise analysis was first discussed by Moore (20) and Cohn (21, 22). These methods have grown rapidly in usefulness and are now almost a field in themselves. Noise analysis has been treated thoroughly in a recent monograph by Thie (23) and in the proceedings of a conference (24) held at the University of Florida in 1963. Recent papers (31, 32, 33) have discussed two detector cross correlation measurements of space dependent transfer functions by noise techniques.

Pile oscillator work has been reported many times. The best such work involving space dependent effects was done by Hansson and Foulke (25). Their work on the NORA reactor forms the basis for a great many of the calculations reported in this thesis.

Wave propagation work has been continued primarily at the University of Florida using small accelerator type neutron sources. Many systems have been studied (26 through 30) including two region systems and also multiply-

ing media. The status of these techniques was thoroughly covered at the Symposium on Neutron Noise, Waves, and Pulse Propagation held at the University of Florida in February, 1966.

Each of the experiments discussed encountered one consistent difficulty. It was necessary to perform complicated experiments, i.e., to produce a wave having a pure fundamental mode in space, in order that their results might be compared with theory. It is clear that if a more elaborate mathematical model, which considered irregular geometries and arbitrary sources, were available, then there should be some trade off between hard experiments and a simple analysis or a simple experiment involving an extensive computer analysis.

Purpose of the Research

The preceding sections lay the background for the work done in this study. The interest in space-time analysis, or to be more specific, in modulated source problems is evidenced by the volume of the literature on the subject. It is clear that before large power reactors can be allowed to operate on fully automatic control systems as conventional power plants are today, there must be thorough understanding of the space dependent dynamics of the system. It is also the case that current techniques of analysis are either extremely costly or are limited to very simple systems. In addition, experimental work in spatial kinetics is hampered by the necessity of producing in the laboratory the idealized model for which analytical solutions are available.

The problem undertaken in this work was to find some simple method by which the analysis of dynamics experiments (in particular modulated

neutron experiments) could be undertaken for real systems such as heterogeneous, multiregion reactors with irregular boundaries. The purpose is not to create a new theory nor to prove an existing one, but to provide the experimentalist with a tool with which he may study more complex systems than are now possible.

The work described in the thesis centers around the description of the model in a form suitable for solution with existing statics codes and demonstration of its validity through the analysis of pile oscillator, wave propagation, and reactor noise experiments. In addition, a proposed experiment involving the relatively new technique of two detector reactor noise measurements is outlined for obtaining data from the GTRR for comparison with calculated values.

CHAPTER II

THEORETICAL ANALYSIS

This chapter contains the derivation of the equations used in the complex source model, first in the form of one-group diffusion theory for simplicity in the discussion, and then the extension to the two-group telegrapher's equations. It is shown how the model may be interpreted so as to use existing statics codes for the solution and some general remarks are made about properties of the derived equations.

Description of the Complex Source Model

We may describe the method using the one-group diffusion equation

$$\nabla \cdot D(\vec{x}) \nabla \phi(\vec{x}, t) - \Sigma_r(\vec{x})\, \phi(\vec{x}, t) + S_p(\vec{x}, t) + S_D(\vec{x}, t) + S_o(\vec{x}, t) \qquad (1)$$

$$= \frac{1}{v} \frac{\partial \phi(\vec{x}, t)}{\partial t} .$$

Here $\phi(\vec{x}, t)$ is the space- and time-dependent flux. D is the diffusion coefficient, Σ_r is the total removal cross section including fission and transverse leakage, and v is the neutron velocity. $S_p(\vec{x}, t)$ is a source term representing the prompt neutrons arising from fission, and is given by the equation

$$S_p(\vec{x}, t) = (1 - \beta)\, \nu\Sigma_f(\vec{x})\, \phi(\vec{x}, t) \qquad (2)$$

where β is the delayed neutron fraction, ν is the mean number of neutrons per fission, and Σ_f is the fission cross section. $S_D(\vec{x}, t)$ is another source term representing the delayed neutron contribution, and is given by

$$S_D(\vec{x}, t) = \sum_i \gamma_i \lambda_i C_i(\vec{x}, t) \tag{3}$$

with the precursor densities $C_i(\vec{x}, t)$ given by

$$\frac{\partial C_i(\vec{x}, t)}{\partial t} = \beta_i \nu \Sigma_f(\vec{x})\ \phi(\vec{x}, t) - \lambda_i C_i(\vec{x}, t) \tag{4}$$

and γ_i equal to the effectiveness factor for delayed neutrons of group i. All source terms are in units of neutrons per unit volume per unit time.

Finally, $S_o(\vec{x}, t)$ is a source term which represents the external disturbance. Small changes in the configuration of the reactor (i.e., reactivity changes) may be treated as being equivalent to positive or negative external sources wherever the assumption of linearity is valid.(22) This formulation is then a complete description of the linear, zero-power, space-dependent kinetics of the reactor.

All of the time-dependent quantities in the above equations may be resolved into a steady part, dependent on position only, plus a fluctuating part dependent on position and time. The steady parts obey the above equations with all time derivatives and S_o equal to zero. When the appropriate subtractions are made, it is found that Equations 1 through 4 are satisfied by the fluctuating parts alone. (If the mean flux is not steady

(e.g., if the reactor is on a period) a similar decomposition can still be made.)

We may now restrict ourselves to the consideration of sinusoidal disturbances, and write

$$\phi(\vec{x}, t) = \underline{\phi}(\vec{x})\ e^{j\omega t} \tag{5}$$

where $\underline{\phi}(\vec{x})$ is a complex amplitude dependent on position. The amplitudes $\underline{S}_p$, $\underline{S}_D$, $\underline{S}_o$, and $\underline{C}_i$, also position-dependent, may be similarly defined.

Substituting into Equation 4, we obtain

$$\underline{C}_i = \frac{\beta_i \nu \Sigma_f \underline{\phi}}{j\omega + \lambda_i} \tag{6}$$

and, from Equation 3,

$$\underline{S}_D = \nu \Sigma_f \underline{\phi} \sum_i \frac{\gamma_i \lambda_i \beta_i}{j\omega + \lambda_i} \tag{7}$$

while Equation 2 yields

$$\underline{S}_p = (1 - \beta)\ \nu \Sigma_f \underline{\phi} \tag{8}$$

and Equation 1 gives

$$D\ \nabla^2 \underline{\phi} - \left(\Sigma_r + \frac{j\omega}{v} \right) \underline{\phi} + \underline{S}_p + \underline{S}_D + \underline{S}_o = 0\ . \tag{9}$$

Determination of $\underline{\phi}$ for a given $\underline{S}_o$ constitutes a solution to the problem.

Extension of this treatment to a multigroup model poses no difficulties. An equation similar to Equation 9 is required for each group, with the appropriate intergroup coupling terms included. (These terms have real coefficients.) In addition, the contributions of the various sources to the various groups must be weighted according to the energy distributions of the source neutrons. The quantity $\nu\Sigma_f\underline{\phi}$ appearing in Equations 7 and 8 must now be summed over all groups. Extension to higher-order approximations to the transport equations is also straightforward. For example, the telegrapher's equation, having a second time derivative, required a term proportional to $\omega^2\underline{\phi}$ in Equation 9.

To obtain a solution, a value of ω and the spatial and energy distribution of $\underline{S}_o$ are specified. The neutron balance equations for the statics calculation are then applied to the various amplitudes. To put the equations into the correct form, $\underline{S}_o$ is inserted, the prompt and delayed fission source terms are obtained by multiplying the usual fission source term by the constants $(1 - \beta)$ and

$$\sum_i \frac{\gamma_i \lambda_i \beta_i}{j\omega + \lambda_i},$$

respectively, and the quantity $j\omega/v$ is added to each removal cross section. The resulting inhomogeneous equations are then solved for $\underline{\phi}$ by the usual methods. The magnitude and phase of $\underline{\phi}$ then indicate the magnitude and phase of the reactor's response to the given sinusoidal source of amplitude $\underline{S}_o$ at the frequency ω. For a complete description of the space-

dependent kinetics of the reactor, the calculation must be repeated for various values of ω and various source locations and energies.

Since the various amplitudes are complex, while the usual procedures for solving such equations are designated for real quantities, the above formulation must be elaborated for practical computation. We write

$$\underline{\Phi} = \Phi_R + j\Phi_I$$

where Φ_R and Φ_I are real numbers giving, respectively, the in-phase and quadrature components of $\underline{\Phi}$. The other amplitudes are treated similarly. (Since $\underline{S}_o$ represents the input to the system, its phase is arbitrary.) Equations 7 through 9 then split into two equations each and become, respectively

$$S_{DR} = \nu\Sigma_f \left(\Phi_R \sum_i \frac{\gamma_i \lambda_i^2 \beta_i}{\omega^2 + \lambda_i^2} + \Phi_I \sum_i \frac{\omega\gamma_i \lambda_i \beta_i}{\omega^2 + \lambda_i^2} \right) \tag{10}$$

$$S_{DI} = \nu\Sigma_f \left(-\Phi_R \sum_i \frac{\omega\gamma_i \lambda_i \beta_i}{\omega^2 + \lambda_i^2} + \Phi_I \sum_i \frac{\gamma_i \lambda_i^2 \beta_i}{\omega^2 + \lambda_i^2} \right), \tag{11}$$

$$S_{PR} = (1 - \beta)\, \nu\Sigma_f \Phi_R \tag{12}$$

$$S_{PI} = (1 - \beta)\, \nu\Sigma_f \Phi_I \tag{13}$$

$$D \nabla^2 \phi_R - \Sigma_r \phi_R + \frac{\omega}{v} \phi_I + S_{DR} + S_{PR} + S_{oR} = 0 \qquad (14)$$

$$D \nabla^2 \phi_I - \Sigma_r \phi_I - \frac{\omega}{v} \phi_R + S_{DI} + S_{PI} + S_{oI} = 0 \, . \qquad (15)$$

Thus there are two neutron balance equations for each group, which are intercoupled. The usual methods of handling downscattering could handle the coupling in one direction, and the coupling in the other direction would be treated as an upscattering.

Two-Group Extension

The two-group telegrapher's equations are written as follows:

Fast group:

$$D_1 \nabla^2 \phi_1(\vec{x}, t) - \Sigma_{r1} \phi_1(\vec{x}, t) + S_p(\vec{x}, t) + S_D(\vec{x}, t) + S_1(\vec{x}, t) \qquad (16)$$

$$= \left[\frac{1 + 3D_1 \Sigma_{r1}}{v_1} \right] \frac{\partial \phi_1(\vec{x}, t)}{\partial t} + \frac{3D_1}{v_1^2} \frac{\partial^2 \phi_1(\vec{x}, t)}{\partial t^2}$$

Thermal group:

$$D_2 \nabla^2 \phi_2(\vec{x}, t) - \Sigma_{r2} \phi_2(\vec{x}, t) + \Sigma_{1 \to 2} \phi_1(\vec{x}, t) + S_2(\vec{x}, t) \qquad (17)$$

$$= \left[\frac{1 + 3D_2 \Sigma_{r2}}{v_2} \right] \frac{\partial \phi_2(\vec{x}, t)}{\partial t} + \frac{3D_2}{v_2^2} \frac{\partial^2 \phi_2(\vec{x}, t)}{\partial t^2}$$

Prompt source:

$$S_p(\vec{x}, t) = (1 - \beta) \sum_j \nu\Sigma_{fj}\phi_j(\vec{x}, t) \qquad ; \; j = \text{group number} \tag{18}$$

Delayed source:

$$S_D(\vec{x}, t) = \sum_i \lambda_i C_i(\vec{x}, t) \; ; \tag{19}$$

i = precursor number (assuming $\gamma_i = 1$) .

Precursor densities:

$$\frac{\partial C_i(\vec{x}, t)}{\partial t} = \beta_i \nu \sum_j \Sigma_{fj}\phi_j(\vec{x}, t) - \lambda_i C_i(\vec{x}, t) \tag{20}$$

The external source terms are S_1 and S_2.

Again, the previously described substitutions reduce the preceding equations to two complex equations dependent on $\vec{x}$ and ω but independent of time.

$$D_1\nabla^2\underline{\phi}_1(\vec{x}) - \left(\Sigma_{r1} + \frac{j\omega}{v_1}[1 + 3D_1\Sigma_{r1}] - \frac{3D_1\omega^2}{v_1^2}\right)\underline{\phi}_1(\vec{x}) \tag{21}$$

$$+ \underline{S}_p(\vec{x}) + \underline{S}_D(\vec{x}) + \underline{S}_1(\vec{x}) = 0$$

$$D_2\nabla^2\underline{\phi}_2(\vec{x}) - \left(\Sigma_{r2} + \frac{j\omega}{v_2}[1 + 3D_2\Sigma_{r2}] - \frac{3D_2\omega^2}{v_2^2}\right)\underline{\phi}_2(\vec{x}) \tag{22}$$

$$+ \Sigma_{1\to 2}\,\underline{\phi}_1(\vec{x}) + \underline{S}_2(\vec{x}) = 0$$

As before, each of the underbarred quantities can be separated into real and imaginary components yielding four coupled inhomogeneous differential equations.

Fast real:

$$D\nabla^2\phi_{1R} - \left(\Sigma_{r1} - \frac{3D_1\omega^2}{v_1^2}\right)\phi_{1R} + \frac{\omega(1 + 3D_1\Sigma_{r1})}{v_1}\phi_{1I} + \nu \tag{23}$$

$$\left(1 - \sum_i \frac{\omega^2\beta_i}{\omega^2 + \lambda_i^2}\right)(\Sigma_{f1}\phi_{1R} + \Sigma_{f2}\phi_{2R}) + \nu \sum_i \frac{\omega\lambda_i\beta_i}{\omega^2 + \lambda_i^2}$$

$$(\Sigma_{f1}\phi_{1I} + \Sigma_{f2}\phi_{2I}) + S_{1R} = 0$$

Fast imaginary:

$$D_1\nabla^2\phi_{1I} - \left(\Sigma_{r1} - \frac{3D_1\omega^2}{v_1^2}\right)\phi_{1I} - \frac{\omega(1 + 3D_1\Sigma_{r1})}{v_1}\phi_{1R} + \nu \tag{24}$$

$$\left(1 - \sum_i \frac{\omega^2\beta_i}{\omega^2 + \lambda_i^2}\right)(\Sigma_{f1}\phi_{1I} + \Sigma_{f2}\phi_{2I}) - \nu \sum_i \frac{\omega\lambda_i\beta_i}{\omega^2 + \lambda^2}$$

$$(\Sigma_{f1}\phi_{1R} + \Sigma_{f2}\phi_{2R}) + S_{1I} = 0$$

Thermal real:

$$D_2\nabla^2\phi_{2R} - \left(\Sigma_{r2} - \frac{3D_2\omega^2}{v_2^2}\right)\phi_{2R} + \frac{\omega(1 + 3D_2\Sigma_{r2})}{v_2}\phi_{2I} \tag{25}$$

$$+ \Sigma_{1\to 2\ 1R} + S_{2R} = 0$$

Thermal imaginary:

$$D_2\nabla^2\phi_{2I} - \left(\Sigma_{r2} - \frac{3D_2\omega^2}{v_2^2}\right)\phi_{2I} - \frac{\omega(1 + 3D_1\Sigma_{r2})}{v^2}\phi_{2R} \qquad (26)$$

$$+ \Sigma_{1\rightarrow 2}\phi_{1I} + S_{2I} = 0$$

Notice that the equations in each group are identical except for an interchange of the subscripts R and I and a sign change in the coupling term between real and imaginary flux components. The coefficients of these equations are the usual macroscopic total removal, fission, and downscattering cross sections, Σ_r, Σ_f, $\Sigma_{1\rightarrow 2}$, modified by terms dependent on the velocity v of the particular neutron group and the angular frequency ω. Since the ϕ's which are the solutions to this set of equations are the real and imaginary parts of the complex amplitude either or both of them may be negative.

Utilization of Existing Statics Codes

To see how statics codes may be used to solve this problem, it is necessary to examine the form of Equations 23 through 26. Notice that the four equations are completely coupled. For example, the equation for the fast imaginary component of the flux contains terms proportional to the fast real, thermal real, and thermal imaginary components. The coupling from fast to thermal and from real to imaginary can be treated as downscatter, but the coupling in the other direction from thermal to fast and from imaginary to real will have to be treated as upscatter.

With this in mind, we can renumber the equations in a manner analo-

gous to a few group diffusion problem:

Fast real ≡ group 1

Fast imaginary ≡ group 2

Thermal real ≡ group 3

Thermal imaginary ≡ group 4

The coefficients in Equations 23 through 26 can now be matched one to one with the macroscopic cross sections in a statics code.

Diffusion coefficients:

$$\hat{D}_1 = D_1 \qquad (27)$$
$$\hat{D}_2 = D_1$$
$$\hat{D}_3 = D_2$$
$$\hat{D}_4 = D_2$$

Absorption cross sections:

$$A_1 = \Sigma_{r1} - 3D_1\omega^2/v_1^2 = \hat{\Sigma}_{a1} \qquad (28)$$
$$A_2 = \Sigma_{r1} - 3D_1\omega^2/v_1^2 = \hat{\Sigma}_{a1}$$
$$A_3 = \Sigma_{r2} - 3D_2\omega^2/v_2^2 = \hat{\Sigma}_{a3}$$
$$A_4 = \Sigma_{r2} - 3D_2\omega^2/v_2^2 = \hat{\Sigma}_{a3}$$

Scattering into group 1:

$$C_{1\rightarrow 1} = \left(1 - \sum_i \frac{\omega^2\beta_i}{\omega^2 + \lambda_i^2}\right) \nu\Sigma_{f1} \qquad (29)$$

$$C_{2\to 1} = \frac{\omega(1 + 3D_1\Sigma_{r1})}{v_1} + \nu\Sigma_{f1}\sum_i \frac{\omega\lambda_i\beta_i}{\omega^2 + \lambda_i^2}$$

$$C_{3\to 1} = \left(1 - \sum_i \frac{\omega^2\beta_i}{\omega^2 + \lambda_i^2}\right)\nu\Sigma_{f2}$$

$$C_{4\to 1} = \nu\Sigma_{f2}\sum_i \frac{\omega\lambda_i\beta_i}{\omega^2 + \lambda_i^2}$$

Scattering into group 2:

$$C_{1\to 2} = \frac{-\omega(1 + 3D_i\Sigma_{r1})}{v_1} - \nu\Sigma_{f1}\sum_i \frac{\omega\lambda_i\beta_i}{\omega^2 + \lambda_i^2} = -C_{2\to 1} \qquad (30)$$

$$C_{2\to 2} = \left(1 - \sum_i \frac{\omega^2\beta_i}{\omega^2 + \lambda_i^2}\right)\nu\Sigma_{f1} = C_{1\to 1}$$

$$C_{3\to 2} = -\nu\Sigma_{f2}\sum_i \frac{\omega\lambda_i\beta_i}{\omega^2 + \lambda_i^2} = -C_{4\to 1}$$

$$C_{4\to 2} = \left(1 - \sum_i \frac{\omega^2\beta_i}{\omega^2 + \lambda_i^2}\right)\nu\Sigma_{f2} = C_{3\to 1}$$

Scattering into group 3:

$$C_{1\to 3} = \Sigma_{1\to 2} \qquad (31)$$

$$C_{2\rightarrow 3} = 0$$

$$C_{3\rightarrow 3} = 0$$

$$C_{4\rightarrow 3} = \frac{\omega(1 + 3D_2\Sigma_{r_2})}{v_2}$$

Scattering into group 4:

$$C_{1\rightarrow 4} = 0 \tag{32}$$

$$C_{2\rightarrow 4} = \Sigma_{1\rightarrow 2}$$

$$C_{3\rightarrow 4} = -\frac{\omega(1 + 3D_1\Sigma_{r_2})}{v_2} = -C_{4\rightarrow 3}$$

$$C_{4\rightarrow 4} = 0$$

The input fission cross sections should all be zero since fission has been included in the scattering terms. This is necessary because the codes allow only one fission source and in this problem two are required. The buckling should also be set to zero because transverse leakage was included in the removal cross section.

Finally Equations 23 through 26 are inhomogeneous so a source term must be permitted by the code. Thus, to apply an existing statics code to this problem, the code must provide for the following features:

1. An external source

2. Scattering from any group to any other group

3. Negative flux.

The CRAM code (34), which is a multigroup, multiregion, one or two dimensional diffusion code for the IBM-7094, has these features and can be applied to this problem if the following identifications are made:

1. The external source is represented by a dummy flux group 1 which can be scattered into the appropriate lower group at the sapce point where the source is located.

2. Flux groups 2, 3, 4, and 5 represent the fast real, fast imaginary, thermal real, and thermal imaginary equations, respectively.

3. The coupling from real to imaginary is treated as downscatter and from imaginary to real as upscatter.

4. The macroscopic cross sections are defined by Equations 27 through 32.

It has recently been demonstrated by Johnson (35) that the code EXTERMINATOR (36) can also solve these equations. Since EXTERMINATOR handles the external source problem explicitly, only four energy groups are necessary. No further definitions need be made.

Convergence of the Codes

Thus far nothing has been said about convergence of the codes when the cross sections are defined in the previously described manner. In the normal reactor problem, the coefficients are of the proper sign to yield a nonnegative iteration matrix, i.e., one in which all elements are either positive or zero. In this case all eigenvalues and solution vectors are positive and theorems exist which guarantee convergence of the

iterative method used. CRAM uses the Liebmann technique (37). However, as the cross sections are now defined, the scattering terms give rise to negative off diagonal elements in the iteration matrix and no theorems are available to guarantee convergence. This does not mean that solutions do not exist. It simply means that for any given problem the iteration scheme may, or may not, converge to the solution.

For the above reason it was decided that prior to any work with CRAM, the model should be tested by a code which would solve the equations by a noniterative method such as Choleski matrix inversion or the method of conjugate gradients (38). To do this, a program was written to solve the one dimensional (cylindrical), two-group equations. (See CHARLIE, Appendix B.) If the physics of the model were valid, then direct inversion of the coefficient matrix should produce the correct solutions. The inversion method was first tried for the NORA reactor with excellent results. The calculations are described in the pile oscillator section of Chapter III. The conjugate gradient method produced identical results but was found to require roughly three times the number of steps as was theoretically necessary to find the solution to within acceptable error limits. (The theoretical number of steps is equal to the dimension of the coefficient matrix or four times the number of mesh points chosen.) This turned out to be an omen of things to come.

The next step was to run the same set of problems with CRAM. A normal reactor problem of the size chosen (4 groups and 25 mesh points) will converge in 15 to 20 iterations. The first problem attempted (a frequency of $\omega = 1$ radian/sec) required approximately 50 iterations. In spite of the long running time, the problem converged uniformly and

the results were identical to those obtained previously. At higher frequencies, the code converged more rapidly, but less uniformly, until at 320 radians per second no solution could be obtained. As the frequency was decreased to 0.01 radians per second, the rate of convergence became very sluggish and finding solution was at best impractical. Over the frequency range of interest, however, the code was found to reproduce the results obtained by matrix inversion and to be practical although slow.

Johnson (35) has shown that EXTERMINATOR first showed similar behavior, but when used with the option of "group rebalancing" convergence improved markedly. This can be explained on a physical basis by realizing that the real and imaginary flux components look like two reactors, one real and one imaginary, which are very loosely coupled. It is exactly these conditions for which group rebalancing is required. The precise mathematical reason why EXTERMINATOR will find the solution to a given problem while CRAM fails is not understood. Perhaps a thorough mathematical study of this class of problems will shed new light on existing iteration techniques and also produce new methods with improved convergence rates.

One other interesting point was noted. The rate of convergence depends on the reactivity of the system. For a just critical reactor, convergence was slow but speeded up as the reactor was made either subcritical or supercritical. Similar behavior was found for the conjugate gradient method. Convergence is slow because the coefficient matrix is nearly singular for a critical reactor. Only the inclusion of the ω term prevents singularity.

General Remarks on Properties of the Equations

The complex source model described is a method for computing the complex magnitude of the response of a system to some external disturbance. One of the tests of any theory is to examine its behavior in certain limiting cases. For this model, we have one such test when $\omega = 0$. Making this substitution into Equations 23 through 26, it is seen that the equations uncouple, ϕ_R becomes identical to ϕ_I, and we are left with the two-group steady state diffusion equations. Thus, the solution for any problem with $\omega = 0$ is the fundamental mode flux distribution in the system. Mathematically the static case forces the imaginary components to be zero.

Note that the static case can be used as a criticality condition. If ω is set to zero and the equations are made honogeneous by the elimination of the external source S_o, then in order for there to be a solution the determinant of the coefficient matrix must vanish. To achieve this condition, a search may be made on any of the cross sections, the transverse buckling, or the position of a boundary.

This raises the question of the behavior of the equations for a subcritical, critical, or supercritical reactor with a finite source and $\omega = 0$. The subcritical case is quite straightforward. Physically, a subcritical reactor may maintain a steady flux in the presence of an external source of neutrons. For this case, the phase angle is zero and the gain is proportional to the static flux.

$$\text{GAIN} \equiv (\phi_R^2 + \phi_I^2)^{\frac{1}{2}}$$

$$\text{PHASE} \equiv \tan^{-1} (\phi_I/\phi_R)$$

The critical reactor of course cannot remain stationary with a source and mathematically as $\omega \rightarrow 0$, $\phi_R \rightarrow \infty$ and $\phi_I \rightarrow -\infty$. That is gain $\rightarrow \infty$ and phase $\rightarrow$ $-90°$. No solution is possible when $\omega = 0$.

The supercritical system is a bit peculiar. The supercritical reactor cannot remain stationary with or without a source, but it turns out that the equations do have a unique solution. The observed conditions are that $\phi_R < 0$, $\phi_I = 0$, gain is proportional to the flux in the reactor's fundamental mode, and the phase angle is $-180°$. For $\omega > 0$, plots of gain and phase are shown for the NORA reactor in Figures 3 and 4. This behavior shows that the model is the space dependent extension of the Incremental Linear Equivalent System equations of Carter (39).

Several things should be said with regard to the source term S_o. Since the source represents the input to the system, its magnitude and phase are arbitrary. The equations are linear so the magnitude of the response is directly proportional to the source strength. Changing the sign of the source from positive to negative is simply a phase shift of 180° and the phase of the response changes by 180°. The location of the source in space and in energy presents the most interesting situation. Clearly all points in a reactor are not equally important and a source in the core should give a larger response than the same source near the outer boundary. As discussed by Keepin (40), the response amplitude of the system is proportional to the product of the source strength and the adjoint flux at the location of the source. By moving the source from point to point it is possible, though inefficient, to extract the adjoint flux from the model.

Although the equations are derived for the P-1 approximation

(telegrapher's equation), it is a trivial matter to reduce them to the diffusion approximation. Brehm (41) has shown that P-1 theory tends to overcorrect the space dependence at high frequencies and in reality diffusion theory is a better approximation to the transport solution. (Below 1000 rad/sec there is practically no difference in the three approximations.) If diffusion theory is desired, simply drop the $3D\omega^2/v^2$ and $3D\Sigma_r$ terms from the definition of the cross sections in Equations 28 through 32. No other changes are required. Brehm also shows how transport effects may be taken into account by defining a frequency dependent diffusion coefficient. For one energy group assuming isotropic scattering and small absorption, Brehm gives

$$D = \frac{1}{3\Sigma_t(1 - i\omega')} \left[1 + \frac{4}{5}(1 - C) + \frac{108}{175}(1 - C)^2 + \frac{396}{875}(1 - C)^3 + \ldots \right] \tag{33}$$

where

$$C \equiv \frac{\nu\Sigma_f + \Sigma_s}{\Sigma_t(1 - i\omega')} \quad \text{and} \quad \omega' \equiv \omega/v\Sigma_t$$

This effect can easily be included in the model.

The size of the mesh used in the numerical solution of the equations is important. The mesh spacing must be small in comparison with the complex relaxation length of the disturbance or serious errors may result. This effect is discussed more fully in Chapter III under wave propagation. In general, for frequencies greater than 1000 radians per

second the complex source problem will require a mesh smaller than the corresponding statics problem. Below this frequency no difference is expected.

Each of the above mentioned properties has been observed while making the calculations presented in Chapter III. These points will be reemphasized as they occur in the analysis of each type of modulated neutron experiment.

CHAPTER III

ANALYSIS OF EXPERIMENTS

Analysis of different types of modulated neutron experiments requires slightly different interpretations of the model for each experiment. This chapter discusses three basic types, pile oscillator, wave propagation, and noise measurements. For each type, the numerical calculations are compared with experimental data.

Pile Oscillator

The theory of an oscillating absorber in a reactor was first described by Weinberg and Schweinler (18). Quoting Weinberg,

> . . . if the oscillation is very slow the pile intensity fluctuates as a whole, the neutron flux at any point having the same phase as at any other point . . . . If the oscillation is fast, or if the detector is close to the absorber the fundamental no longer predominates. . . . Since the higher harmonics all have different phases (because the coefficients in the series are complex), the phase of the neutron intensity oscillation will change from point to point. Close to the absorber the intensity will be in phase with the motion of the absorber since the local neutron depression caused by the absorber will be the major part of the intensity fluctuation. Far from the absorber the neutron intensity will tend to move more and more toward the phase of the fundamental. . . . The disturbance set up by the oscillating absorber is therefore wave-like: the absorber sends out damped waves of neutron intensity which are reflected at the boundary. As will be shown below, the wave-length of the traveling disturbance is short at high frequency and long at low frequency. It is for this reason that the disturbance has the same phase everywhere at low frequencies, and has a varying phase at high frequency.

This behavior may be described by a space-dependent "transfer function," which gives the reactor's response, observed at a given point, to a sinusoidal disturbance introduced elsewhere. The term "transfer func-

tion" is used here in its classical electrical-engineering sense as a relation between input and output. No connection is implied with the familiar "reactivity transfer function" of space-independent kinetics. Since reactivity is an integral or whole-reactor parameter, specification of the reactivity effect of an input (e.g., an oscillating absorber) does not uniquely specify the input in a space-dependent situation. (That is, a large number of different configuration changes could give the same reactivity change, and yet induce completely different dynamic effects.) Therefore, there is no such thing as a space-dependent reactivity transfer function.

For the case of the pile oscillator, the transfer function can be obtained by a very simple interpretation of the described model. Here the source term S_o is made to represent the varying absorption of the oscillator, and is placed in the spatial regions and energy groups in which the oscillator operates. Cohn (22) has shown that this approximation is valid as long as the disturbance is small and the system remains linear. The calculated $\underline{\Phi}$ may then be directly compared with the observed response to the oscillator at various detector locations.

The NORA Reactor

The first reactor chosen for analysis was the NORA (25) reactor, a heavy water moderated, enriched uranium critical assembly located in Kjeller, Norway, for which the space dependent transfer function had been determined experimentally by use of a pile oscillator. The two-group model with the telegrapher's equations was solved by CHARLIE using matrix inversion and also using the method of conjugate gradients. Cross sections, including fourteen groups of delayed neutrons, were obtained from P. T.

Hansson (43) and were the same set as used for the original analysis of NORA. (See Appendix C for a complete description of the reactor.) The mesh chosen consisted of 26 space points graduated from a spacing of 4 cm at the center line (near the pile oscillator) to 12 cm at the outer edge. A fine mesh spacing is not necessary in this problem because large flux gradients are not present.

Since the shape of the transfer function is sensitive to reactivity, it was necessary to adjust the axial buckling to make $k_{eff} = 1$. This was accomplished by setting $\omega = 0$ in Equations 23 through 26. When this is done, the equations uncouple and ϕ_R becomes identical to ϕ_I. Hence, with the source set to zero, the determinant of the coefficient matrix must be zero for criticality. By adjusting B_Z^2 until the determinant was zero, the final critical B_Z^2 was found to agree with the experimental value to within the error limits reported.

The pile oscillator was represented by a source term in the thermal real group (since the source is an input to the system its phase is arbitrary) and located at the reactor centerline.

Calculations were made with values of ω ranging from 0.001 to 1000 radians per sec and the results closely reproduce the reported experimental results for gain and phase shift, as shown in Figures 1 and 2. The results shown are for the thermal group only. The fast group results are similar in shape but have less pronounced space effects.

That these equations represent the I L E S transfer function (39) can be seen from Figures 3 and 4. The curve for location A has been recalculated for the reactor subcritical and for supercritical. Both gain and phase have a behavior at low frequencies which is characteristic of

the I L E S model. The parameter used to adjust criticality was B_Z^2, which ranged from 0.000545 to 0.000562 corresponding to k_{eff} values of 1.0035 and 0.9977. These calculations were repeated using CRAM. The results are found to reproduce the experimental values and the previous calculations over the range of the experimental data. (See Figures 5 and 6.) Convergence of the problems is slow. For low frequencies ($\omega = 1$ radian/sec), fifty iterations were required and the convergence was very uniform. At progressively higher frequencies, the rate of convergence became more rapid but less uniform. These symptoms indicate that further work is necessary to find a better iteration scheme for this type problem. Currently, CRAM uses the Liebmann technique, but because of negative terms in the off diagonal elements of the coefficient, matrix convergence is not guaranteed. At extremely high frequencies (greater than 320 radians/sec), CRAM was unable to find the solution, although no problem was encountered with the matrix inversion method. This may indicate that the iteration technique used in CRAM may be entering an unstable region. Very low frequencies present another problem in which the technique becomes sensitive to criticality as shown by the dashed lines in Figures 5 and 6. Attempts to do two-dimensional calculations using the CRAM code have shown much more severe convergence problems.

The phase shift for the supposedly critical reactor begins to turn up at about 0.04 radians/sec. This behavior is typical of a slightly subcritical reactor. The gain plot for the supercritical case shows another peculiarity. Although the phase angle properly goes to -180° at low frequencies, the gain does not show a peak as expected. Apparently this discrepancy is due to the failure of CRAM to converge for low fre-

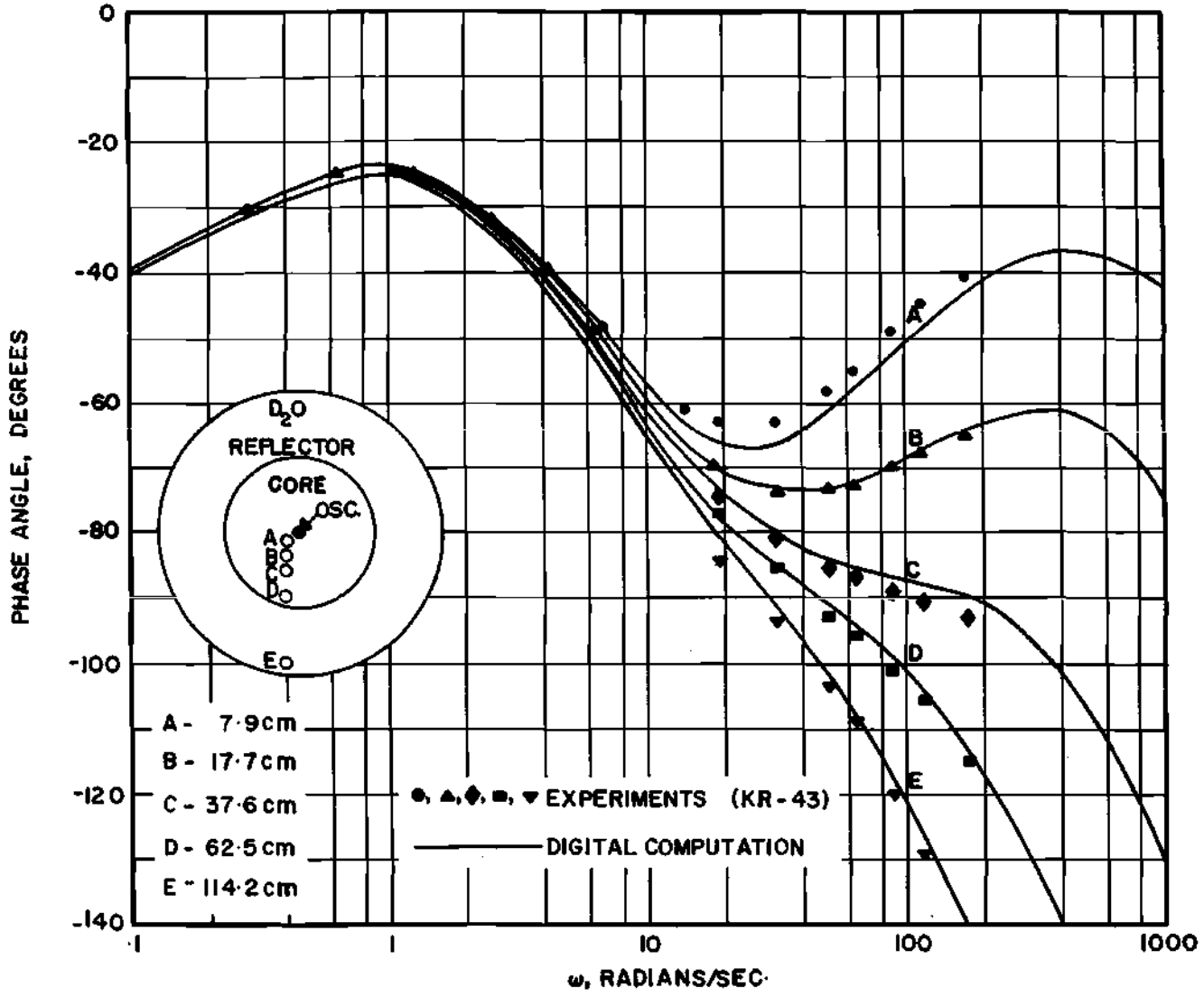

Figure 1. Space Dependent Phase Shift for the NORA Reactor

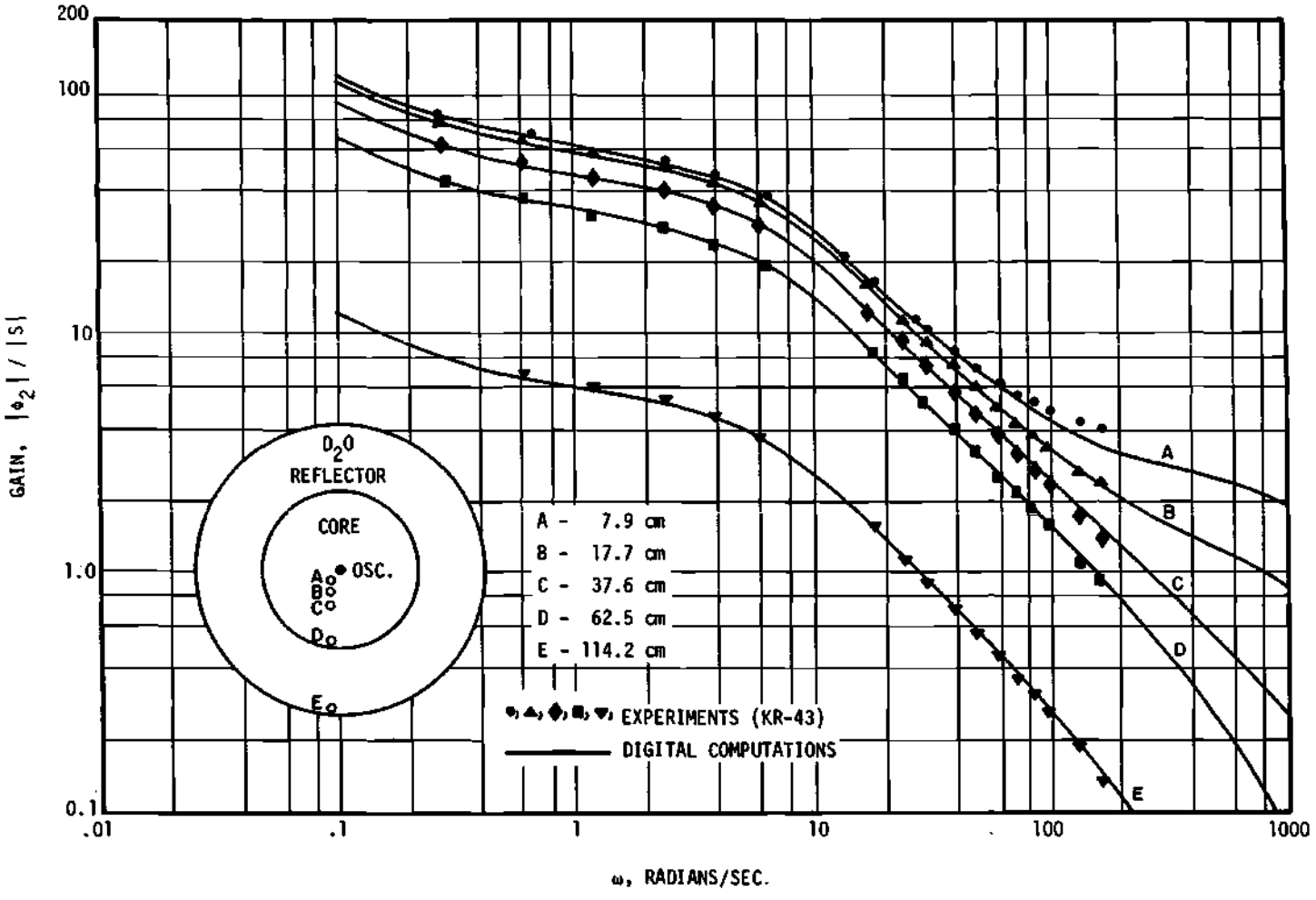

Figure 2. Space Dependent Gain for the NORA Reactor

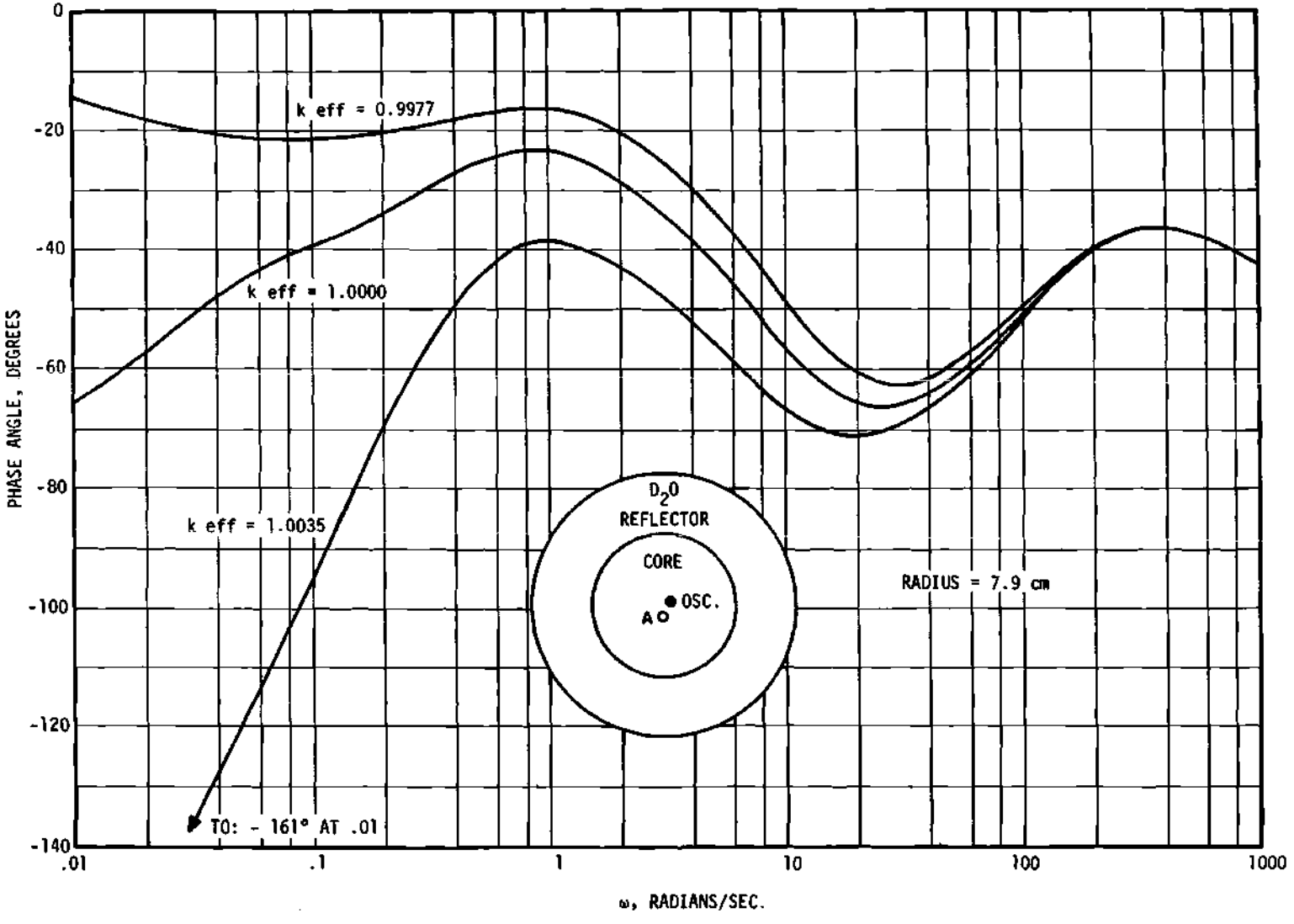

Figure 3. Effect of Criticality on Phase Shift for the NORA Reactor

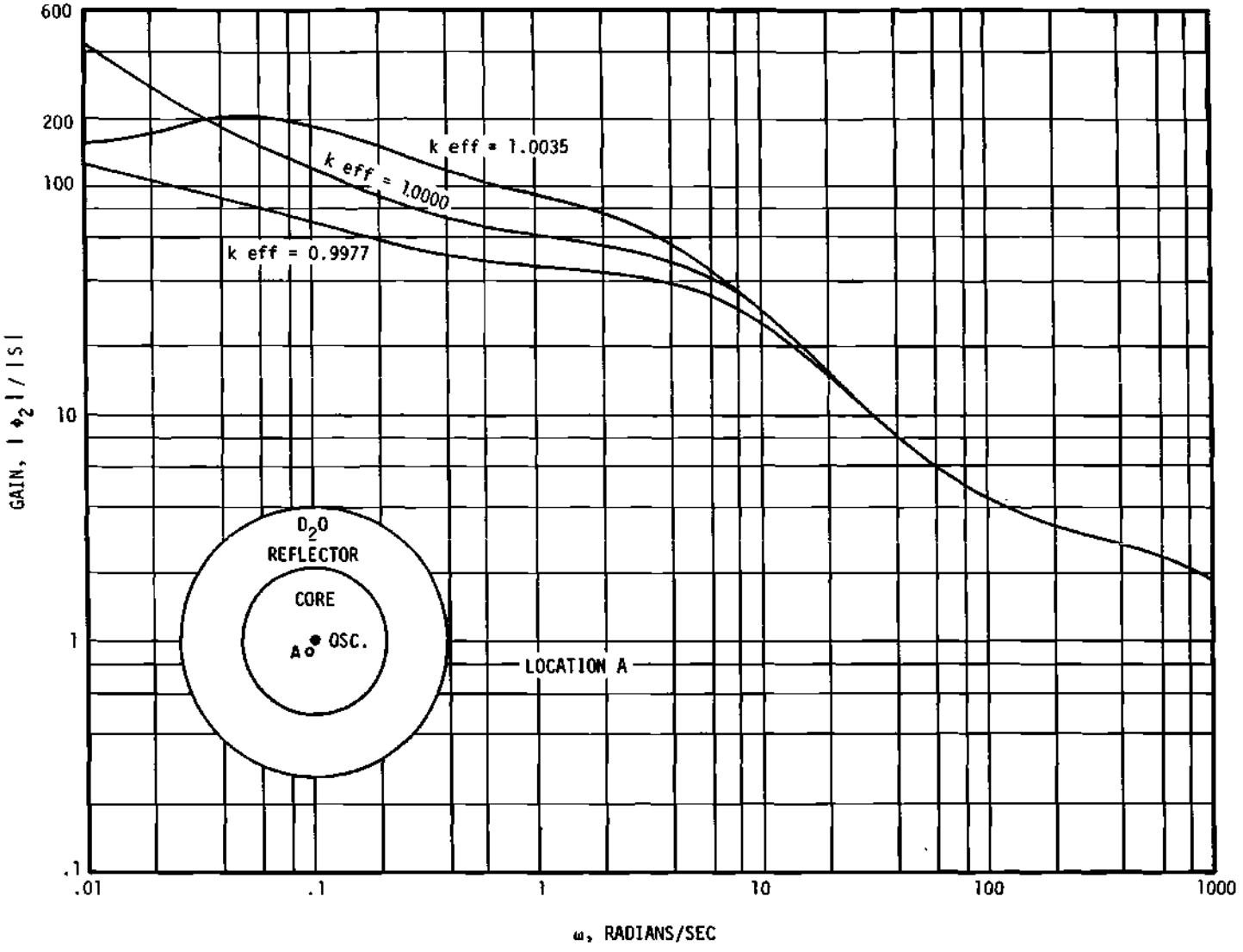

Figure 4. Effect of Criticality on Gain for the NORA Reactor

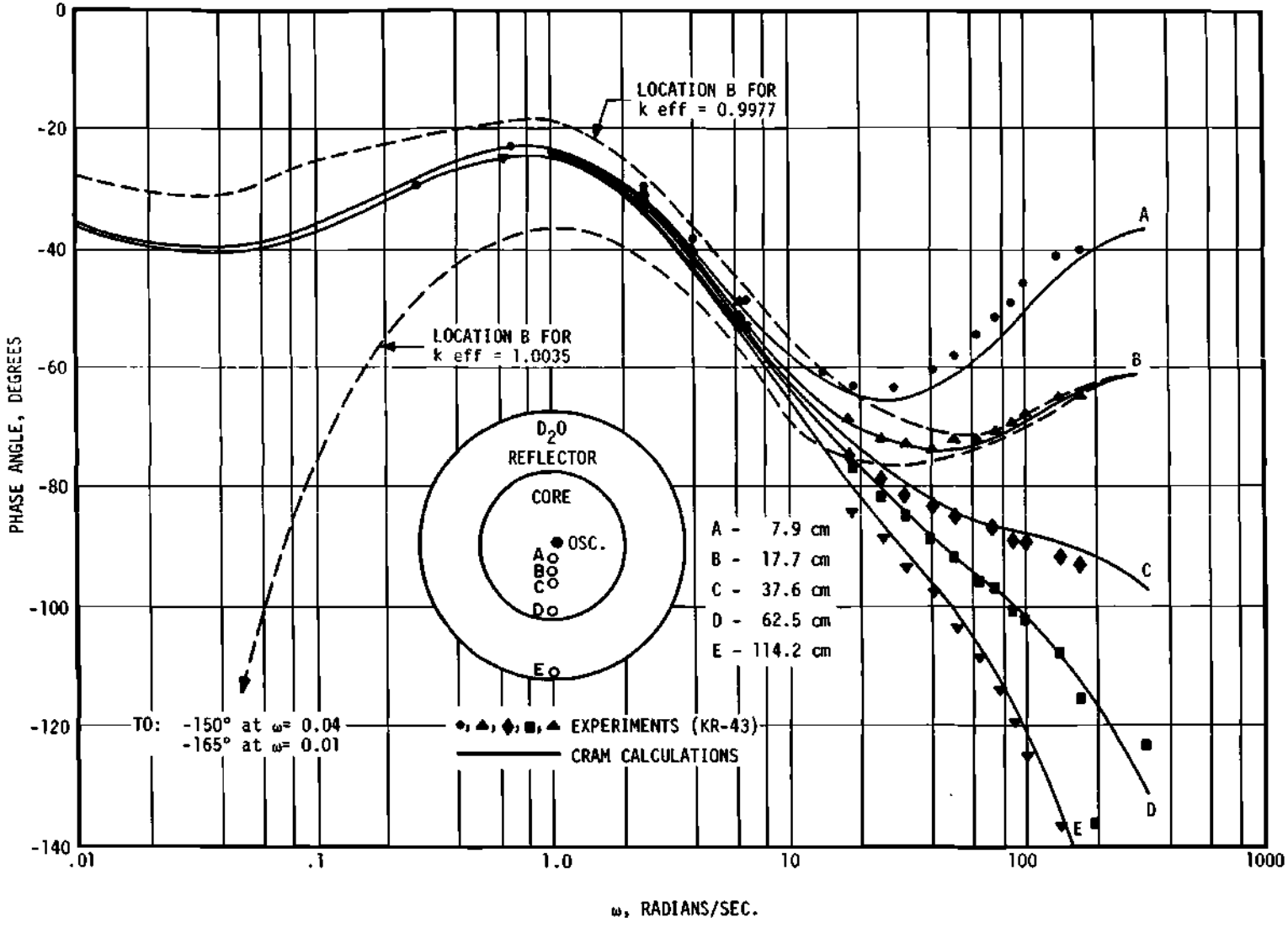

Figure 5. Space Dependent Phase Shift from CRAM for the NORA Reactor

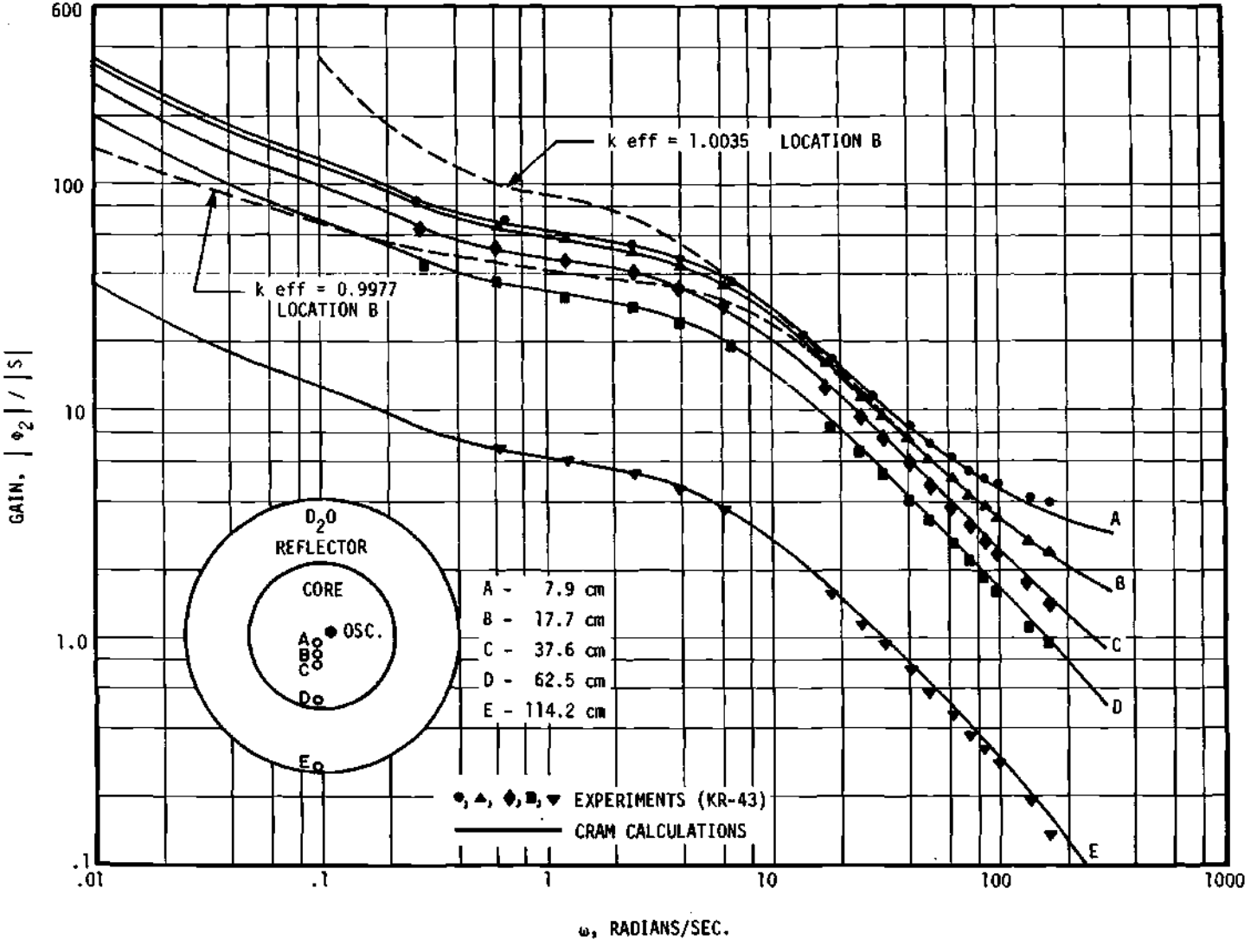

Figure 6. Space Dependent Gain from CRAM for the NORA Reactor

quencies. The problems were terminated after 200 iterations. Johnson (35) shows that EXTERMINATOR with the group rebalancing option eliminates these difficulties.

The Georgia Tech Research Reactor

Pile oscillator measurements have been made on the GTRR by Johnson (35,44). Although in his experiment the pile oscillator was placed off the reactor centerline and would require a two-dimensional code for a proper analysis, it was of interest to see if the low frequency data would compare with calculations in which the oscillator was placed in the center of the core. CHARLIE with the diffusion equation option was used for these calculations. A complete description of the reactor including the preparation of the cross sections is given in Appendix C.

The fast and thermal space dependent transfer functions are shown in Figures 7 through 10. The experimental data shows agreement with the theory in the low frequency (space independent) region; however, it begins to deviate from the assumed model at about two radians per second. This result points out the problems that might be encountered in attempting to use a one-dimensional model when two-dimensions are required. The relative positions of the oscillator and detector are shown by the "X" and triangle respectively.

Another form for presenting the results is a plot of the gain versus radius as a function of frequency. This is done for the thermal group in Figures 11 and 12. The curve labeled static flux on the gain plot was computed using CRAM as a normal two-group reactor problem. The other curves were calculated with CHARLIE. This figure indicates dramatically how the amplitude of the complex flux response at low frequencies becomes

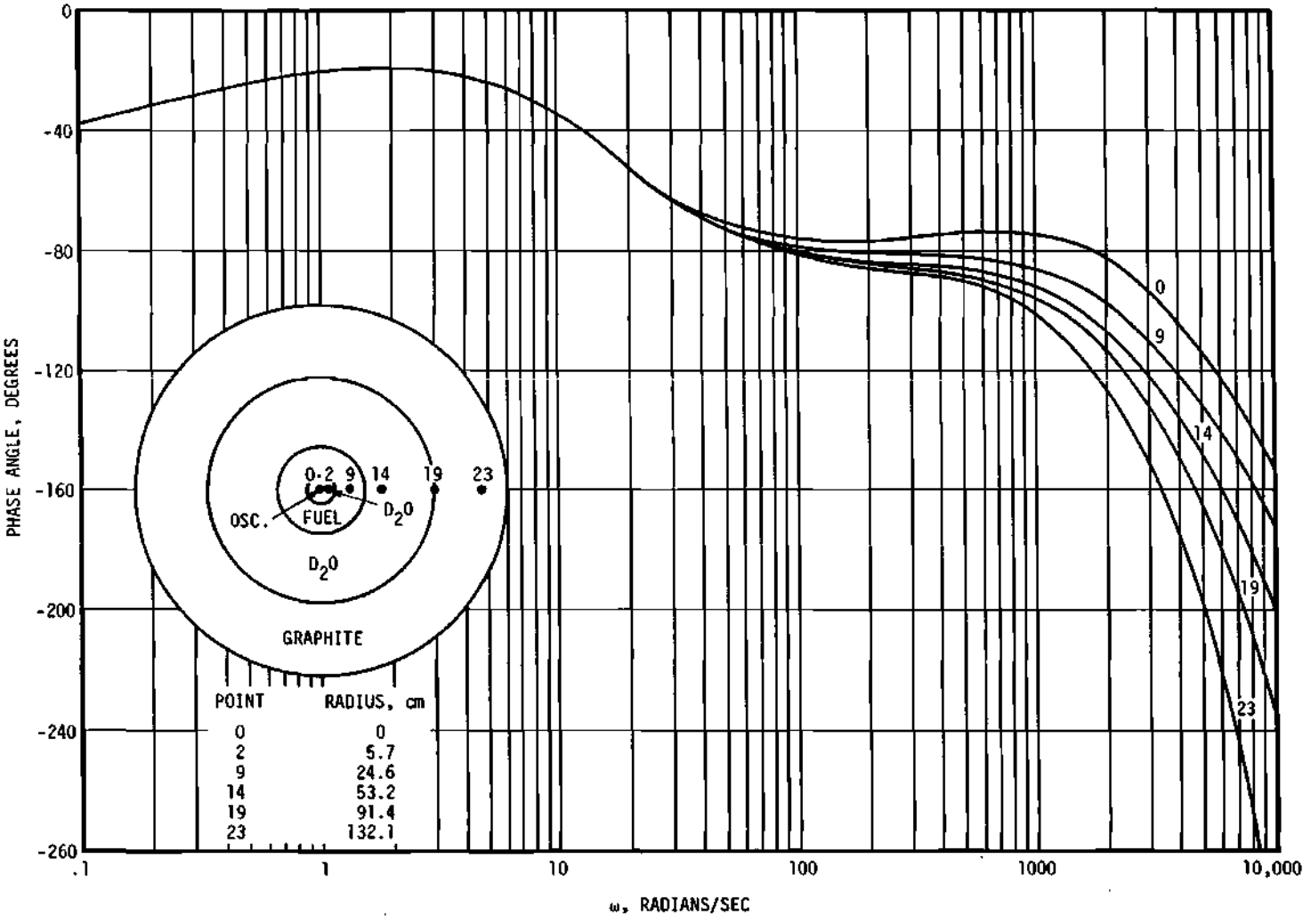

Figure 7. Space Dependent Fast Flux Phase Angle for a GTRR Pile Oscillator Experiment

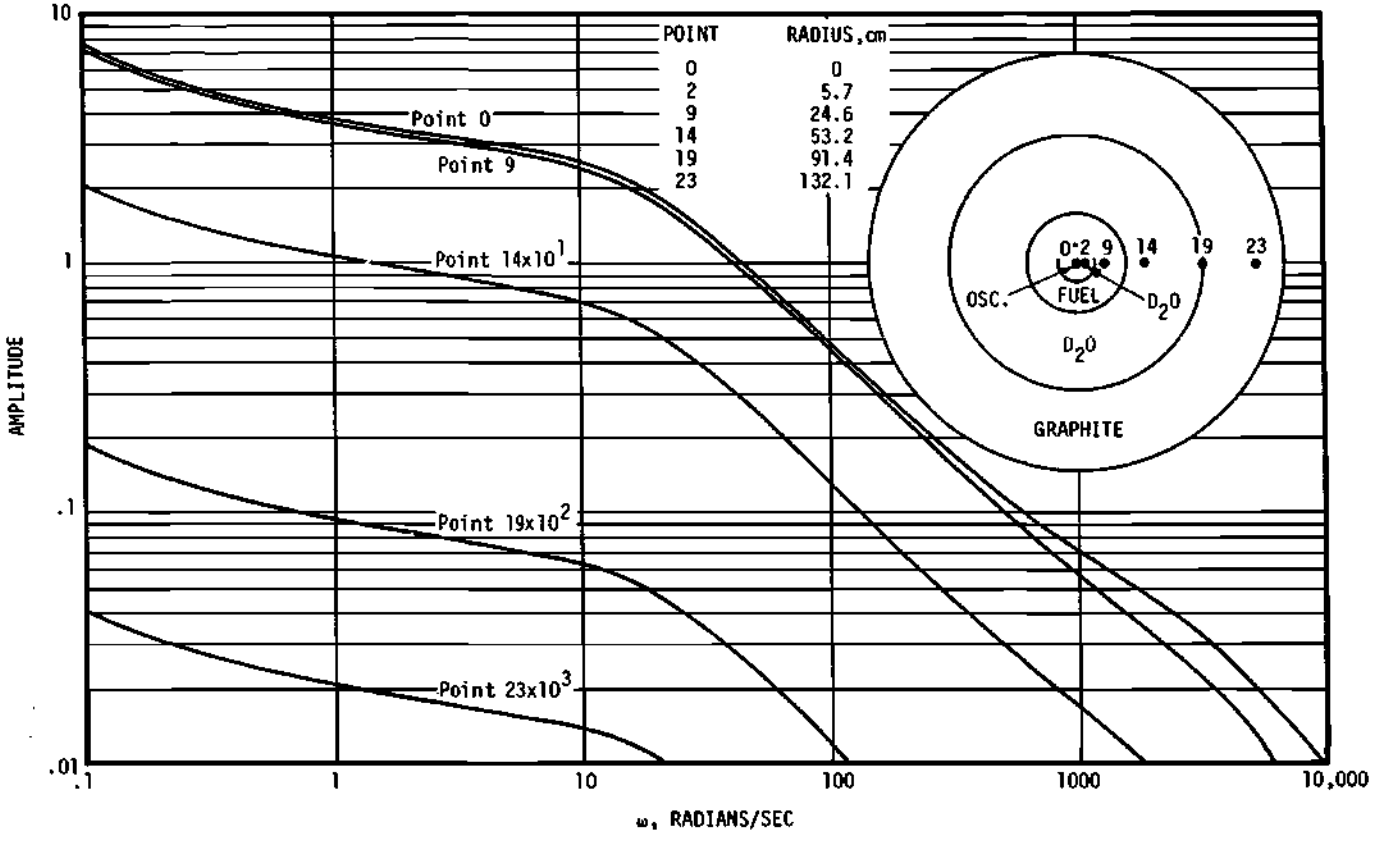

Figure 8. Space Dependent Fast Flux Amplitude for a GTRR Pile Oscillator Experiment

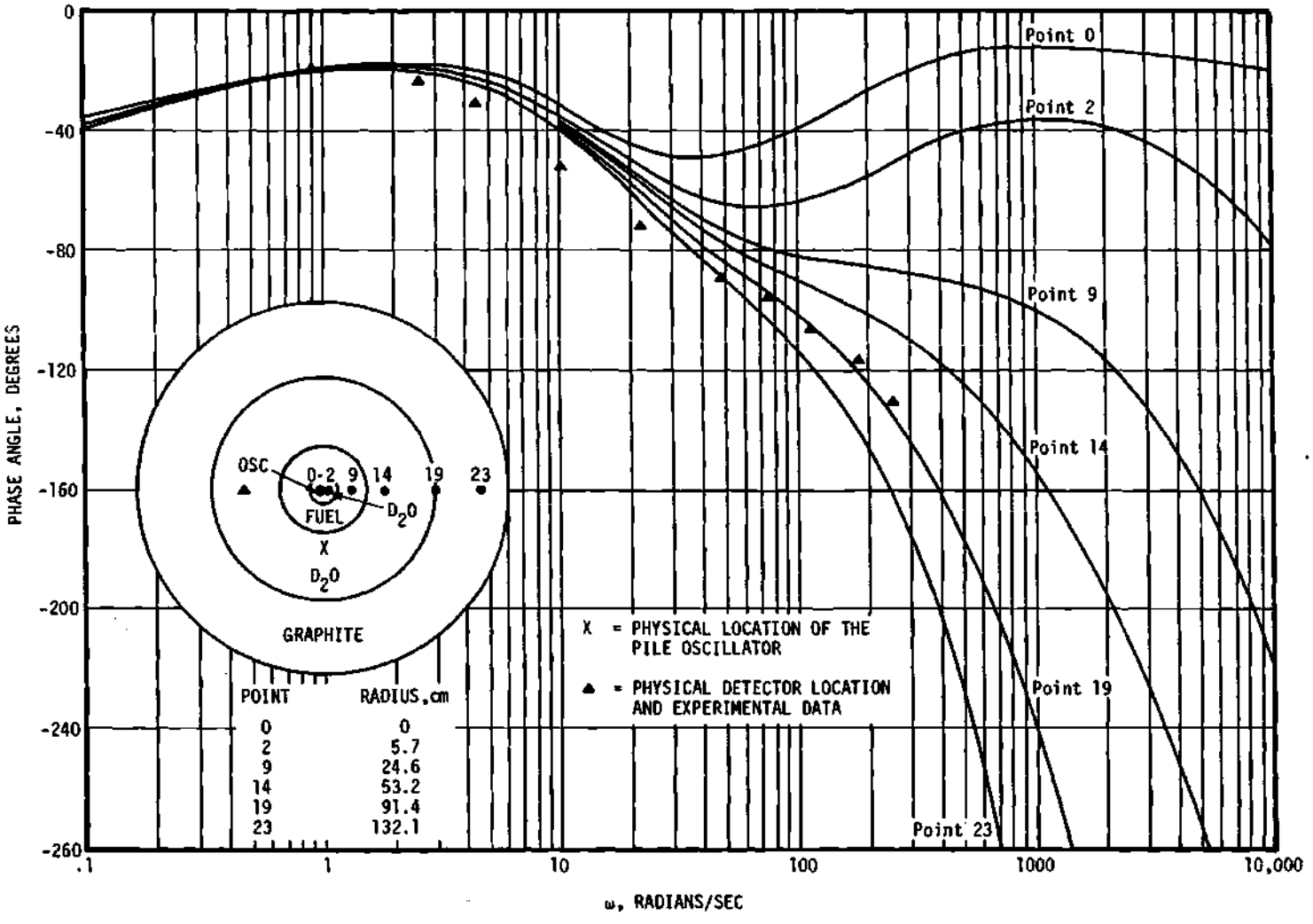

Figure 9. Space Dependent Thermal Flux Phase Angle for a GTRR Pile Oscillator Experiment

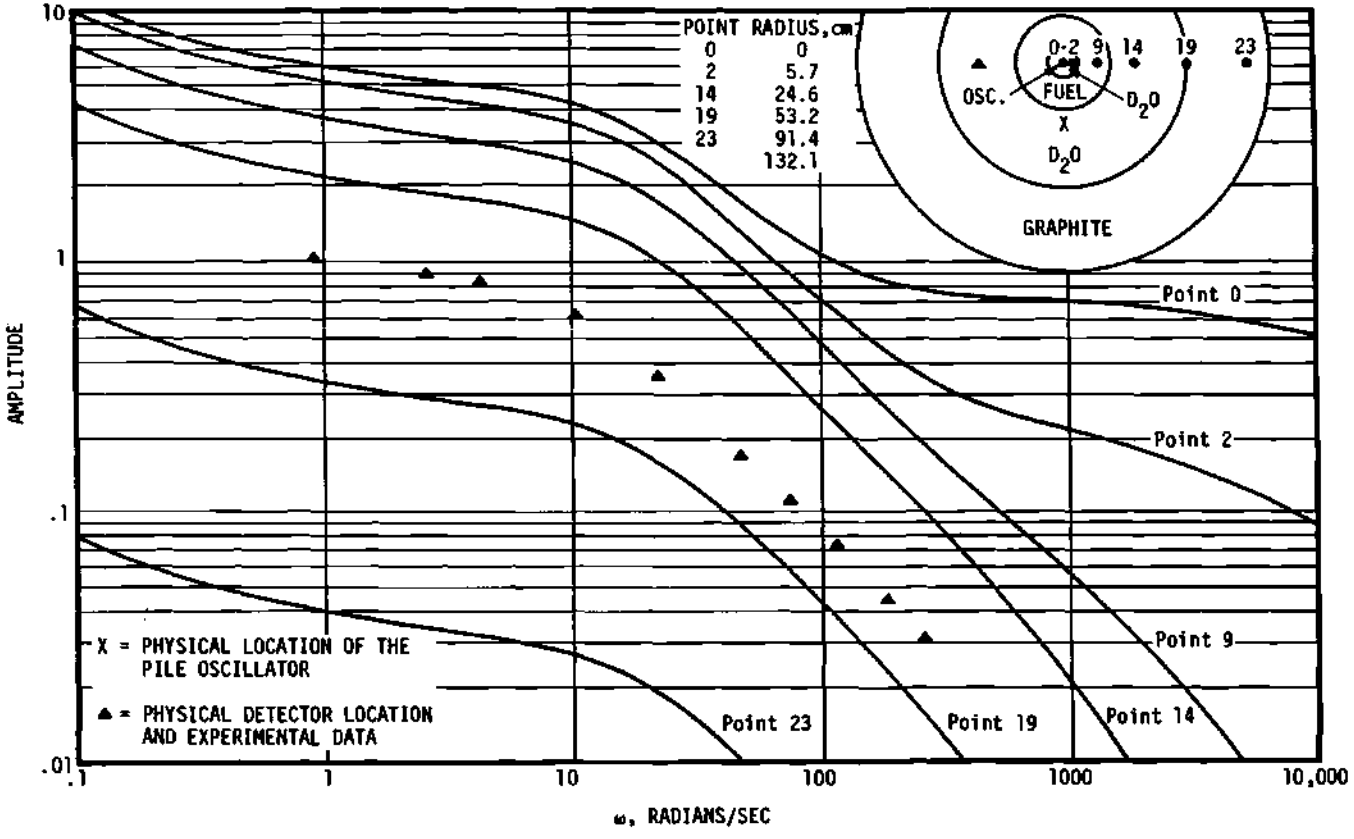

Figure 10. Space Dependent Thermal Flux Amplitude for a GTRR Pile Oscillator Experiment

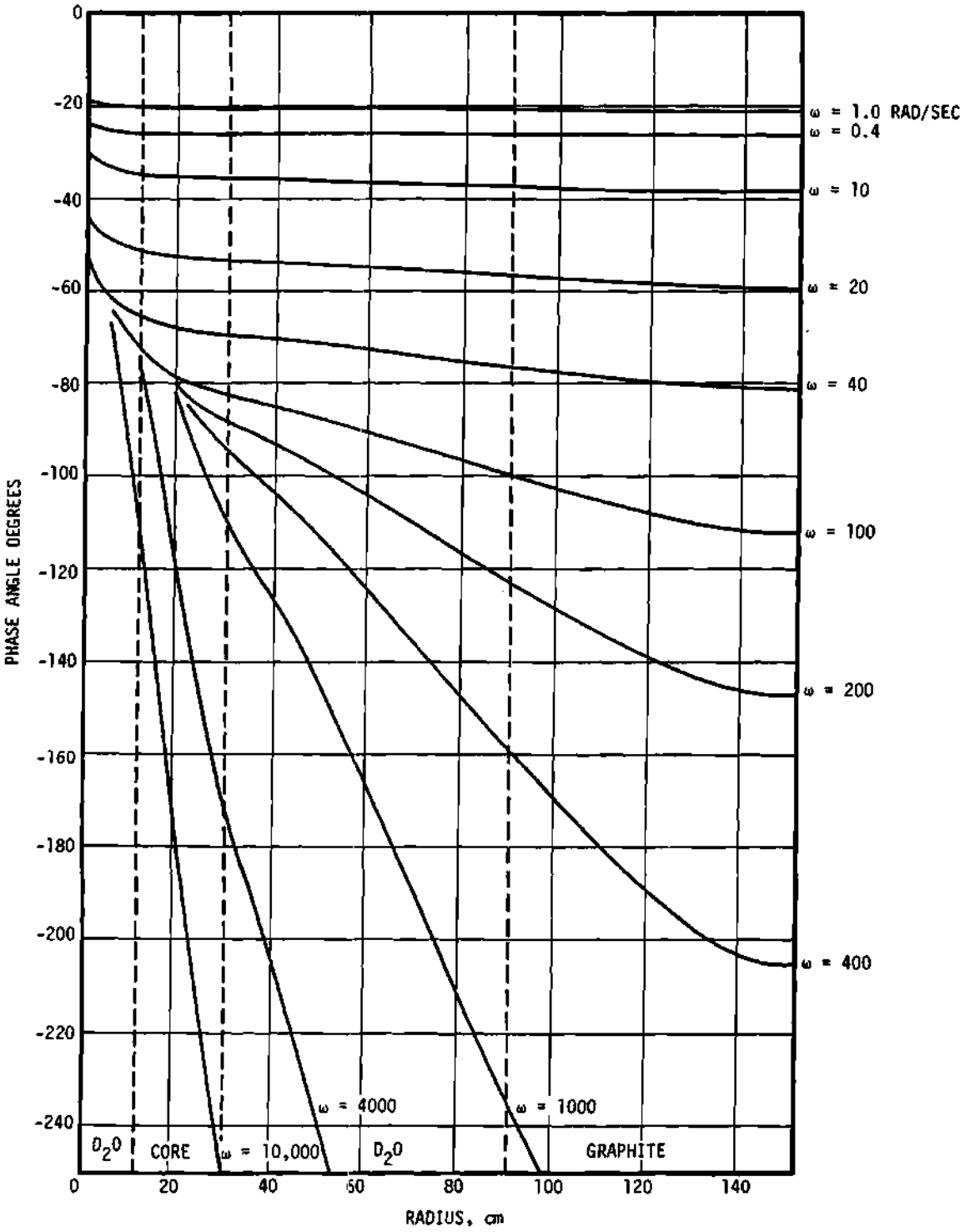

Figure 11. Thermal Flux Phase Angle versus Radius for a GTRR Pile Oscillator Experiment

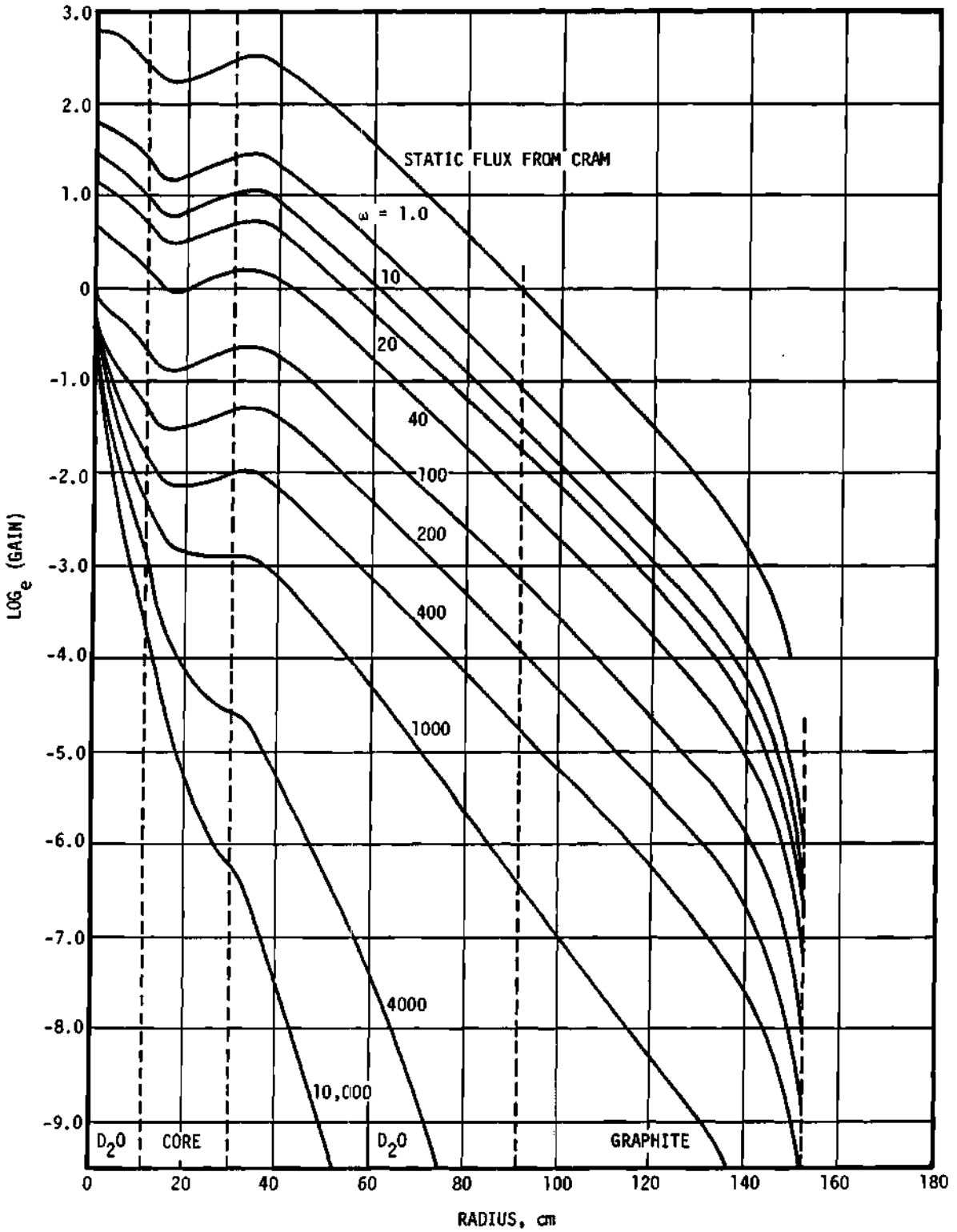

Figure 12. Thermal Flux Amplitude versus Radius for a GTRR Pile Oscillator Experiment

proportional to the fundamental mode flux. At high frequencies, the rapidly decreasing slope of the curves demonstrates how the disturbances are attenuated and shifted in phase rapidly as they propagate through the reactor.

The gain and phase curves for $\omega = 4000$ and 10,000 radians/sec are redrawn to a different scale in Figures 13 and 14. The changes in slope of both curves may be caused by the waves being reflected at the interface between regions and at the boundary of the system or because the wavelength of the disturbance is not long compared to the mesh spacing. Further calculations are needed to determine the nature of the effect. If it is a reflection phenomenon, then transport theory is needed to study the effect in any detail, but it would be satisfying if diffusion theory indicates that such effects are present.

Wave Propagation

The original work on neutron wave experiments was done by Raievski and Horowitz (19). The main idea behind the experiment is to place a modulated source of neutrons in a moderating and diffusing medium. The oscillating source produces waves which propagate through the medium. As they travel they are attenuated and shifted in phase. A measurement of the complex relaxation length will allow determination of the transport mean free path and absorption cross section of the medium. More recently Moore (15) introduced the concept of the dispersion law which relates the amplitude damping and the phase shift of the wave to the frequency.

The Dispersion Law

The dispersion law may be obtained easily for the case of the one-group diffusion equation for an oscillating plane source in an infinite

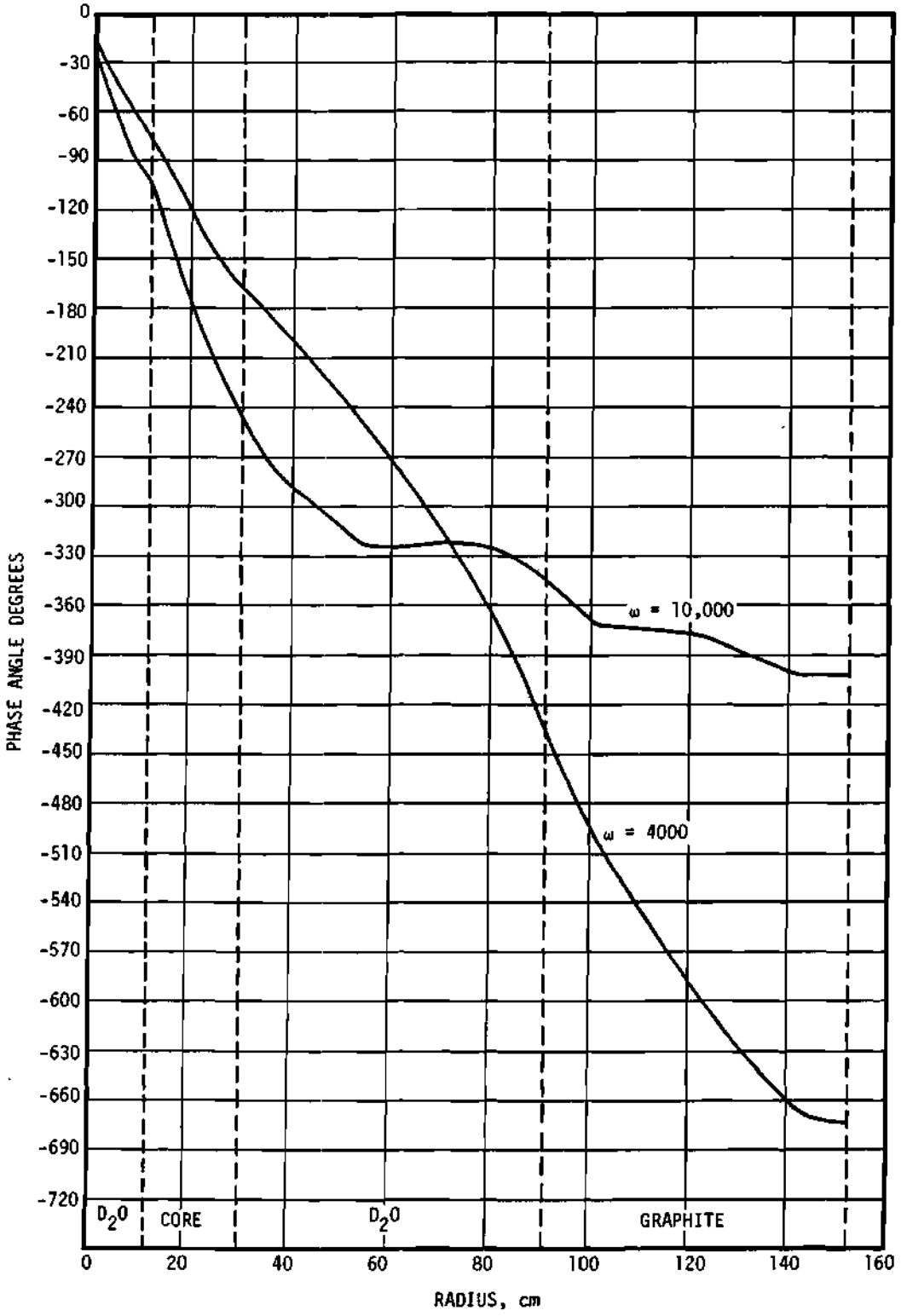

Figure 13. Thermal Flux Phase Angle versus Radius for a GTRR Pile Oscillator Experiment

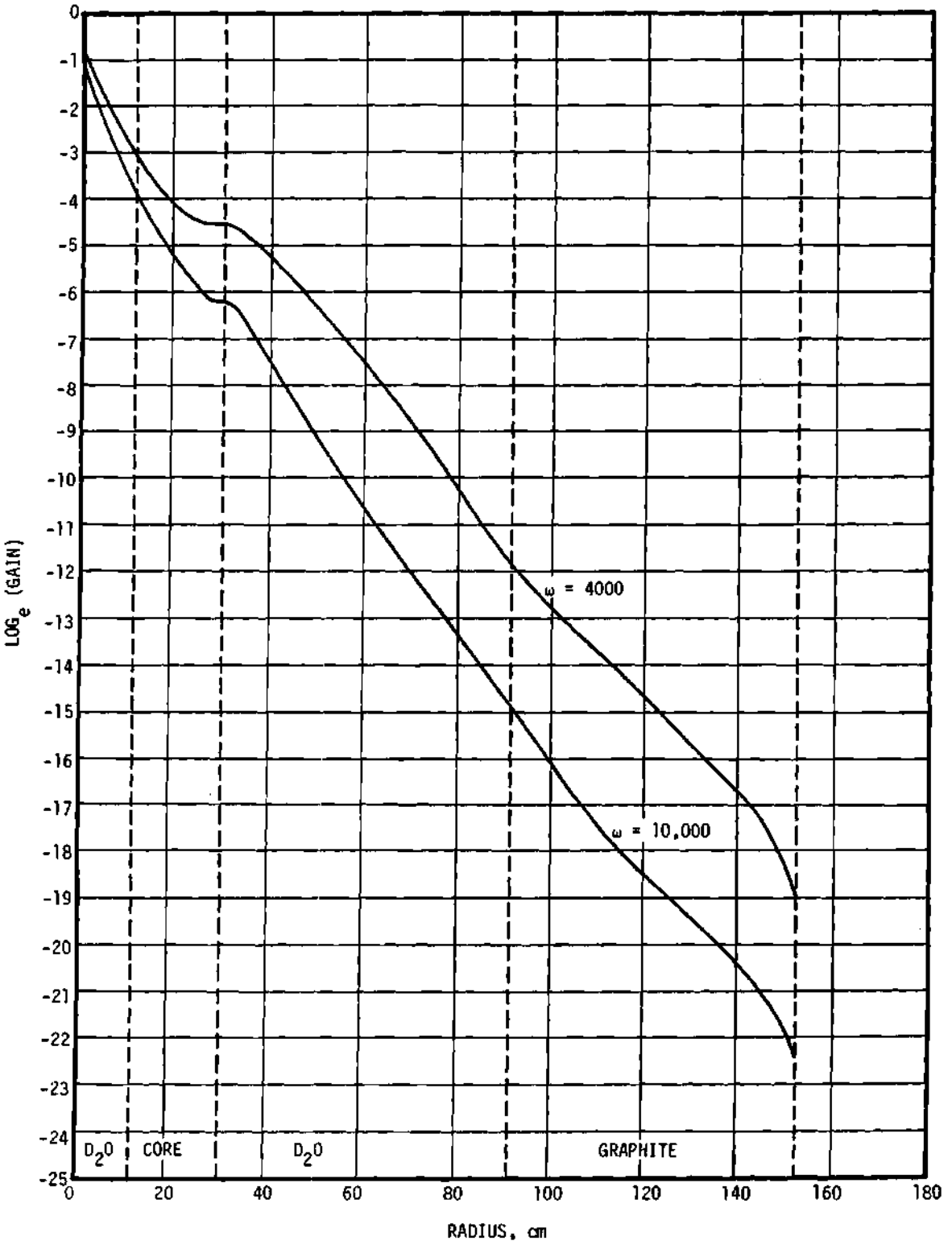

Figure 14. Thermal Flux Amplitude versus Radius for a GTRR Pile Oscillator Experiment

medium.

$$D \frac{\partial^2}{\partial x^2} \phi(x,t) - \Sigma_a \phi(x,t) = \frac{1}{v} \frac{\partial}{\partial t} \phi(x,t) \qquad (1)$$

This equation has a solution in the form

$$\phi(x,t) = e^{-kx + i\omega t} \qquad (2)$$

where k is the inverse complex relaxation length. Substituting 2 into 1 gives

$$k^2 = \left[\frac{1}{D} \Sigma_a + \frac{i\omega}{v}\right] .$$

Separating k into its real and imaginary parts, $k = \mathcal{L} + i\zeta$, yields

$$\zeta = \frac{\omega}{2Dv\mathcal{L}} \qquad (3)$$

$$\mathcal{L}^2 = \frac{1}{2}\left[\frac{\Sigma_a}{D} + \sqrt{\left(\frac{\Sigma_a}{D}\right)^2 + \left(\frac{\omega}{Dv}\right)^2} \right] \qquad (4)$$

The relation between $\mathcal{L}$ and ζ for any ω is the dispersion law for the medium. Note that it is independent of the geometry of the system and that for $\omega = 0$, $\mathcal{L} = \frac{1}{L}$, and $\zeta = 0$.

As the wave propagates through the medium, its spatial distribution is

$$\phi(x) = e^{-(\mathcal{L} + i\zeta)x} . \qquad (5)$$

The amplitude and phase of the disturbance are

$$\text{GAIN} = e^{-\mathcal{L}x} \tag{6}$$

and

$$\text{PHASE} = -\zeta x \ . \tag{7}$$

Thus a measurement of the gain and phase shift of a wave are measurements of $\mathcal{L}$ and ζ or the dispersion law of the medium.

The telegrapher's equation yields

$$\zeta = \frac{\omega(1 + 3D\Sigma_a)}{2Dv\mathcal{L}} \tag{8}$$

and

$$\mathcal{L}^2 = \frac{1}{2}\left[\left(\frac{\Sigma_a}{D} - \frac{3\omega^2}{v^2} \right) + \sqrt{\left(\frac{\Sigma_a}{D} - \frac{3D^2}{v^2} \right)^2 + \left[\frac{\omega(1 + 3D\Sigma_a)}{Dv} \right]^2} \right] . \tag{9}$$

The complex source model solves Equations 21 and 22 of Chapter II for the complex amplitude of the flux $\underline{\phi}(x)$. This quantity is identical (for plane geometry and one energy group) to the spatial flux distribution given by Equation 5. Gain and phase are given by Equations 6 and 7. For cylindrical geometry which was programmed in CHARLIE, the complex amplitude is

$$\underline{\phi}(r) = K_o(\mathcal{L}r)\ e^{-i\zeta r} \ . \tag{10}$$

Calculations for Graphite and Heavy Water

A simple test was desired to demonstrate the use of the complex source model in computing the dispersion law. One-group calculations were done for graphite using diffusion theory and also for D_2O using both diffusion and P-1 theory. The geometry chosen was a right circular cylinder with height of 500 cm. The mesh spacing, and hence the diameter (since the program is limited to 25 increments), was allowed to vary for each frequency. For low frequencies, the mesh was 10 cm with diameter of 500 cm and, for high frequencies, the mesh was 1.0 cm with diameter of 50 cm. In each case the source was placed in the central mesh region. The calculated gain and phase are plotted in Figures 15 and 16. The $\mathcal{L}$ and ζ were obtained by fitting a K_o Bessel function to the gain curve and a straight line to the phase curves. The curvature at the end is due to the effect of the boundary. As shown in Figure 17, the numerical calculations were found to reproduce the dispersion law given by Equations 3 and 4 exactly.

The effect of the mesh spacing may be seen from the shape of the lower curve. In this calculation, the mesh was held constant at 10 cm for all frequencies. As ω is increased, the wavelength λ and diffusion length L given by

$$\lambda = 2\pi/\zeta$$

$$L = 1/\mathcal{L}$$

become the same order of magnitude as the mesh spacing and the curve

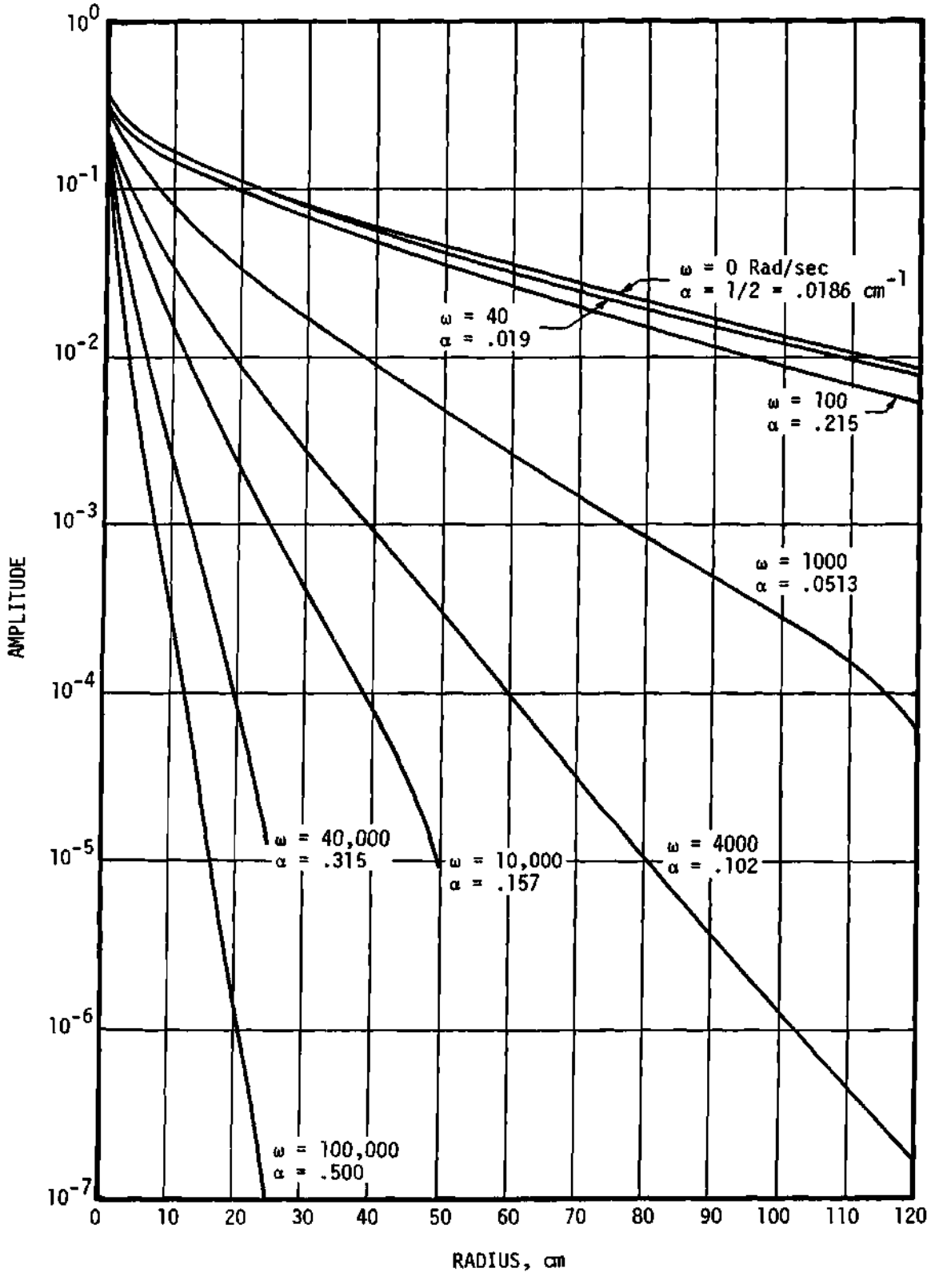

Figure 15. Calculated Amplitude for a Neutron Wave Experiment in AGOT Graphite

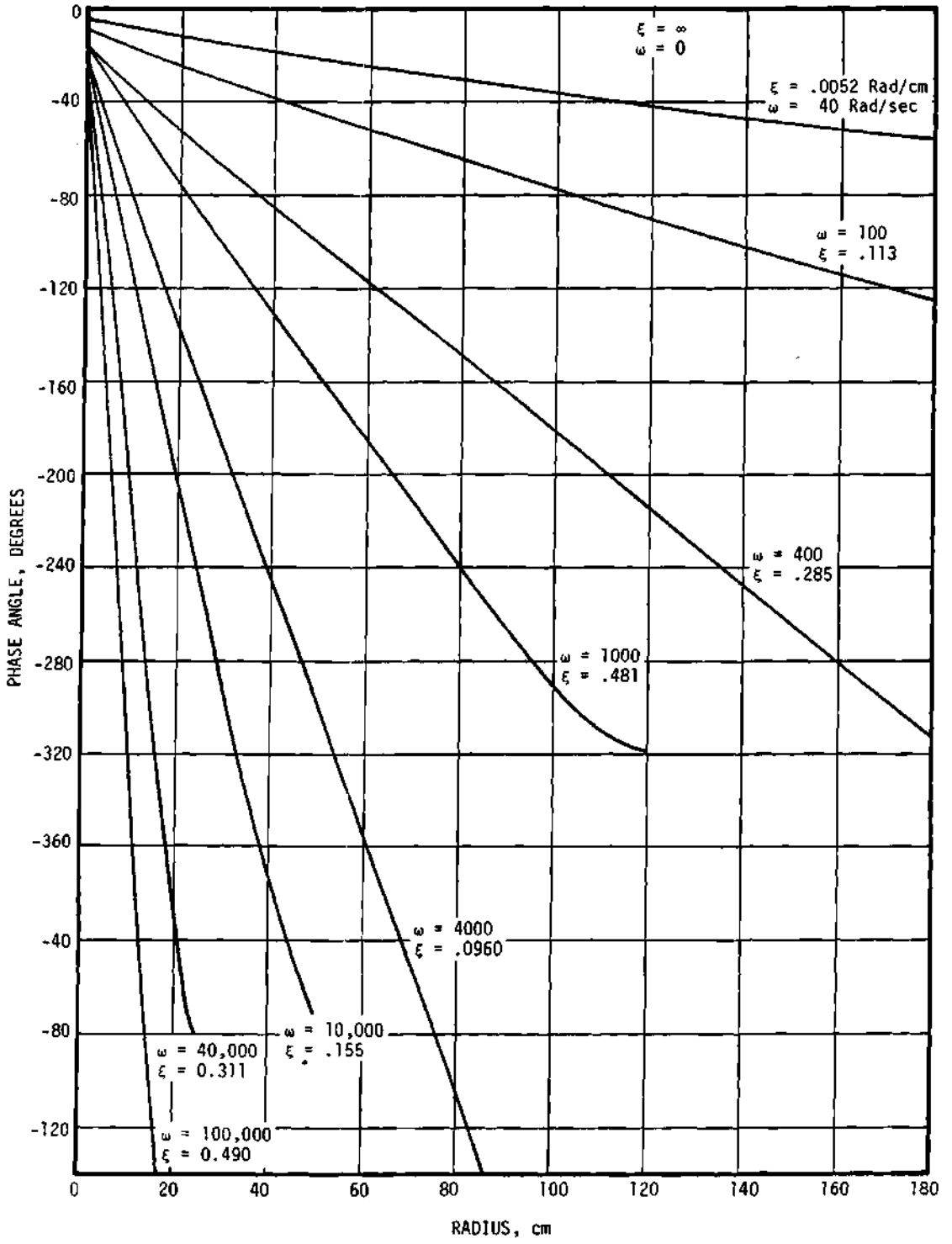

Figure 16. Calculated Phase Angle for a Neutron Wave Experiment in AGOT Graphite

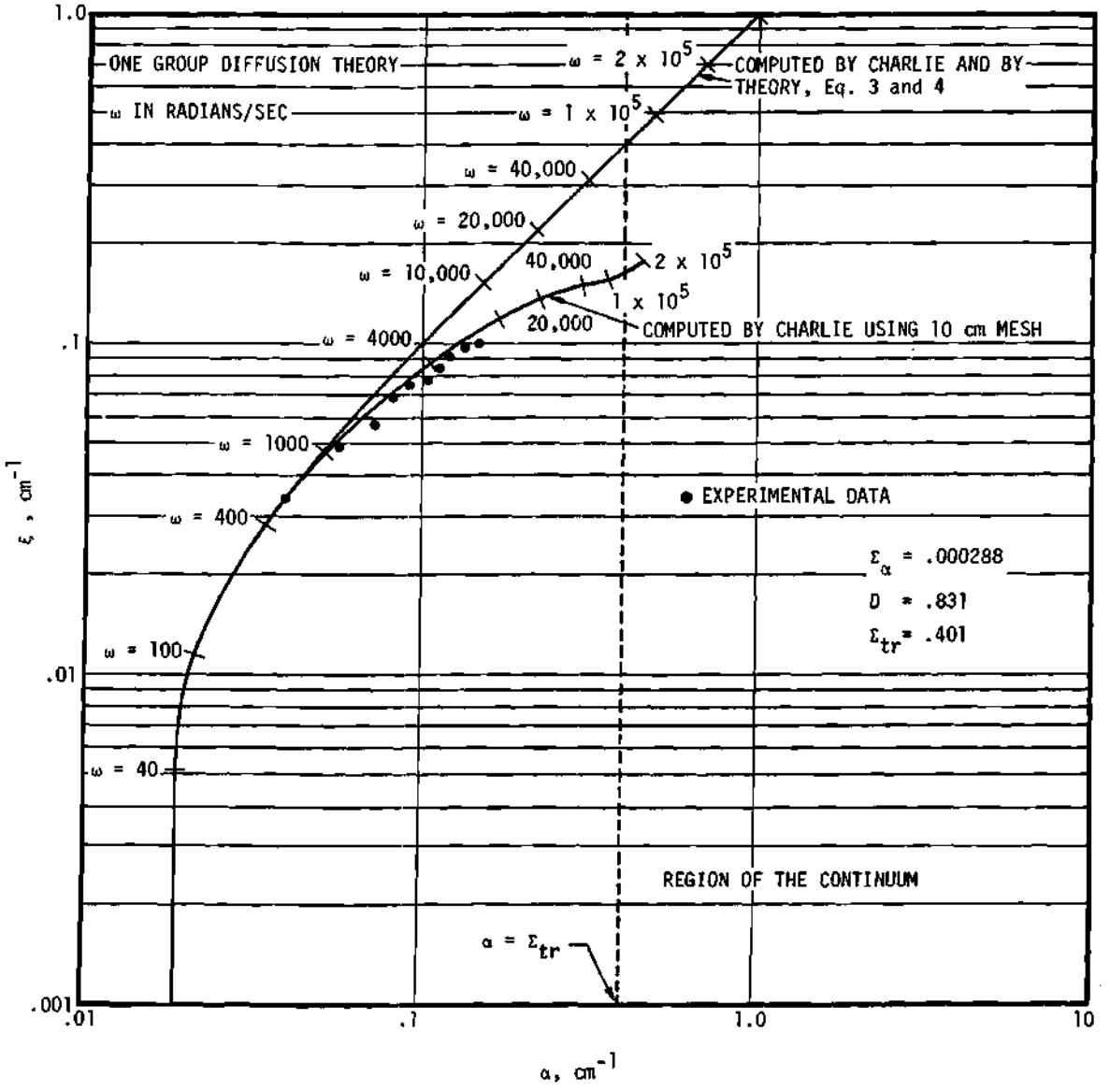

Figure 17. Dispersion Law for AGOT Graphite

falls below the theoretical calculation. The seeming agreement with the experimental points taken from Travelli (45) is accidental. Wavelength, diffusion length, and complex relaxation length are plotted as a function of frequency in Figure 18.

The calculation for heavy water (Figure 19) is intended merely to indicate the differences between the telegrapher's equation and diffusion theory. The numerical calculations are in complete agreement with Equations 3 and 4 or 8 and 9.

Note that once an experimental measurement of the dispersion law has been made for any medium, it is then possible to define a frequency dependent diffusion coefficient such that the diffusion calculation will fit the experimental results. This is nothing more than a fitting technique to measure the frequency dependent diffusion coefficient proposed by Brehm (41).

Noise Analysis

When the current output of an ionization chamber in a reactor operation at a steady flux level is examined, it is found to be composed of an average current plus some seemingly random fluctuations. These fluctuations are not random, however, and as was shown by Moore (20), they contain important information about the dynamics of the reactor.

The observed fluctuations, i.e., reactor noise, arise in the following way: production, absorption, and leakage of neutrons in the reactor are all statistical processes that obey the Poisson distribution.

$$P(r = r_1) = \frac{e^{-\lambda} \lambda^{r_1}}{r_1!}, \text{ for } r_1 = 0, 1, 2, \ldots \qquad (11)$$

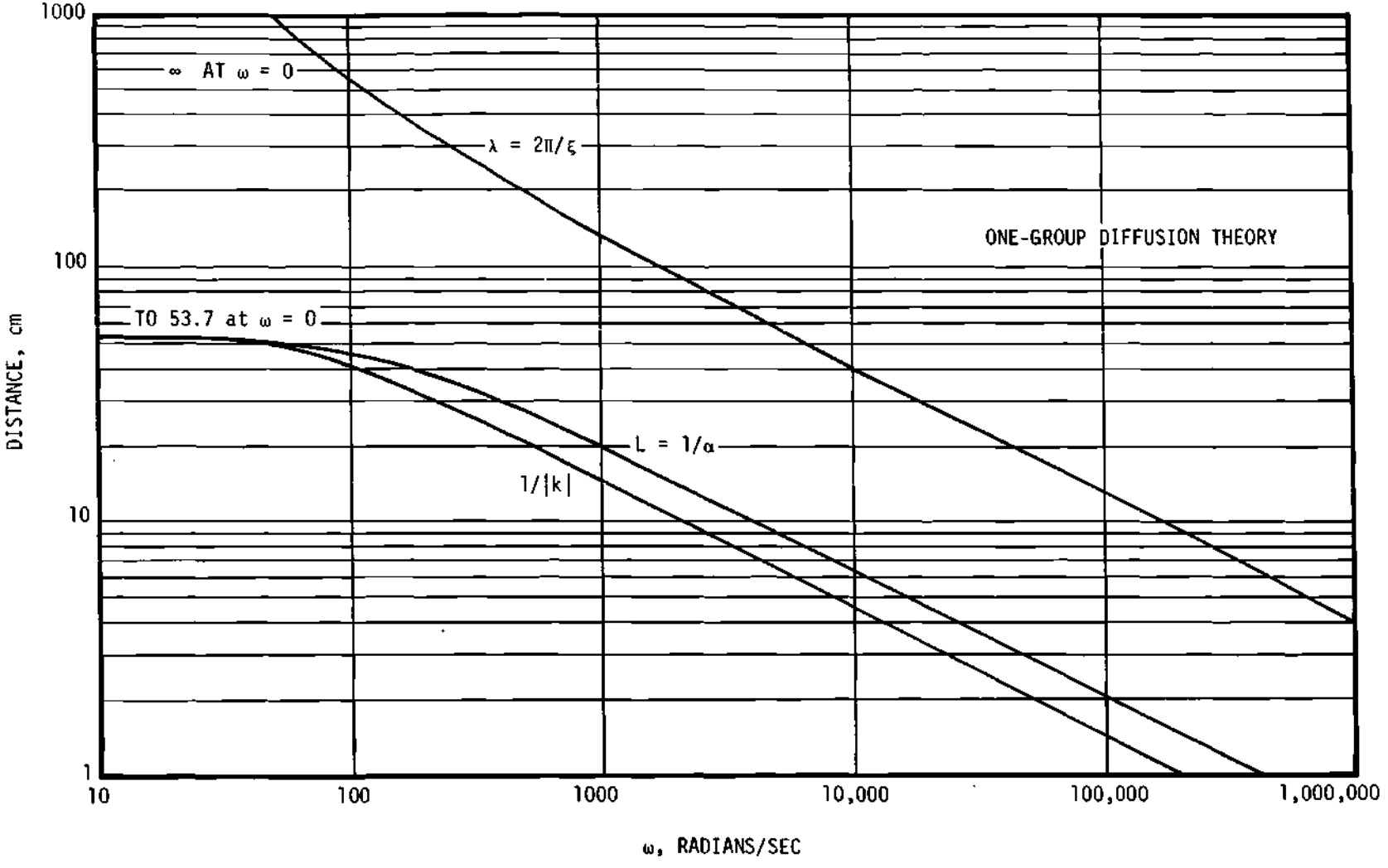

Figure 18. Wavelength, Diffusion Length, and Complex Relaxation Length for AGOT Graphite

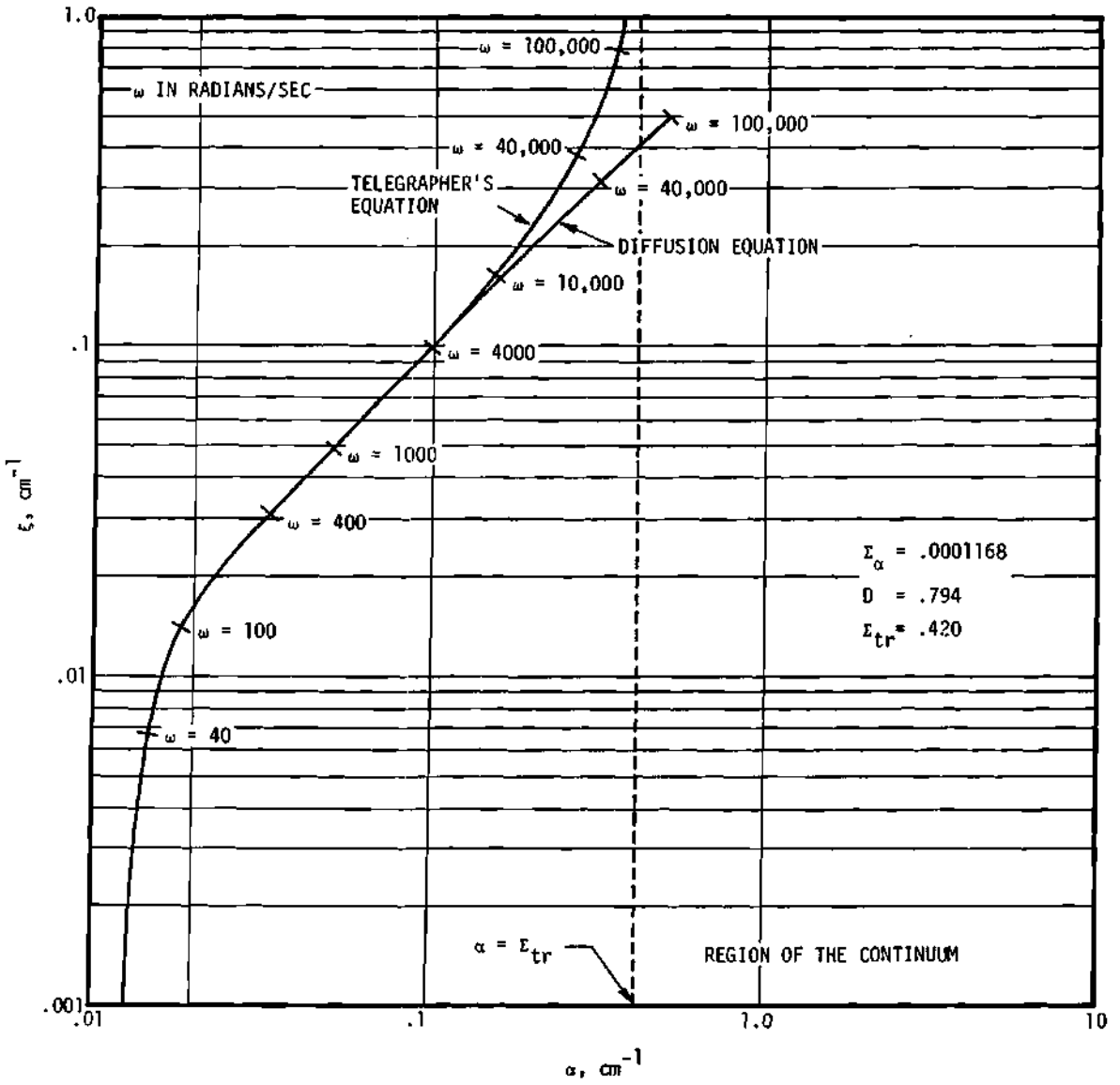

Figure 19. Dispersion Law for Heavy Water

where r = number of events occurring in n trials

$\lambda = np$

p = probability that an event will occur; holds when $p < 0.1$.

These statistical fluctuations can be thought of as a time varying source of neutrons in the reactor.

Cohn (22) pointed out that an analogy could be drawn between the neutron noise and the electron noise in a temperature limited diode. The electron noise is given by the Schottky formula

$$< |I|^2 > = 2e^2\bar{m}$$

where $< |I|^2 >$ = spectral density of the noise current in amps^2

e = electron charge

$\bar{m}$ = average number of electrons flowing per second.

Thus by analogy we can write the spectral density of the reactor noise as:

$$< |S_o|^2 > = 2 \sum_i q_i^2 \bar{m}_i \qquad (12)$$

where q_i = net neutrons produced in occurrence of type i

$\bar{m}_i$ = average number of reactions of type i per second.

Note that the noise spectral density is independent of frequency and thus we say that the noise is "white."

The noise equivalent source for the case of a one energy group, space independent reactor is given by the terms in Table 1. Substituting the terms in Table 1 into Equation 12 yields

Table 1. Contributions to the Noise Equivalent Source for a Space Independent Reactor

Nature of process	Average rate of occurrence	Net number of neutrons produced
1. Non-productive absorption including leakage	$\frac{n}{\ell^*}\frac{A}{A+F}$	- 1
2. Fission giving rise to N prompt neutrons	$\frac{n}{\ell^*}\frac{F}{A+F}P_N$	N - 1

P_N = probability that N neutrons are produced

A = macroscopic absorption cross section including leakage

F = macroscopic fission cross section

$$< |S_o|^2 > = \frac{2n}{\ell^*(A + F)} \left[A + F \sum_{N=1}^{\infty} (N - 1)^2 P_N \right] . \qquad (13)$$

Using the criticality condition

$$\frac{\bar{\nu}F}{A + F} = k_{eff} = 1$$

and that

$$\sum_{N=1}^{\infty} P_N = 1 \quad ; \quad \sum_{N=1}^{\infty} NP_N = (1 - \beta)\bar{\nu} \approx \bar{\nu}$$

we obtain

$$< |S_o|^2 > = \frac{2n}{\ell^*} \left[\frac{\bar{\nu}^2 - \bar{\nu}}{\bar{\nu}} \right] . \qquad (14)$$

Here we have defined $\bar{\nu}^2 \equiv \sum_{N=1}^{\infty} N^2 P_N = 4.36$ for U^{235}.

The response of the reactor to this source can be obtained by multiplying the source strength times the reactor transfer function

$$n(\omega) = T(\omega)\ S_o(\omega)$$

or

$$< |n(\omega)|^2 > = |T(\omega)|^2 < |S_o(\omega)|^2 > . \qquad (15)$$

The transfer function for the one group, space independent reactor is known to be

$$T(\omega) = \frac{\ell^*}{j\omega L + B} \qquad (16)$$

where

$$L = \ell^* + \sum_i \frac{\lambda_i \beta_i}{\omega^2 + \lambda_i^2}$$

$$B = \beta - \sum_i \frac{\lambda_i^2 \beta_i}{\omega^2 + \lambda_i^2}$$

Finally the response of a space independent system is given by

$$< |n(\omega)|^2 > = \frac{2n\,\ell^*}{(\omega L)^2 + B^2} \left(\frac{\overline{\nu^2} - \overline{\nu}}{\overline{\nu}} \right) . \qquad (17)$$

To include spatial effects in the calculation of the reactor noise, it is necessary to know both the magnitude and location of the equivalent noise sources and the transfer functions connecting these sources with the response of the reactor. When each of these is known, the overall response, in terms of the power spectrum, cross power spectrum, and transfer function between two detector locations, is simply a matter of combining the individual responses in the proper manner.

First consider the transfer function relating a given source location and energy with the response at each point and energy within the reactor. The complex source method calculates the reactor's response $\underline{\phi}_i(E, \vec{x})$ to a given source, $S_i'(E_n, \vec{x}_j)$ for each frequency of interest.

$$\underline{\phi}_i(E, \vec{x}) = H(E, \vec{x}, E_n, \vec{x}_j)\; S_i'(E_n, \vec{x}_j)\, \Delta V \qquad (18)$$

where $\vec{x}$ = response point

$\vec{x}_j$ = source point

E = response energy

E_n = source energy

$S_i'(E_n, \vec{x}_j)$ = source of type i per unit volume

ΔV = volume of the source region

Thus the transfer function H can be readily calculated by dividing the calculated response by the source magnitude and its volume. Here it is implicitly assumed that the volume is small enough so that the source and transfer function are relatively uniform over the region.

To calculate the magnitude of the noise equivalent source, it is necessary to consider the statistical fluctuation in the reaction rates of each physical process (e.g., absorption, fission, or leakage) which adds or removes neutrons in some region in the reactor. The basic equation for the source power spectral density can be computed from the Schottky formula.

$$|S_i|^2 = 2\, m_i\, q_i^2 \tag{19}$$

where $|S_i|^2$ = noise source in neutrons^2/sec per unit bandwidth

q_i = net number of neutrons produced in the reaction of type i

m_i = rate of reaction i

Here the source spectral density is independent of frequency.

In the two-group diffusion theory model the following reactions can occur:

Fast absorption ($q_{a1} = -1$):

$$|S_{a1}(\vec{x})|^2 = 2\, \phi_1(\vec{x})\, \Sigma_{a1}(\vec{x})\, \Delta V\, (-1)^2 \tag{20}$$

Thermal absorption ($q_{a2} = -1$):

$$|S_{a2}(\vec{x})|^2 = 2\,\phi_2(\vec{x})\,\Sigma_{a2}(\vec{x})\,\Delta V\,(-1)^2 \tag{21}$$

Downscatter out of group 1 ($q_{s_1} = -1$):

$$|S_{s1}(\vec{x})|^2 = 2\,\phi_1(\vec{x})\,\Sigma_{1\to 2}(\vec{x})\,\Delta V\,(-1)^2 \tag{22}$$

Downscatter into group 2 ($q_{s_2} = +1$):

$$|S_{s2}(\vec{x})|^2 = 2\,\phi_1(\vec{x})\,\Sigma_{1\to 2}(\vec{x})\,\Delta V\,(+1)^2 \tag{23}$$

Fission in fast group producing N fast neutrons ($q_{f1,1} = N - 1$):

$$|S_{f1,1}(\vec{x})|^2 = 2\,\phi_1(\vec{x})\,\Sigma_{f1}(\vec{x})\,\Delta V \sum_{N=1}^{\infty} P_N(N-1)^2 \tag{24}$$

where P_N = probability of producing N neutrons

$$\sum_{N=1}^{\infty} P_N = 1$$

$$\sum_{N=1}^{\infty} NP_N = (1-\beta)\,\bar{\nu} \approx \bar{\nu}$$

$$\sum_{N=1}^{\infty} N^2 P_N = \bar{\nu}^2$$

Fission in thermal group producing N neutrons in the fast group ($q_{f_{1,2}} = N$):

$$|S_{f_{1,2}}(\vec{x})|^2 = 2\,\phi_2(\vec{x})\,\Sigma_{f_2}(\vec{x})\,\Delta V \sum_{N=1}^{\infty} P_N(N)^2 \qquad (25)$$

Fission in thermal group removing a neutron ($q_{f_2} = -1$):

$$|S_{f_2}(\vec{x})|^2 = 2\,\phi_2(\vec{x})\,\Sigma_{f_2}(\vec{x})\,\Delta V\,(-1)^2 \qquad (26)$$

Partial current crossing a boundary from k to j moving to the right (J^+) ($q = \pm 1$):

$$|S_{kj}(\vec{x})|^2 = 2\left(\frac{\phi(\vec{x})}{4} - \frac{D_k}{2}\,\frac{\partial\phi(\vec{x})}{\partial x}\right)\Delta A\,(\pm 1)^2 \qquad (27)$$

where D = diffusion coefficient

Partial current crossing a boundary from j to k moving to the left (J^-) ($q = \pm 1$):

$$|S_{jk}(\vec{x})|^2 = 2\left(\frac{\phi(\vec{x})}{4} + \frac{D_j}{2}\,\frac{\partial\phi(\vec{x})}{\partial x}\right)\Delta A\,(\pm 1)^2 \qquad (28)$$

Equations 20 and 21 apply to both fast and thermal groups.

Not all of the above processes are independent. For example, the scattering of a neutron from fast to thermal means that there is a loss of one neutron in the fast group and simultaneous gain of one neutron in the thermal group. Figure 20 shows the relationship between these equations. When the processes are connected, as indicated by arrows crossing

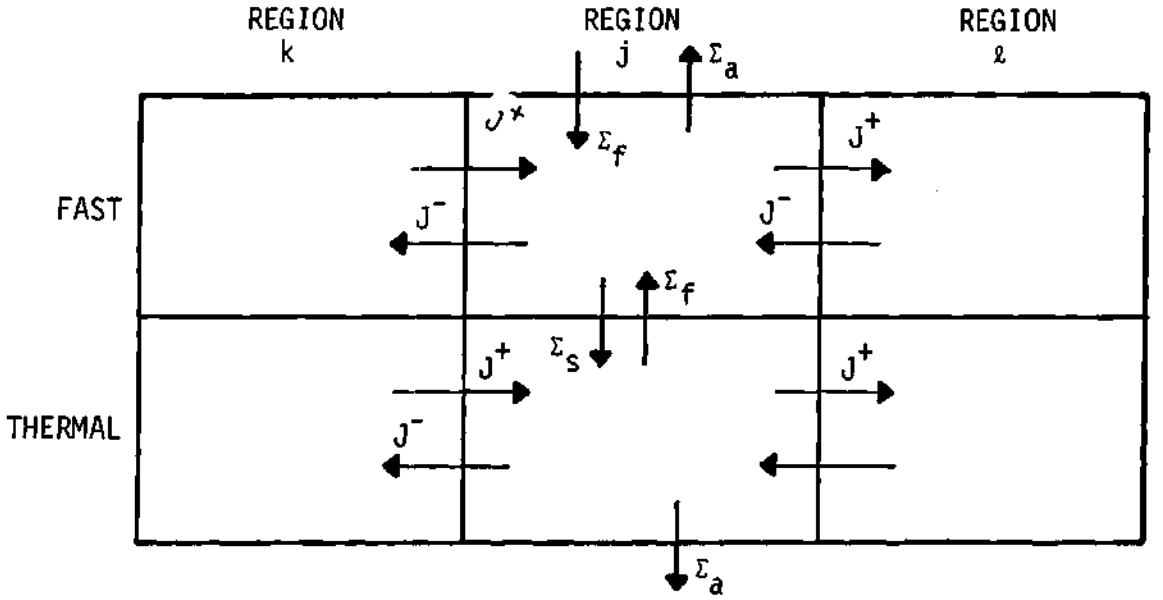

Figure 20. Source Mechanisms for a Typical Reactor Region

boundaries between blocks, the sources are in phase and the response of the reactor to each of the sources adds linearly.

Thus with the aid of Figure 20, we can write a set of equations (one for each arrow in the diagram) which represents the response of the reactor to each separate physical process occurring in region j.

Fast absorption:

$$\underline{\phi}_{a1}(E,\vec{x}) = H(E,\vec{x},E_1,\vec{x}_j)|S_{a1}(\vec{x}_j)| \tag{29}$$

Thermal absorption:

$$\underline{\phi}_{a2}(E,\vec{x}) = H(E,\vec{x},E_2,\vec{x}_j)|S_{a2}(\vec{x}_j)| \tag{30}$$

Downscatter:

$$\underline{\phi}_{12}(E,\vec{x}) = -H(E,\vec{x},E_1,\vec{x}_j)|S_{s1}(\vec{x}_j)| + H(E,\vec{x},E_2,\vec{x}_j)|S_{s2}(\vec{x}_j)| \tag{31}$$

Fast fissions:

$$\underline{\phi}_{f1}(E,\vec{x}) = H(E,\vec{x},E_1,\vec{x}_j)|S_{f1,1}(\vec{x}_j)| \tag{32}$$

Thermal fissions:

$$\underline{\phi}_{f2}(E,\vec{x}) = H(E,\vec{x},E_1,\vec{x}_j)|S_{f1,2}(\vec{x}_j)| - H(E,\vec{x},E_2,\vec{x}_j)|S_{f2}(\vec{x}_j)| \tag{33}$$

Fast current in from the left (entering j from k):

$$\underline{\phi}_{kj}(E,\vec{x}) = H(E,\vec{x},E_1,\vec{x}_j)|S_{kj}(\vec{x}_j)| - H(E,\vec{x},E_1,\vec{x}_k)|S_{kj}(\vec{x}_j)| \tag{34}$$

Fast current in from the right (entering j from ℓ):

$$\underline{\phi}_{\ell j}(E,\vec{x}) = H(E,\vec{x},E_1,\vec{x}_j)|S_{\ell j}(\vec{x}_j)| - H(E,\vec{x},E_1,\vec{x}_\ell)|S_{\ell j}(\vec{x}_j)| \qquad (35)$$

Fast current out to the left (entering k from j):

$$\underline{\phi}_{jk}(E,\vec{x}) = - H(E,\vec{x},E_1,\vec{x}_j)|S_{jk}(\vec{x}_j)| + H(E,\vec{x},E_1,\vec{x}_k)|S_{jk}(\vec{x}_j)| \qquad (36)$$

Fast current out to the right (entering ℓ from j):

$$\underline{\phi}_{j\ell}(E,\vec{x}) = - H(E,\vec{x},E_1,\vec{x}_j)|S_{j\ell}(\vec{x}_j)| + H(E,\vec{x},E_1,\vec{x}_\ell)|S_{j\ell}(\vec{x}_j)| \qquad (37)$$

Equations similar to 27, 28, 29, and 30 apply for the thermal group. Thus for each source location there are thirteen terms which contribute to the overall response.

To combine the preceding thirteen equations for region j as well as the corresponding equations for other source regions, we note that each of the equations is independent of the others and thus their phase relationship is random. Under these conditions, the power spectrum at point $\vec{x}_a$ and energy E_n is,

$$P(E_n,\vec{x}_a) = \sum_i |\underline{\phi}_i(E_n,\vec{x}_a)|^2 \qquad (38)$$

where the summation is taken over all source regions and neutron processes.

The cross power spectrum between points $\vec{x}_a$ and $\vec{x}_b$ is,

$$P(E_n, \vec{x}_a, E_m, \vec{x}_b) = \sum_i \underline{\phi}_i(E_n, \vec{x}_a)^* \underline{\phi}_i(E_m, \vec{x}_b) \tag{39}$$

and the transfer function is,

$$T(E_n, \vec{x}_a, E_m, \vec{x}_b) = \frac{P(E_n, \vec{x}_a, E_m, \vec{x}_b)}{P(E_n, \vec{x}_a)} . \tag{40}$$

A complete description of the reactor noise would require that the preceding calculations be carried out in three dimensions. In view of the long running times experienced with two dimensional calculations (35), such an attempt would be completely impractical. The alternative is to return to a one dimensional model with relatively large source regions. These approximations assume the large source regions to oscillate in phase with the effect of distorting the frequency response within the source region but leaving the response outside these regions relatively undisturbed.

A computer program has been written (NOISE, Appendix B) which will calculate the noise power spectral density at each mesh point in a reactor as well as the cross power spectral density and transfer function between any two specified locations. The equations programmed are 13 through 33. Calculations using the code are discussed below.

Noise Calculation for the GTRR

To calculate the response of the reactor to a distributed noise source, it is necessary to define the source regions which will be used.

The regions were chosen by referring to the static flux distributions calculated by CRAM (see Figure 21). Since the flux in both fast and thermal groups drops off rapidly past 50 cm, it was decided to limit the number of source regions to four. The regions are defined as follows:

1. Central D_2O out to 11.43 cm
2. First fuel ring from 11.43 to 19.05 cm
3. Second fuel ring from 19.05 to 30.22 cm
4. Reflector from 30.22 to 50.12 cm.

A complete description of the reactor is given in Appendix C. The cross sections used were obtained from some preliminary results of Johnson (35) by assuming a flat flux across the reactor for averaging purposes. The following calculations could be improved by using properly weighted values for the cross sections.

The transfer function from both fast and thermal sources in each of the regions was obtained from CHARLIE by sequentially stepping a uniformly distributed source from region 1 to region 4. The complex amplitude of the flux response was punched into cards for each source energy, location, and frequency. For these calculations, the neutron detectors were not included in the description of the reactor. This was done because it is not possible (in one dimension) to correctly represent a detector located off the centerline. This omission is not precisely accurate because the detection of a neutron breaks the chain related process in which the neutron was participating and thus changes the character of the noise.

Amplitude and phase plots for each source location and energy are shown in Figures 22 through 29. The response points shown (0, 14, and 19) are the centerline, 53.2 cm, and 91.4 cm radius. The thermal flux curves

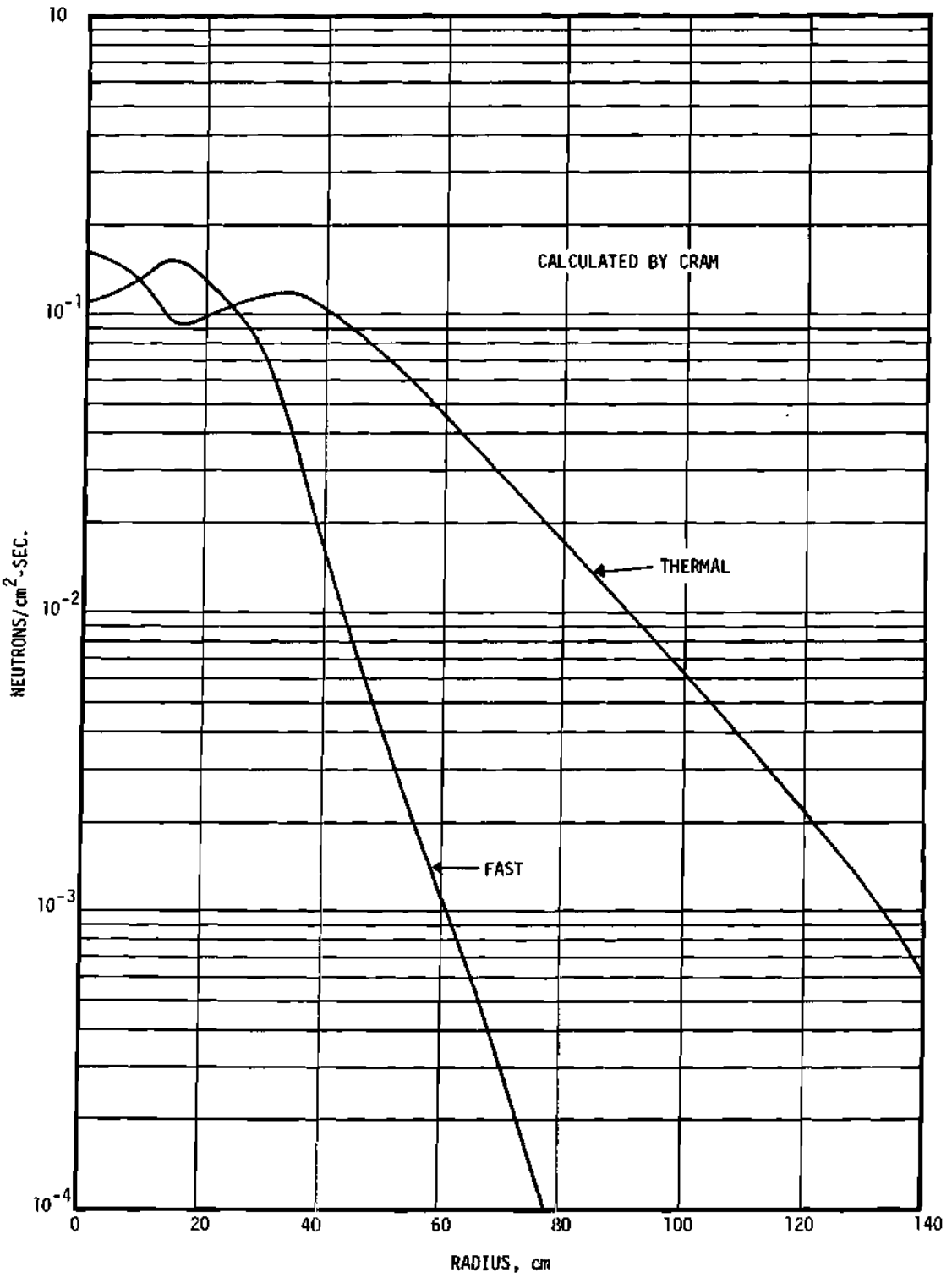

Figure 21. Static Fluxes for the GTRR

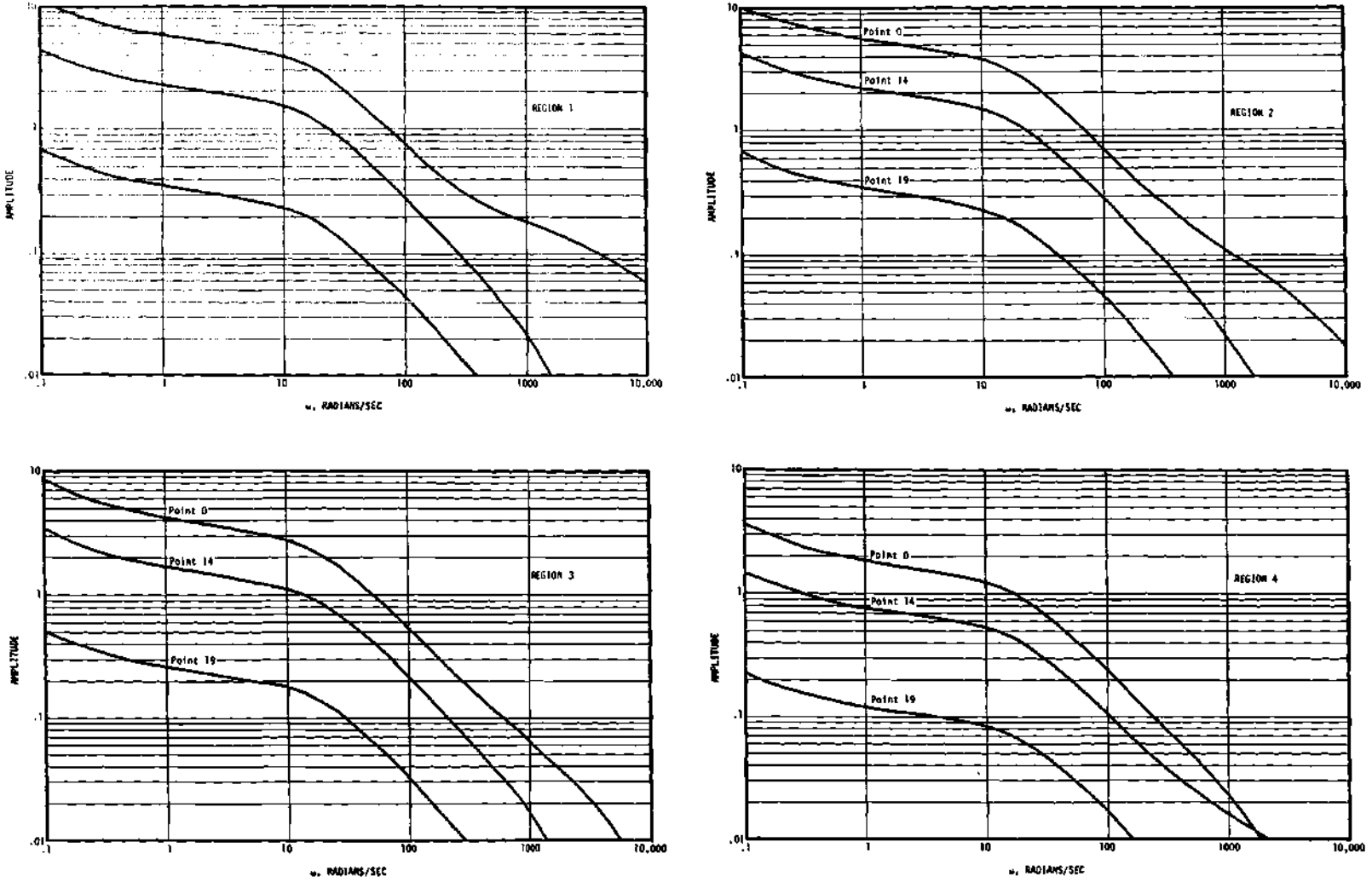

Figure 22. Thermal Flux Amplitude for a Distributed Thermal Source in the GTRR

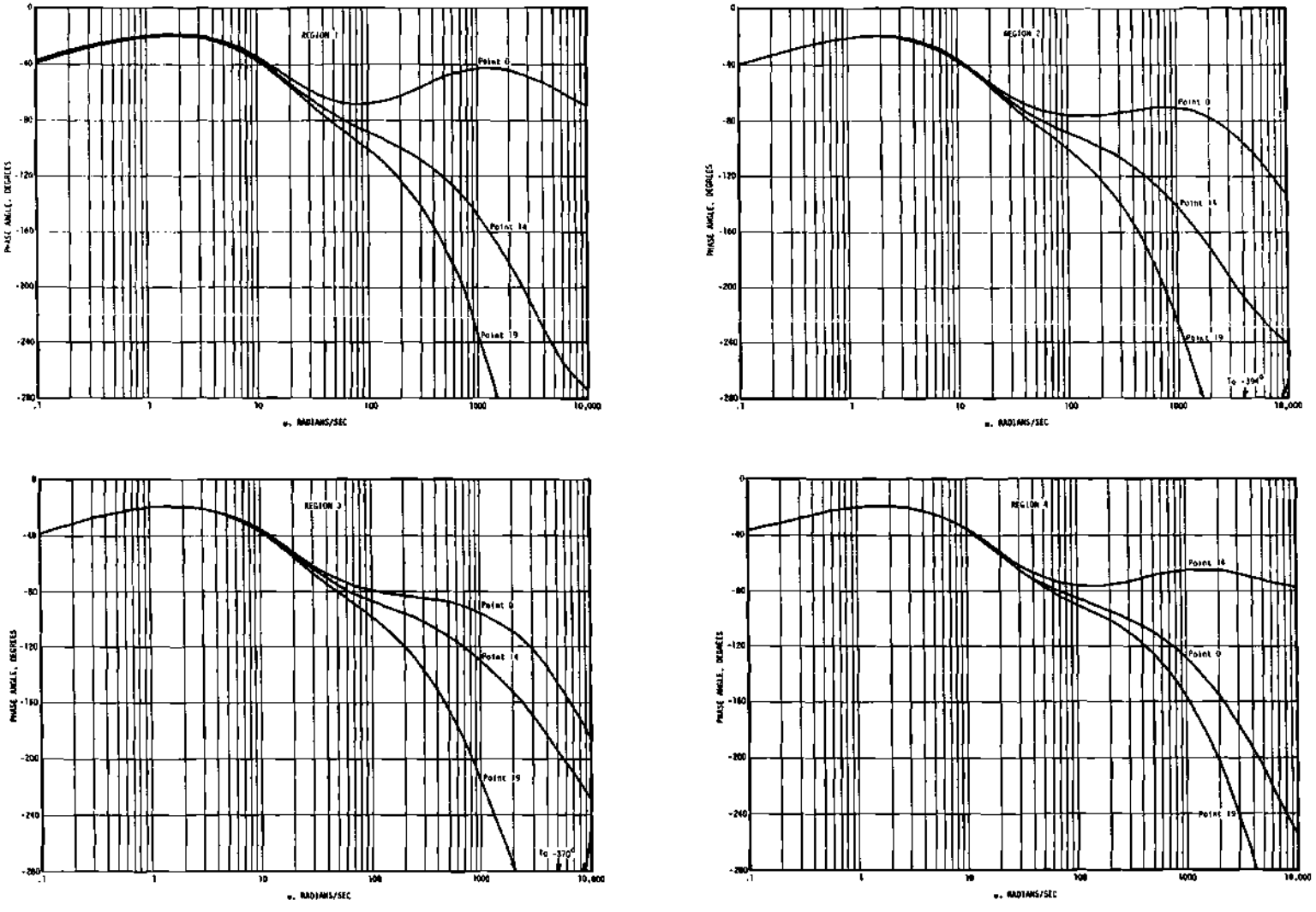

Figure 23. Thermal Flux Phase Angle for a Distributed Thermal Source in the GTRR

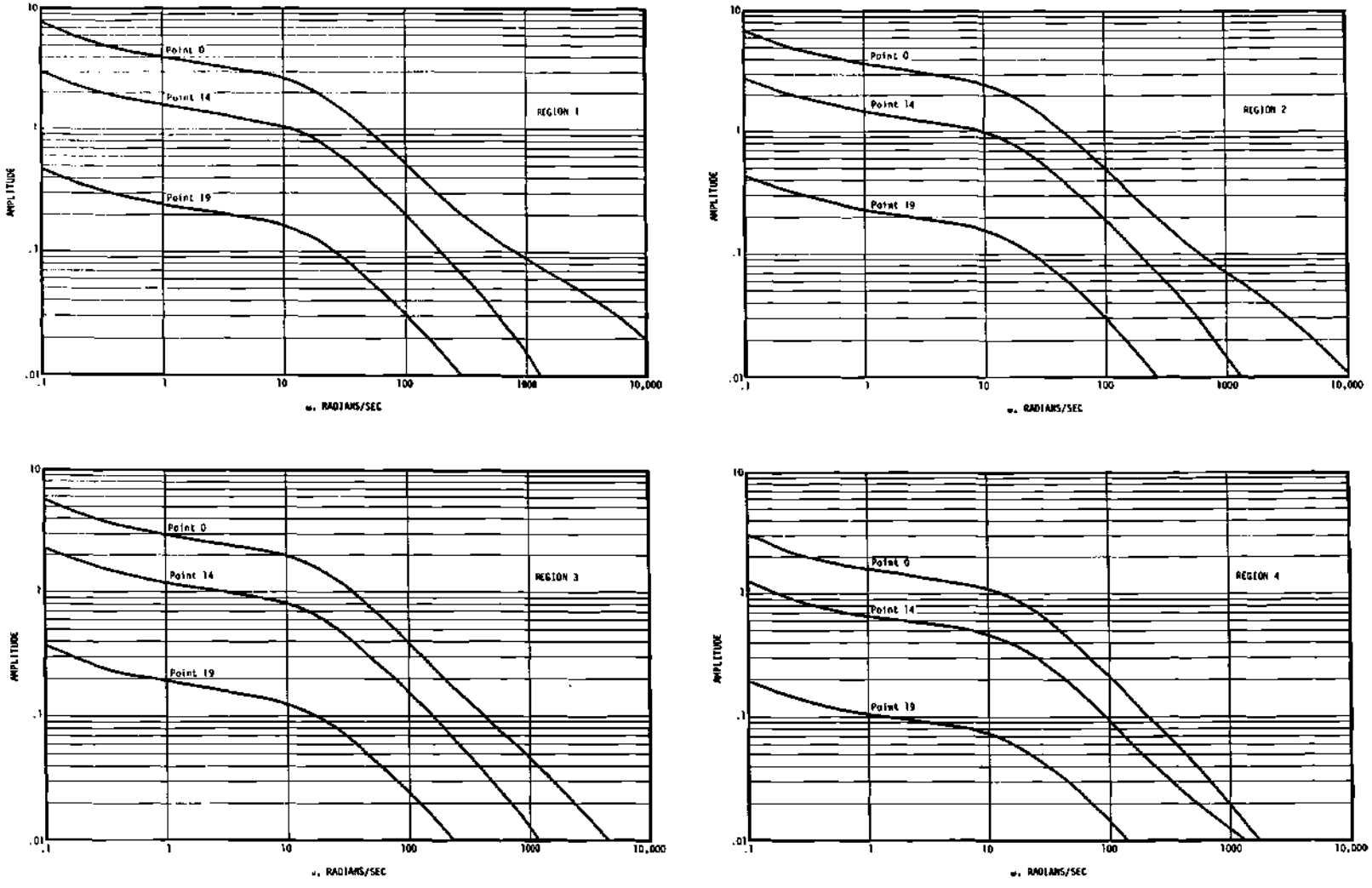

Figure 24. Thermal Flux Amplitude for a Distributed Fast Source in the GTRR

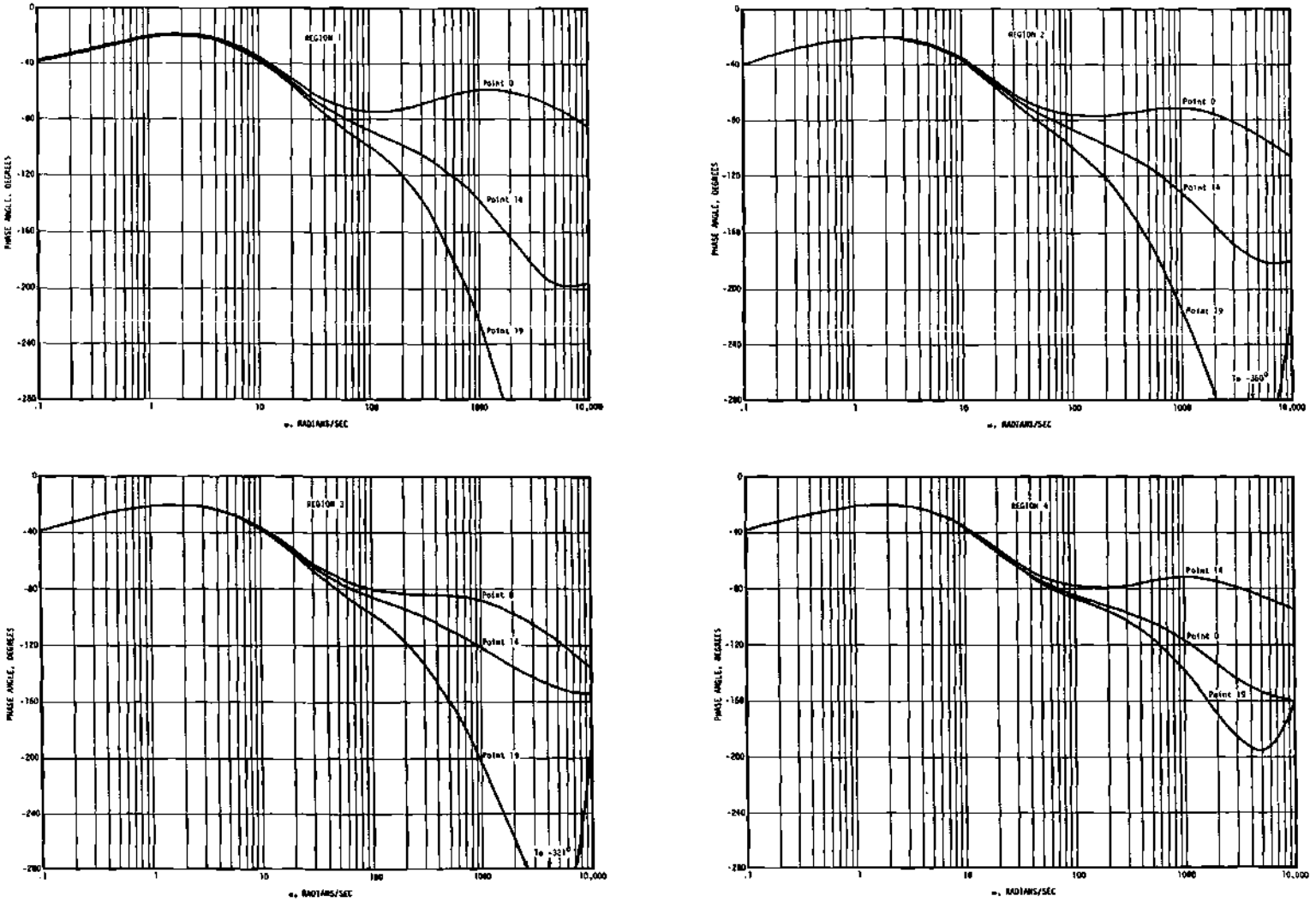

Figure 25. Thermal Flux Phase Angle for a Distributed Fast Source in the GTRR

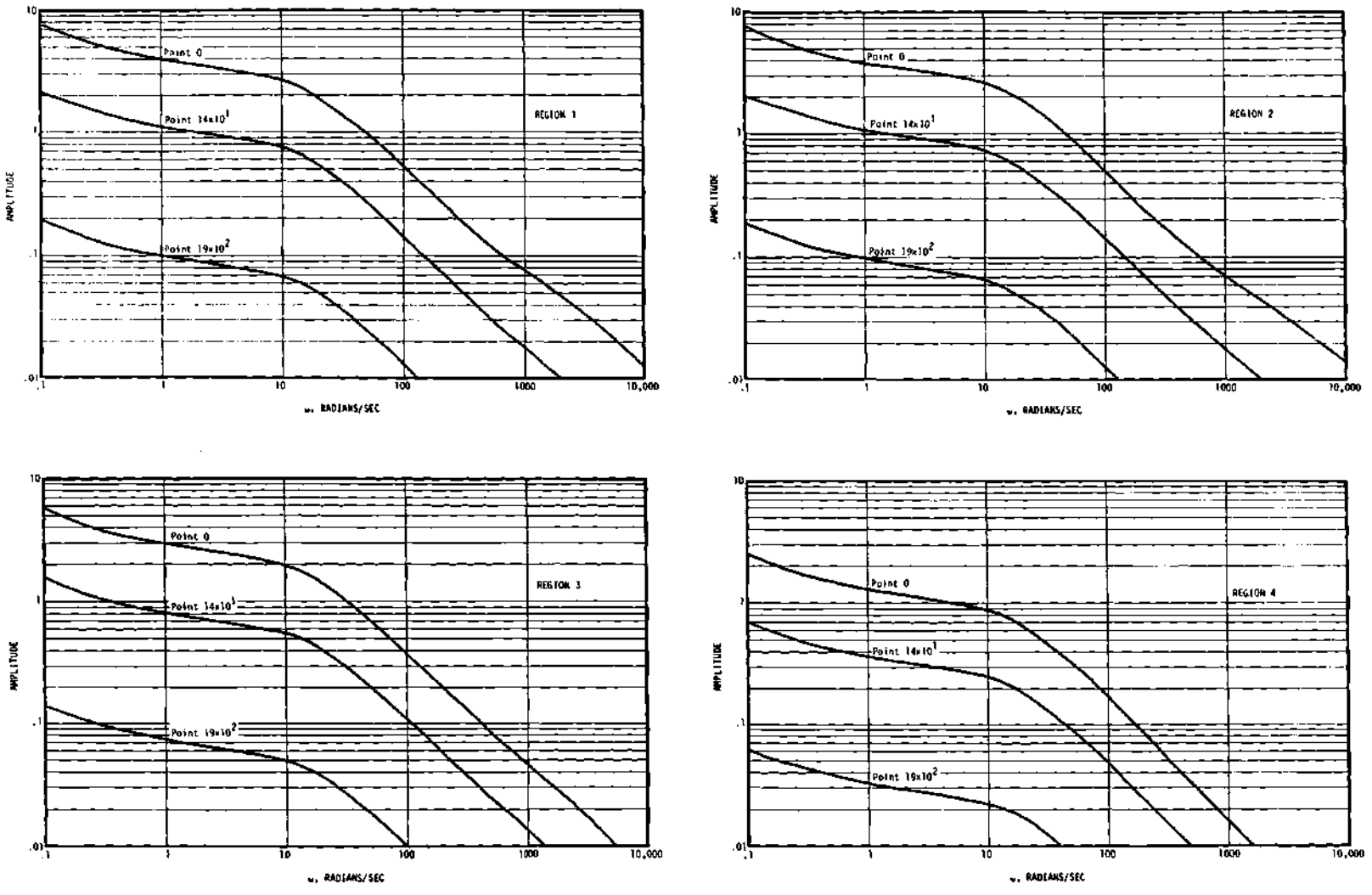

Figure 26. Fast Flux Amplitude for a Distributed Thermal Source in the GTRR

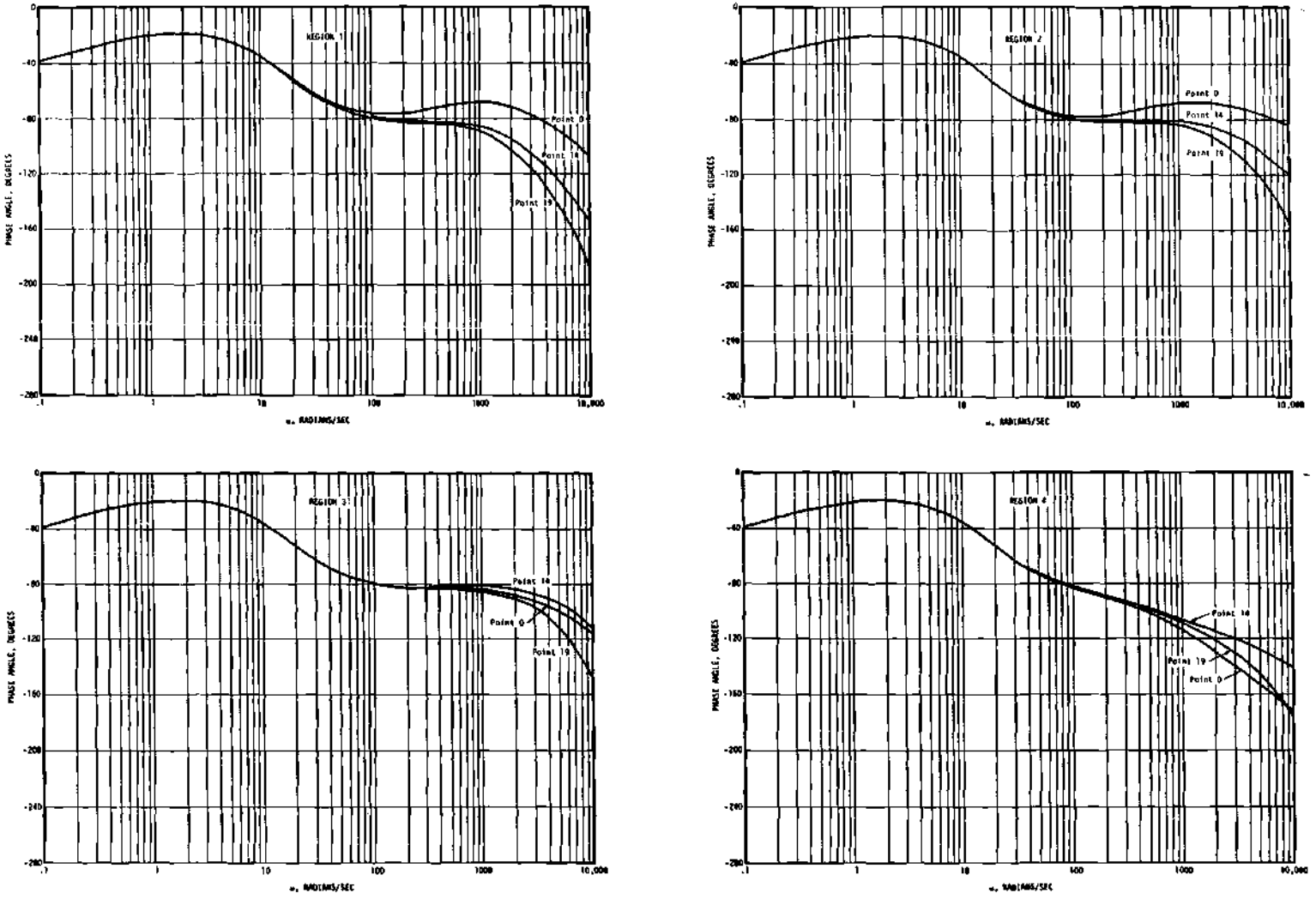

Figure 27. Fast Flux Phase Angle for a Distributed Thermal Source in the GTRR

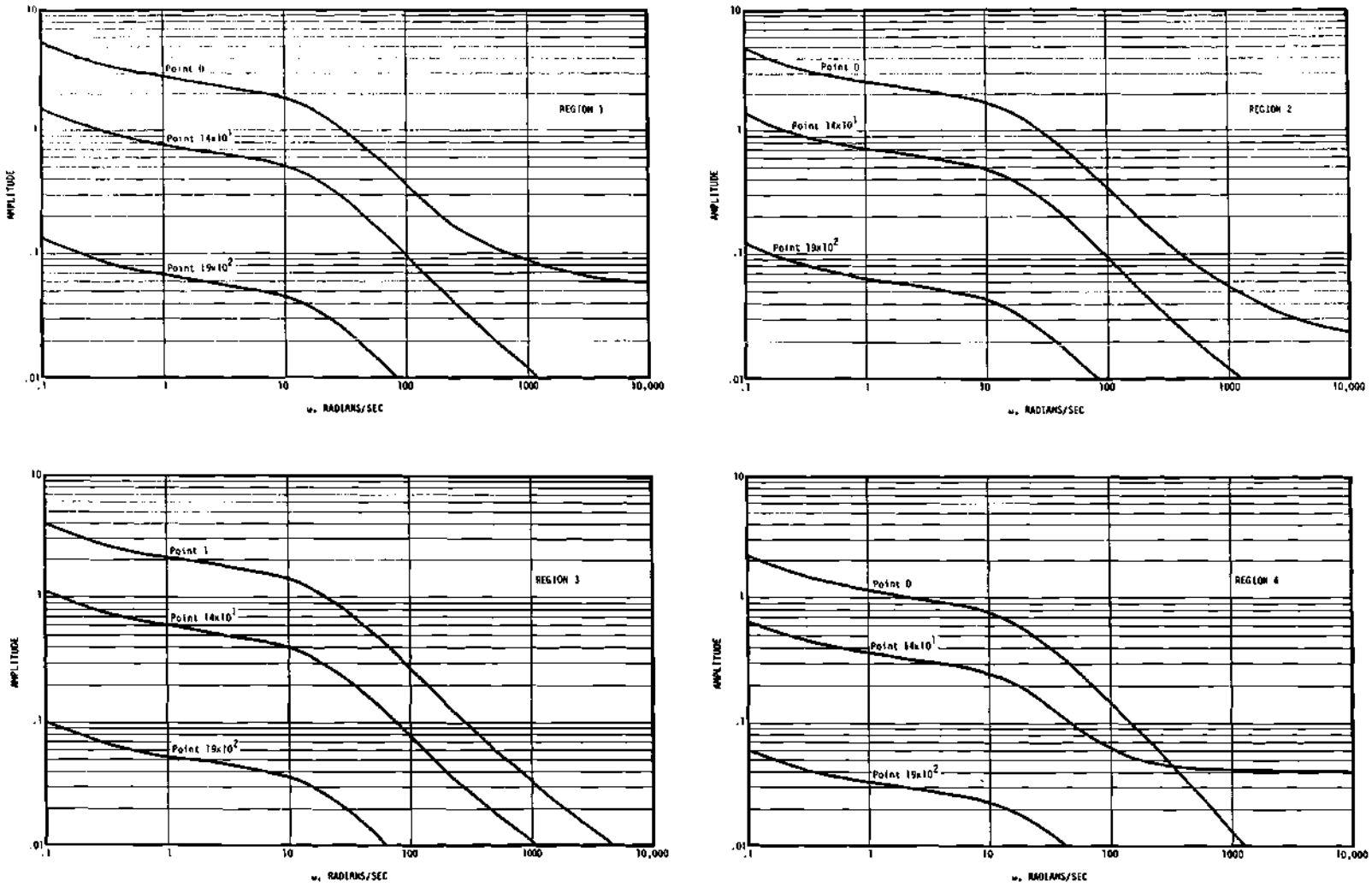

Figure 28. Fast Flux Amplitude for a Distributed Fast Source in the GTRR

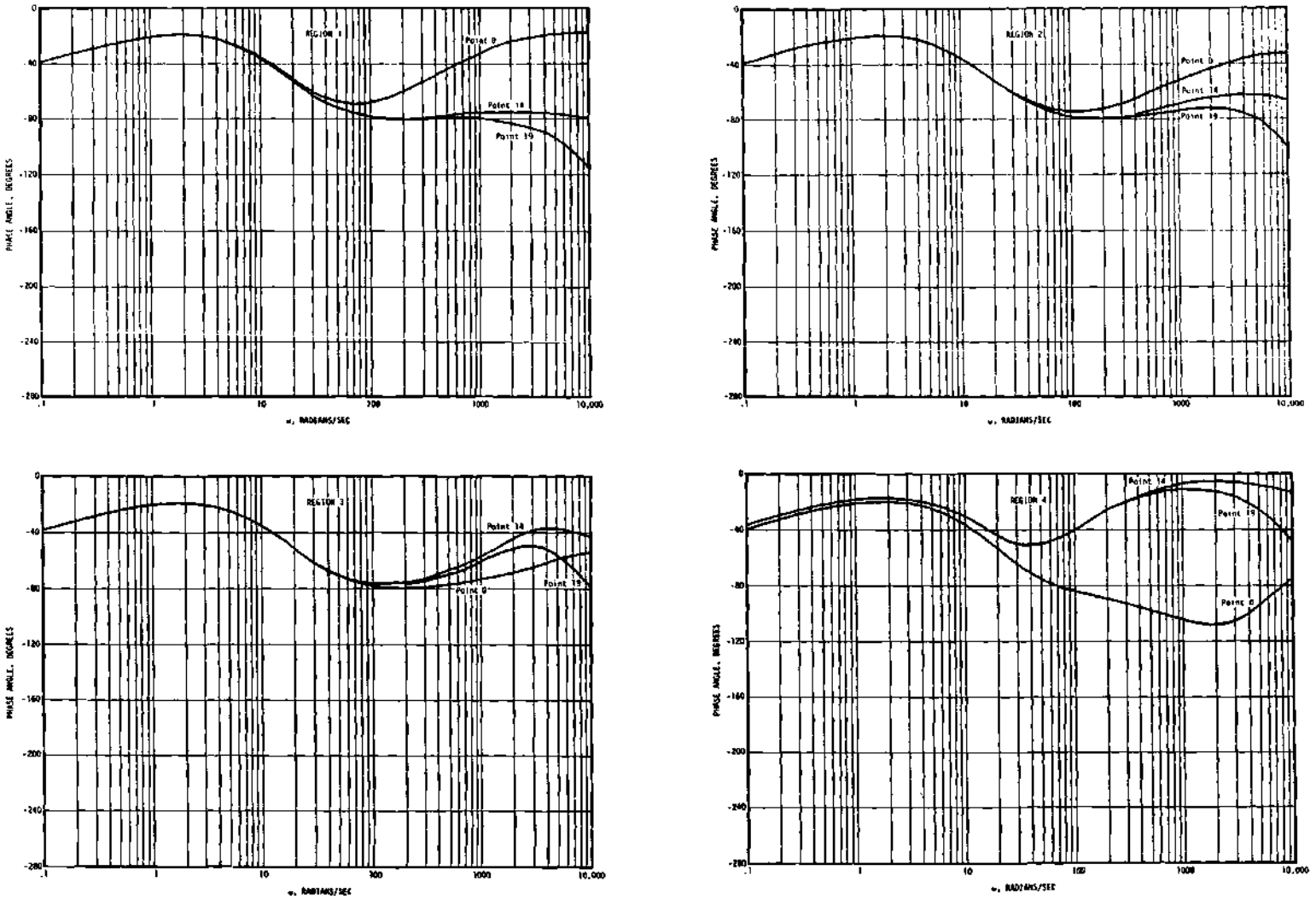

Figure 29. Fast Flux Phase Angle for a Distributed Fast Source in the GTRR

show strong space dependence starting at 20 radians per second for the phase angle and 100 radians per second for the amplitude. The fast flux curves show much less space dependence than the thermal and the phases are not affected below 100 radians per second. At very high frequencies the thermal phase angle for point 19, and to a lesser extent point 14, bends upward, i.e., becomes less negative. This effect may be due to the reflection of the waves from the interface between regions or too large a mesh spacing. At low frequencies, the ratio of the amplitudes of two curves is the ratio of the static flux at the two points in question. Also the ratio of amplitudes at the same point but with the source in different regions is the importance of the source region or the adjoint flux.

The overall effect of the distributed noise source on the reactor and the degree of coupling between two detectors is calculated by NOISE. This program uses as input the complex flux previously calculated, the dimensions of the system, static flux and the gradient of the flux, and the macroscopic cross sections. The amplitudes of the noise equivalent sources are given in Table 2. The calculated power spectral density and transfer functions between two locations are shown for selected points in Figures 30 through 35.

The power spectral density curves show almost no space effect below 100 radians per second. The fact that the amplitude of the transfer function between widely separated points is flat up to 100 radians per second emphasizes this point. A consequence of this is that cross power spectral density techniques may be used to monitor reactor noise when the detection efficiency is so low as to rule out the conventional auto power

Table 2. Noise Equivalent Sources for the GTRR

Source Type	Region			
	1	2	3	4
Fast absorption plus leakage	0.5773	0.8748	1.1011	0.6543
Thermal absorption plus leakage	0.4138	0.9758	1.1099	1.1786
Downscatter out of group 1	1.1149	1.4192	1.9853	1.9056
Downscatter into group 2	1.1149	1.4192	1.9853	1.9056
Fast fission	0.0	0.2875	0.2421	0.0
Thermal fissions as source to 1	0.0	3.4794	3.6245	0.0
Thermal fissions as a sink to 2	0.0	1.6663	1.7358	0.0
Fast partial current moving to the right *	1.8949	3.1020	3.2155	0.9520
Fast partial current moving to the left *	2.3932	2.7818	2.3901	0.7110
Thermal partial current moving to the right *	2.6651	2.3399	3.1972	3.4301
Thermal partial current moving to the left *	1.5132	2.5028	3.3890	3.1218

* Note: These refer to the partial currents at the right hand boundary of each source region.

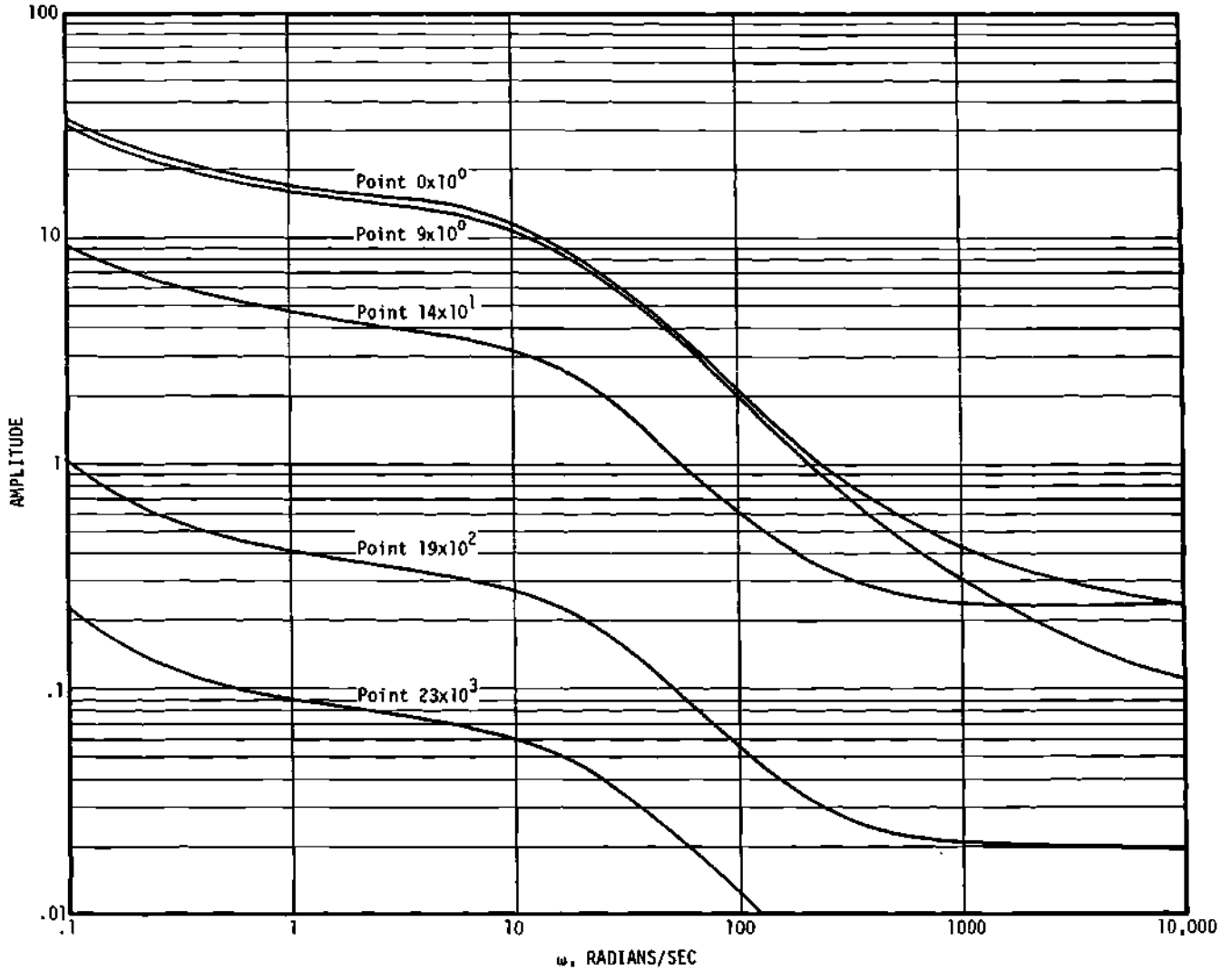

Figure 30. Fast Noise Power Spectral Density for the GTRR

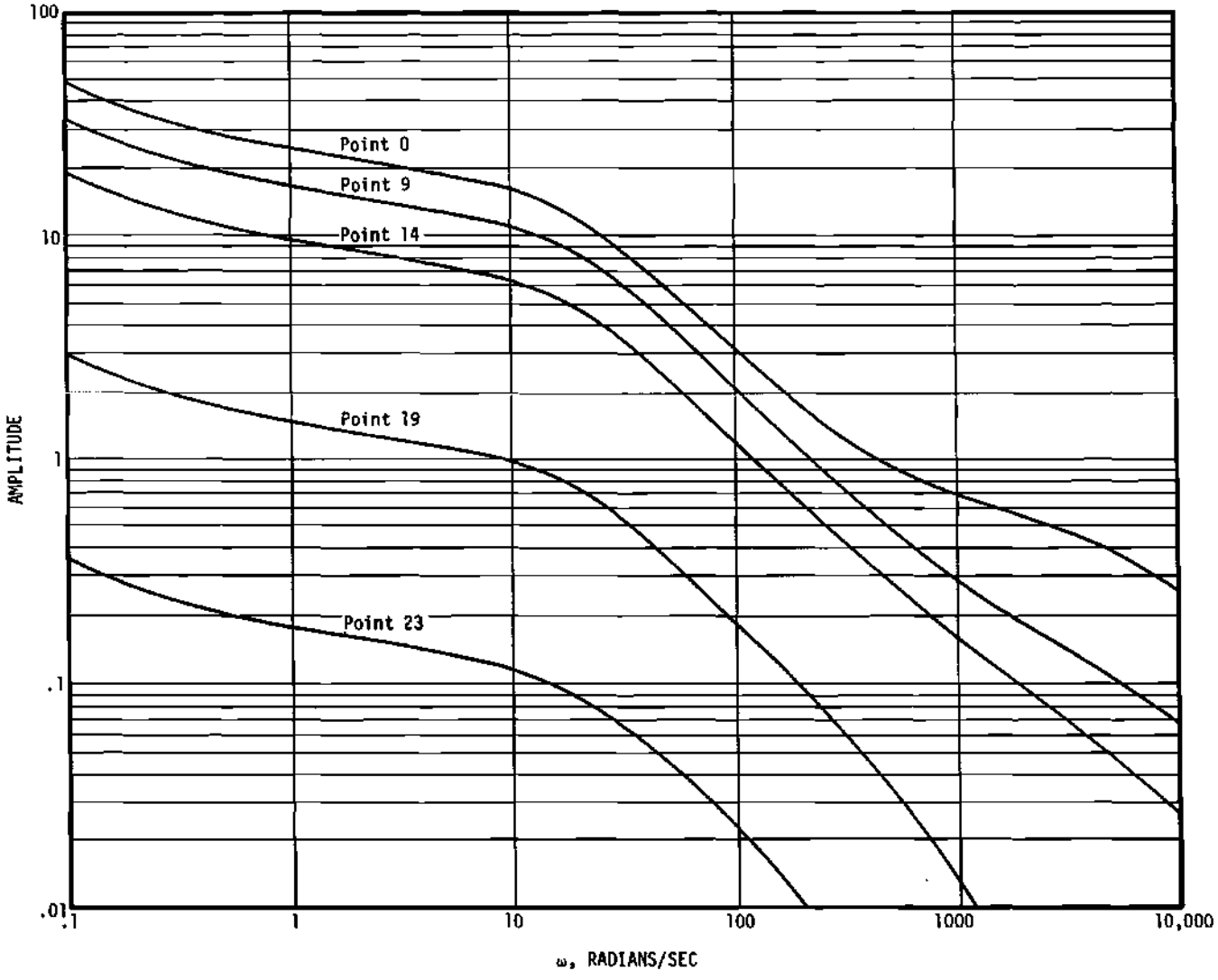

Figure 31. Thermal Noise Power Spectral Density for the GTRR

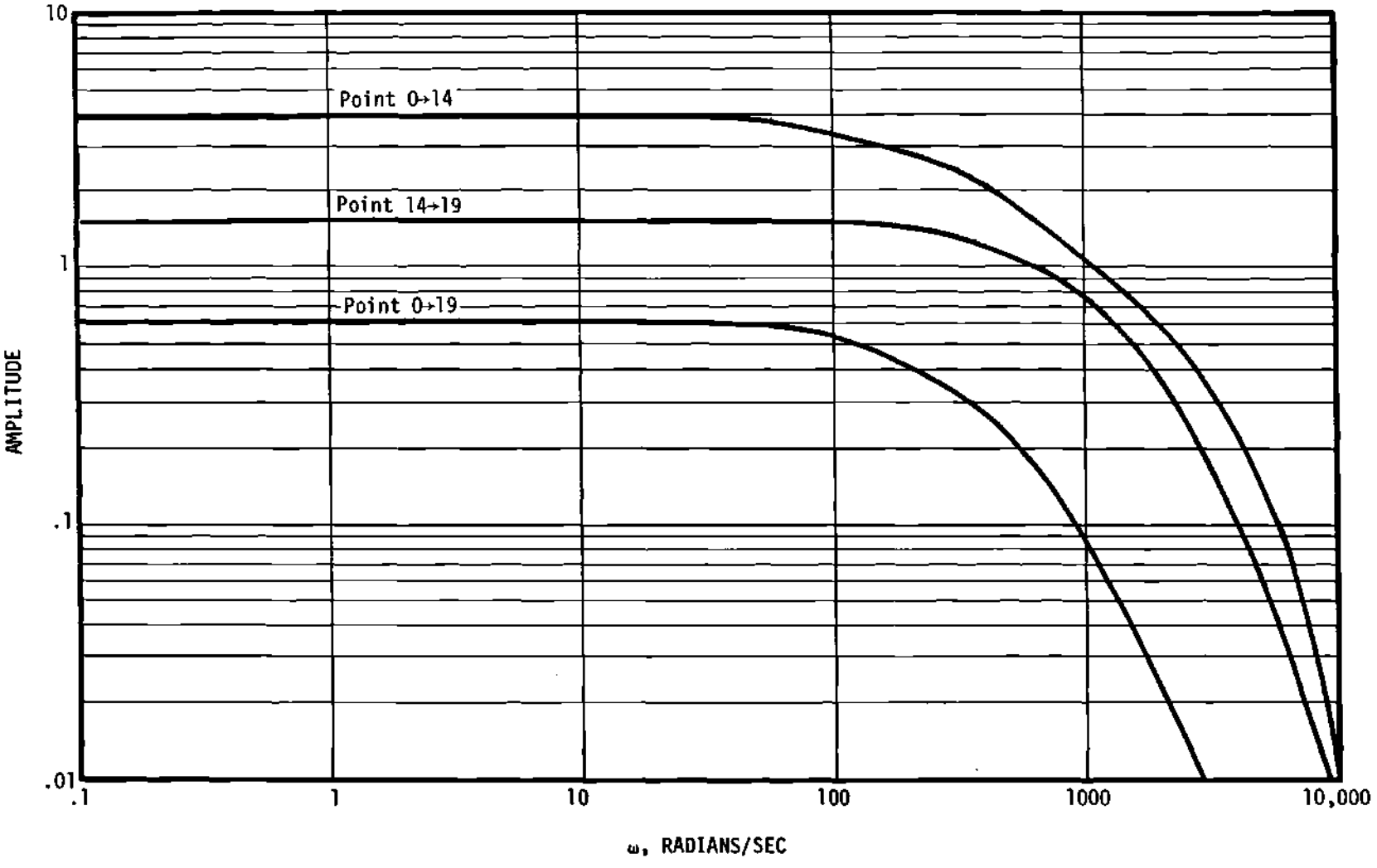

Figure 32. Amplitude of the Thermal Noise Transfer Function Between Detectors in the GTRR

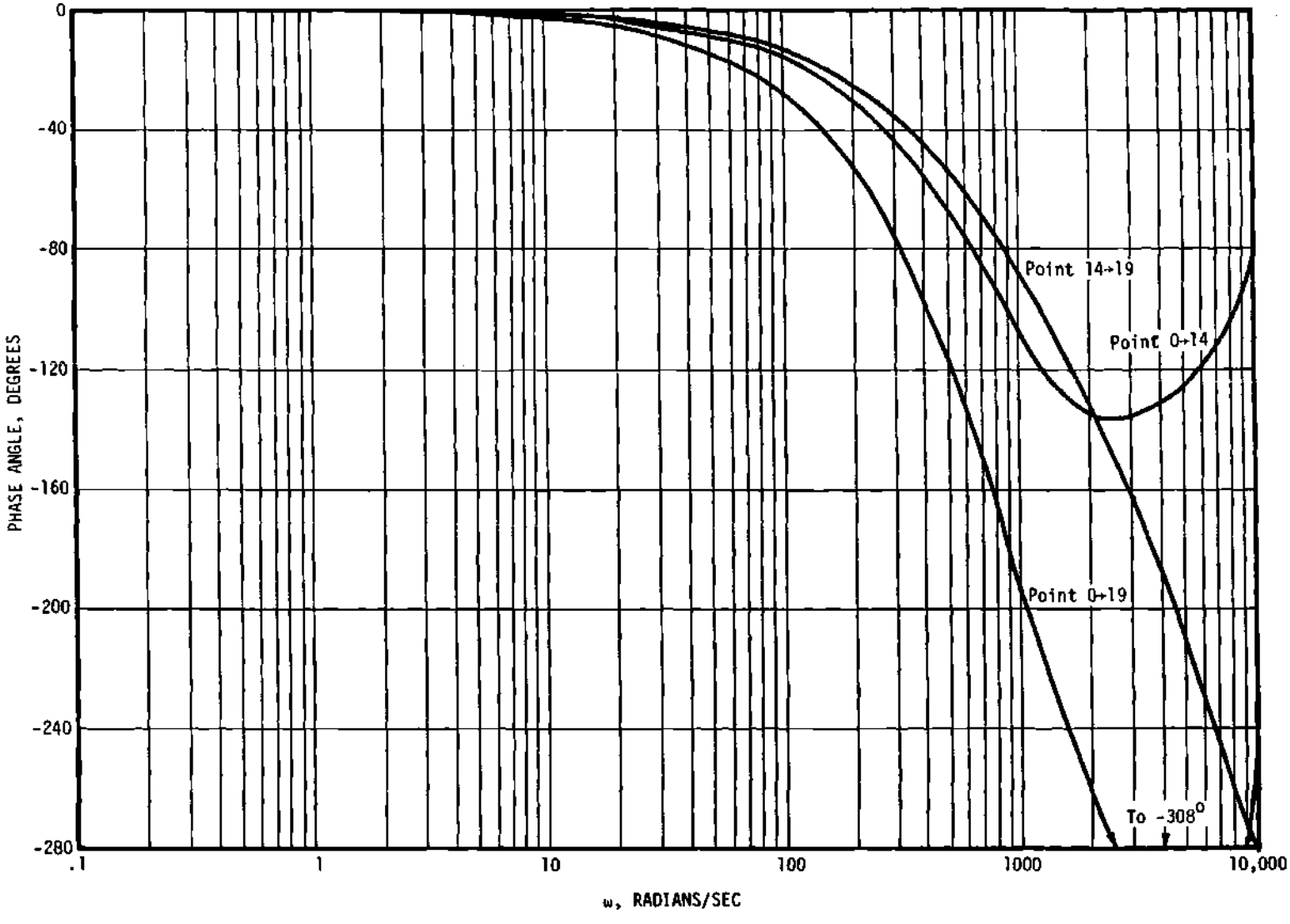

Figure 33. Phase Angle of the Thermal Noise Transfer Function Between Detectors in the GTRR

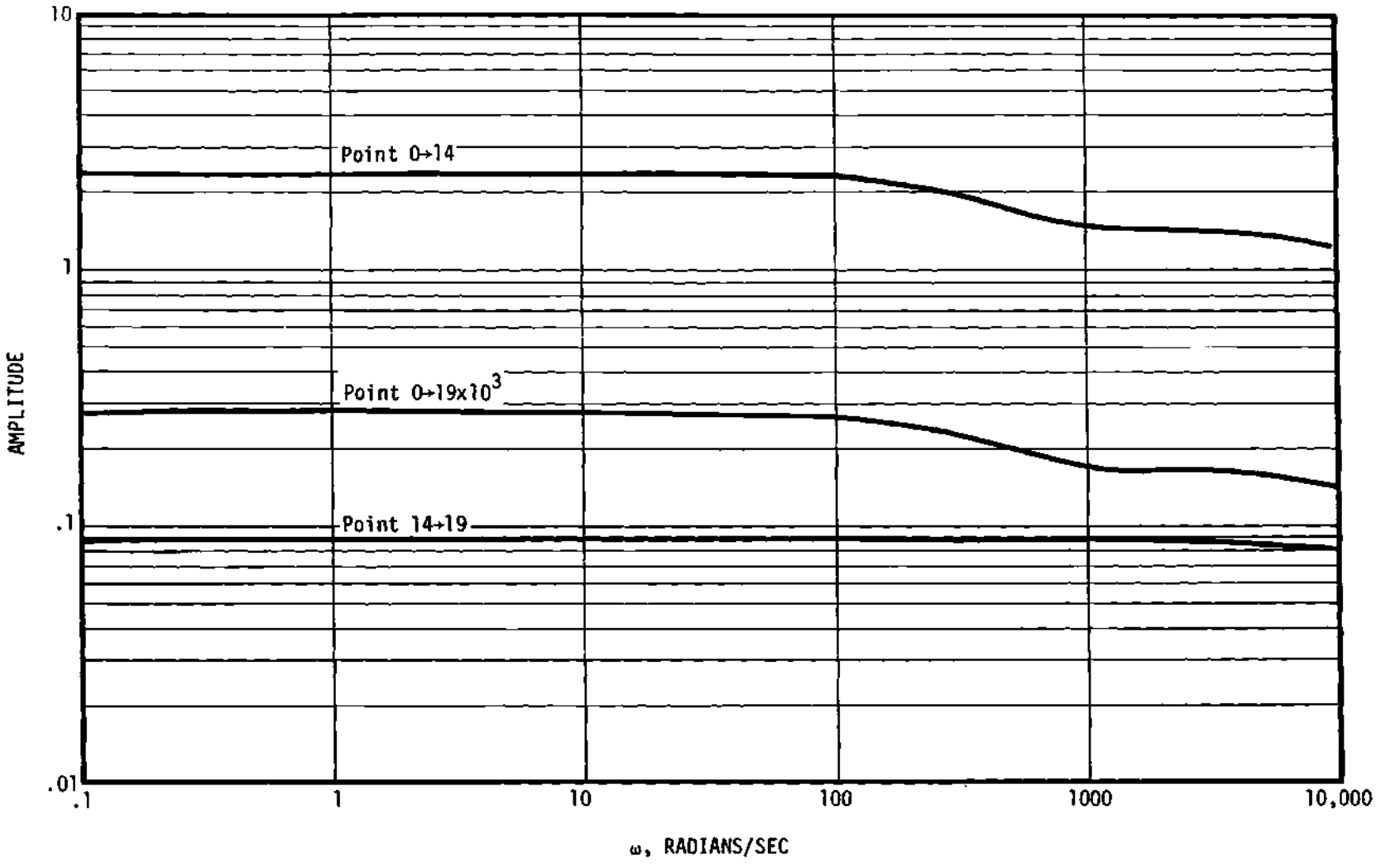

Figure 34. Amplitude of the Fast Noise Transfer Function Between Detectors in the GTRR

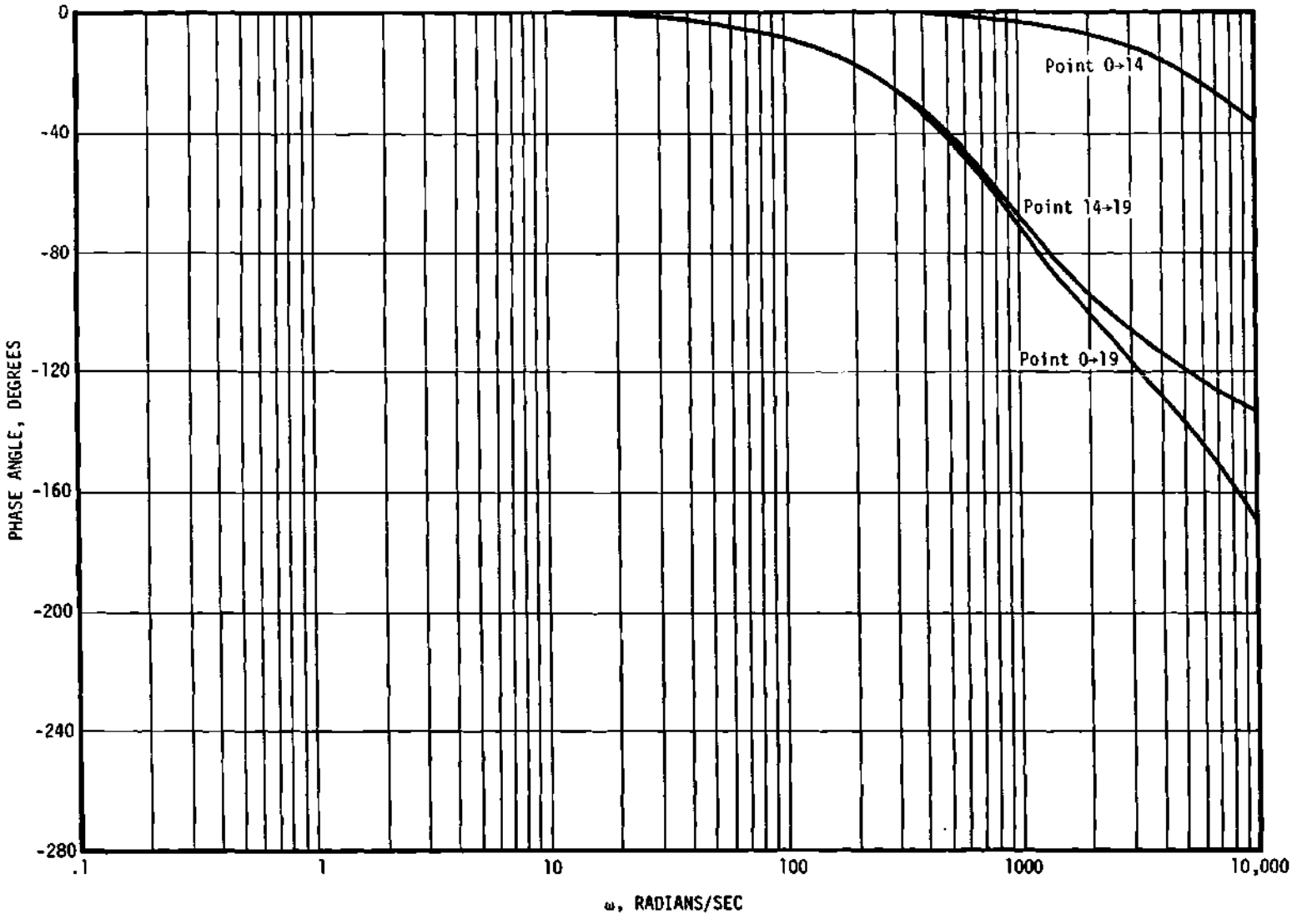

Figure 35. Phase Angle of the Fast Noise Transfer Function Between Detectors in the GTRR

spectrum method. Cross correlation techniques have the advantage of eliminating uncorrelated noise which is present in two signals. Some recent work which has made use of cross correlation methods to extract the transfer function from the uncorrelated noise has been reported in references 31, 32, and 33. At high frequencies, however, the curves show that cross correlation measurements must be interpreted in terms of spatial effects.

CHAPTER IV

PROPOSED NOISE MEASUREMENTS ON THE GEORGIA TECH RESEARCH REACTOR

This chapter will describe proposed two-detector noise measurements to be made on the GTRR. The experiments described here will verify the correctness of the complex source method in predicting the space dependent noise characteristics of a reactor. Specifications of the equipment are discussed first, followed by the procedure for data collection and data reduction.

Noise Analysis System

A schematic diagram of the data collection system is shown in Figure 36. The noise signal is obtained from two, Reuter Stokes, RSN-76A, boron lined, uncompensated ionization chambers. Compensated chambers should not be used for noise measurements because the compensating current adds an uncorrelated noise to the chamber output thus reducing the ratio of correlated to uncorrelated noise. Reference 33 gives a discussion of the effect. The power supplies for the chamber are two battery packs yielding +750 volts each. Batteries are used to eliminate any possibility of 60 or 120 cycle ripple being introduced into the signal. For maximum flexibility in being able to reach any part of the reactor, the chambers should be coupled to 50 feet of Amphenol RG 114 coaxial cable. The total capacitance to ground for both detector and cable will be 570 pico farads.

The signal is then fed into the electrometer amplifiers which are

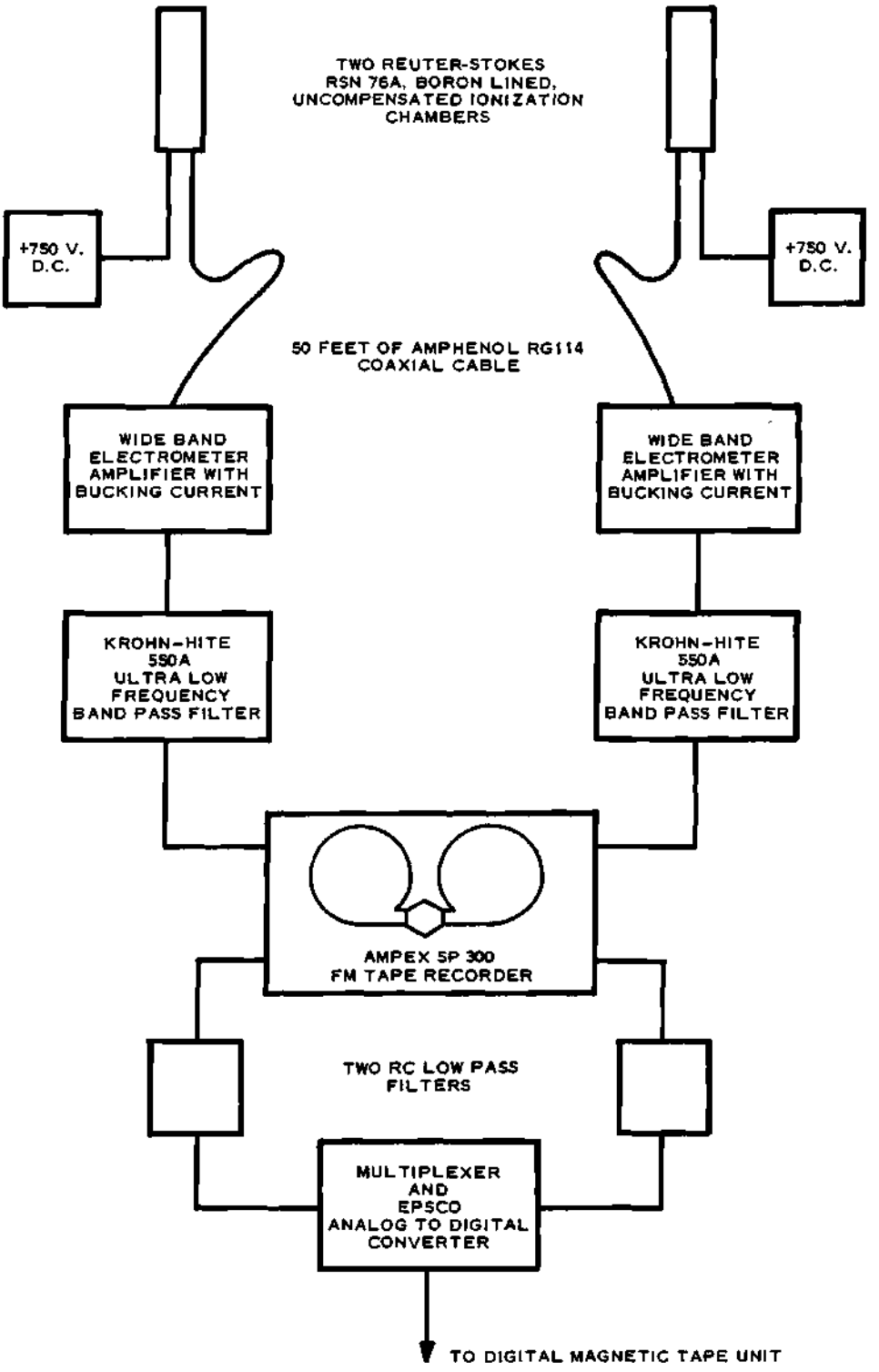

Figure 36. Schematic Diagram of the Reactor Noise Data Collection System

designed to pass d.c. to several kilocycles. The circuit diagram and construction of the electrometers are given by Brookshier (47). Each electrometer is equipped with a range switch with scales from 10^{-4} to 10^{-13} amps and a bucking current which can be adjusted to remove the average d.c. level. This bucking current is supplied from batteries to avoid ripple. After removal of the d.c. the remaining signal is amplified to approximately 5 volts at the output of the electrometers.

The signal at this point contains frequency components well outside the range of interest. These are both the high frequency uncorrelated noise components and also slow drifts in reactor power level. To remove these unwanted frequencies, the signal is put through a Krohn-Hite 550 A ultra low frequency band pass filter. This effectively removes frequencies below 0.01 cps and above 300 cps. The filtered signals are then recorded on two tracks of a four track Ampex SP-300 FM Tape recorder. This recorder has a signal-to-noise ratio of 40 db and four record-reproduce speeds which can be used for frequency shifting. A photograph of the equipment is shown in Figure 37.

To reproduce the data, the tape recorder can be taken to the Lockheed-Georgia Company in Marietta, Georgia, where signal will be digitized using an Epsco analog-to-digital converter. The converter samples the signal at a maximum rate of 200 conversions per second for each channel and will resolve the signal into 999 increments plus the sign. The digitized data are stored on magnetic tape compatible with the IBM-7094 digital computer.

On calibration of the system, two points should be made. Neither the overall gain of the system nor the absolute phase shift of either data channel is important. The only requirements are:

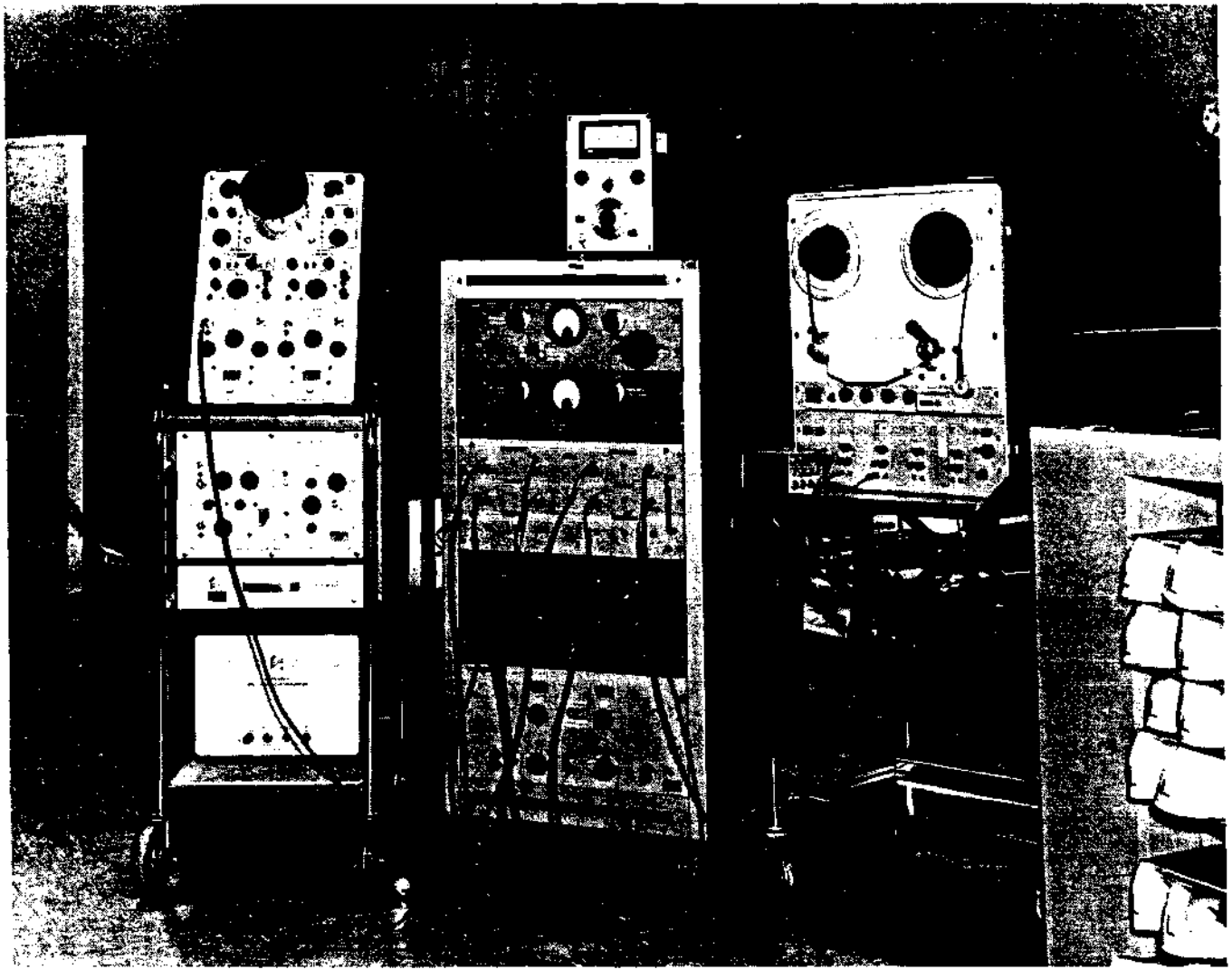

Figure 37. Noise Analysis Instrumentation

1. Linearity of each component over the voltage range expected
2. A flat gain response in both channels from 0.1 cps to 150 cps
3. No interchannel phase shift from 0.1 cps to 150 cps.

If items 2 and 3 are not satisfied, then correction factors will have to be applied to the reduced data.

Each of the components described was found to be linear. Gain and phase of the system were checked in two ways. First, by recording a series of pure sine waves from a Hewlett-Packard audio oscillator on both channels simultaneously, and, second, by recording on both channels the output of a General Radio 1390-B random noise generator. These signals were introduced at the input of the electrometers. The first method allowed gain and phase of each frequency to be measured directly. The gain plot in Figure 38 and the Lissajous figures in Figure 39 show that gain and phase corrections are very small.

The second method allowed the recorded signal to be carried all the way through the digitizing process and reduction by the computer. Actually, two recordings were made since the spectral analysis program does not have sufficient resolution when a frequency band of more than 1.5 decades is being covered. The first record was a high frequency run which included all frequencies up to 300 cps, which was the upper limit of the band pass filter. The second record was limited to 30 cps by changing the decade selector switch on the filter. Analysis of the tape was accomplished by converting from analog to digital information and processing the data with a spectral analysis program. A complete description of the process is given in the following section on the experimental procedure.

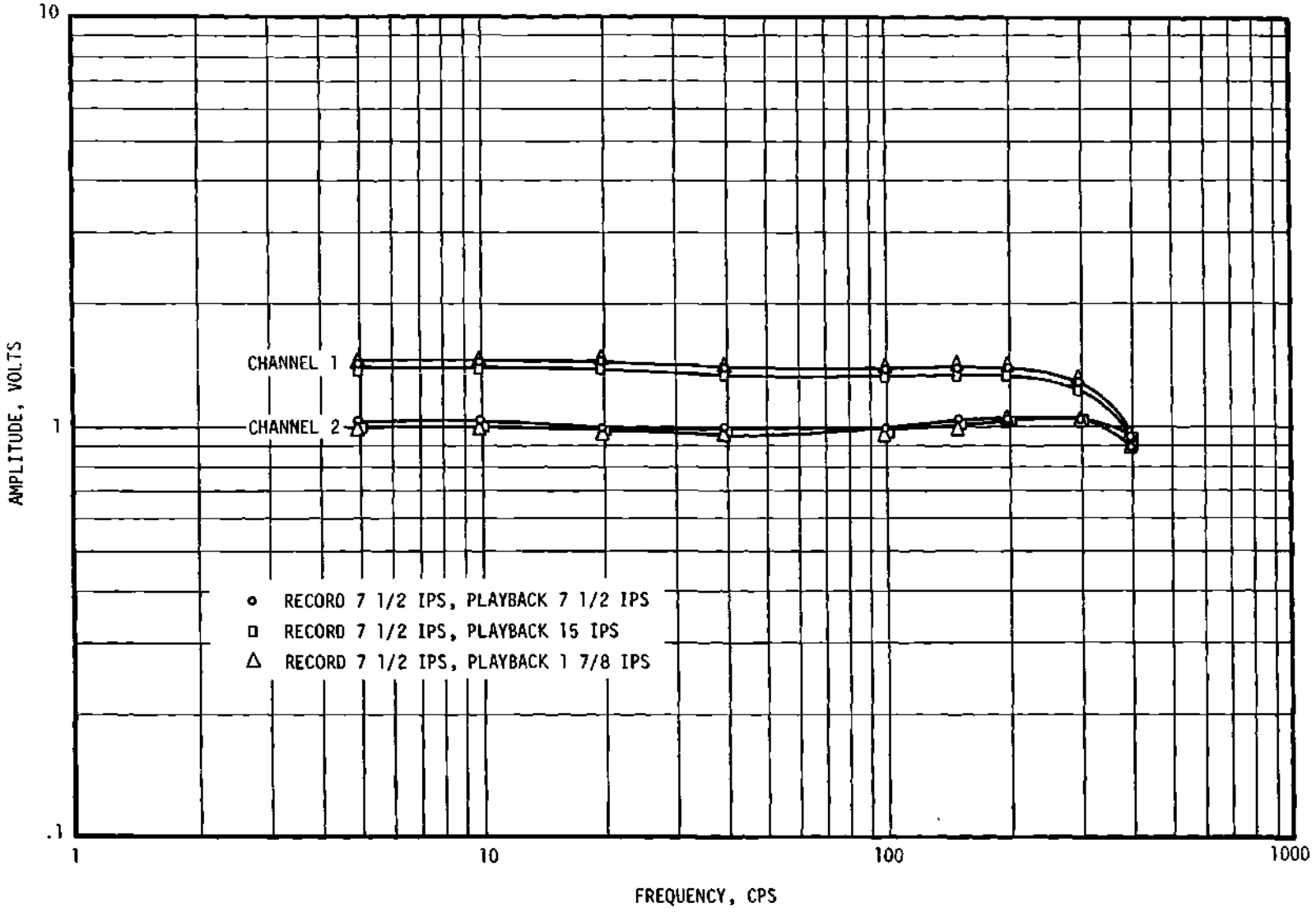

Figure 38. Gain of the Noise Analysis Instrumentation

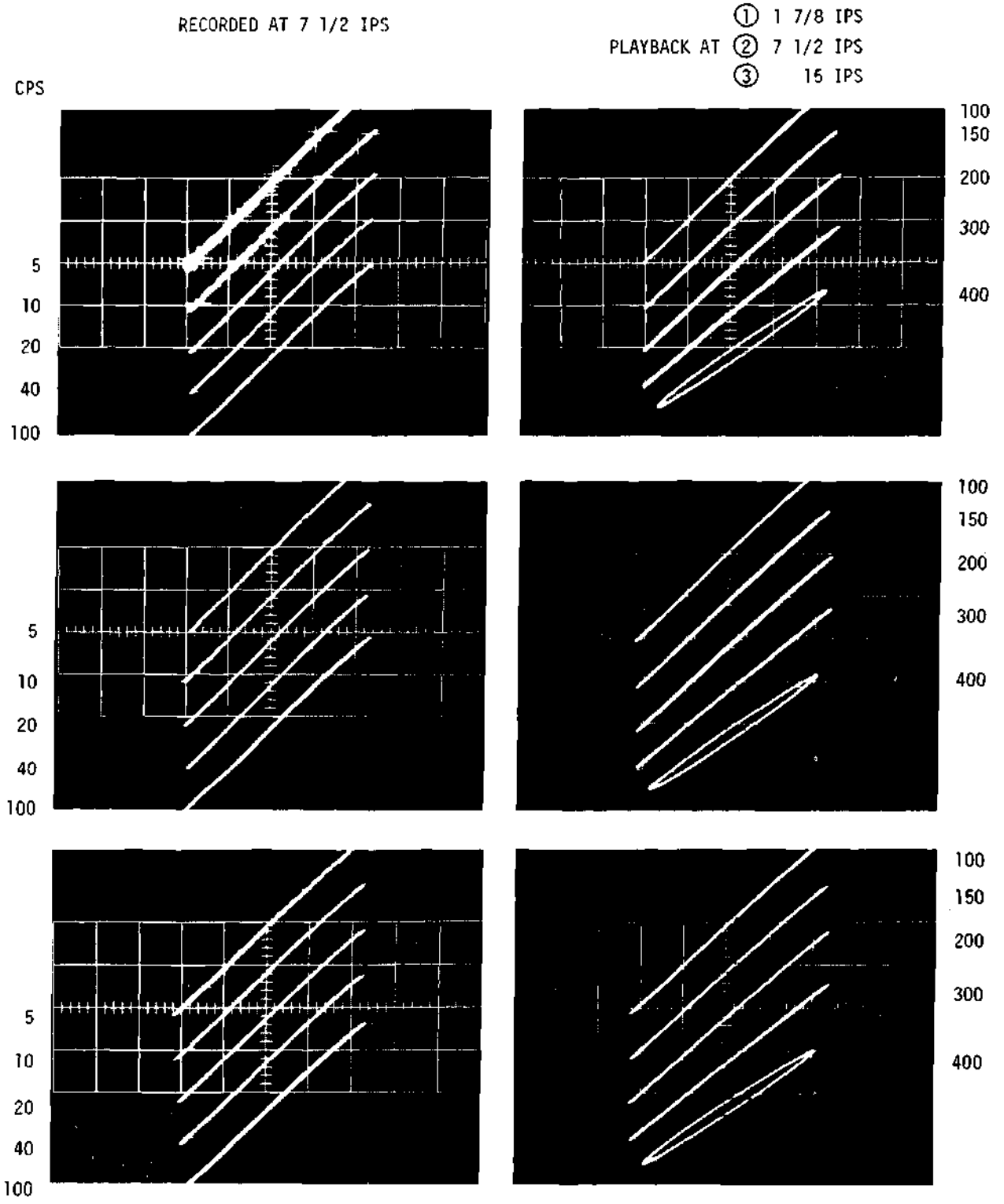

Figure 39. Lissajous Figures Showing Interchannel Phase Shift for the Noise Analysis Instrumentation

Results of the analysis are shown in Figures 40 and 41. The solid line at the top of Figure 40 is the reported power spectral density of the noise generator. The spectrum is white above 100 cps and is down by 6 db at 5 cps. The open points are the result of the numerical analysis for each channel and for the high and low frequency runs. Since the two runs are completely independent and gain adjustments were made on the equipment between runs, it was expected that some renormalization would be necessary. This is accomplished by choosing the frequency points such that the curves would overlap in the 60 to 100 radian per second region. The renormalization was made at 62.8 rad/sec and the adjusted values are shown by the solid points.

The renormalized points agree with the shape of the reported power spectrum between 30 and 1000 rad/sec. About 1000 rad/sec the rolloff due to the band pass filter becomes apparent. The seeming disagreement below 30 rad/sec is not considered significant because specifications for the random noise generator were not given below this frequency.

The relative phase shift between the channels is shown in Figure 41. The large peaks are due to the band pass filters not having precisely the same characteristics near the cut off point; however, this is no problem since the two spectra overlap. The phase shift of two degrees in the low frequency run can be readily compensated in the data analysis.

From the curves presented in Figures 38 through 41, the following conclusions can be drawn:

1. The gain of channel 1 is a factor of 1.5 greater than channel 2
2. The gain of both channels is essentially flat from 30 to 1000

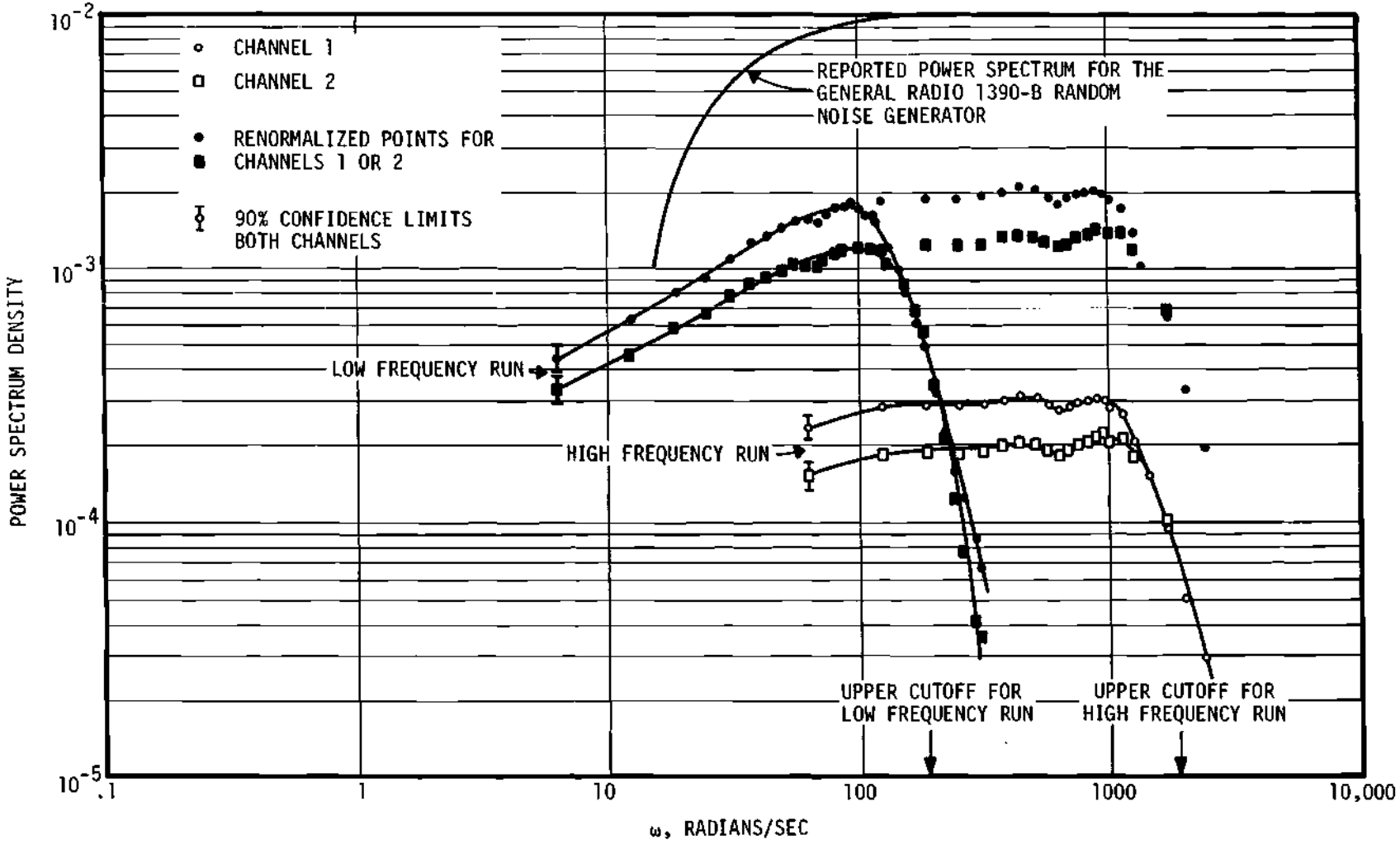

Figure 40. Gain of the Complete Noise Analysis System

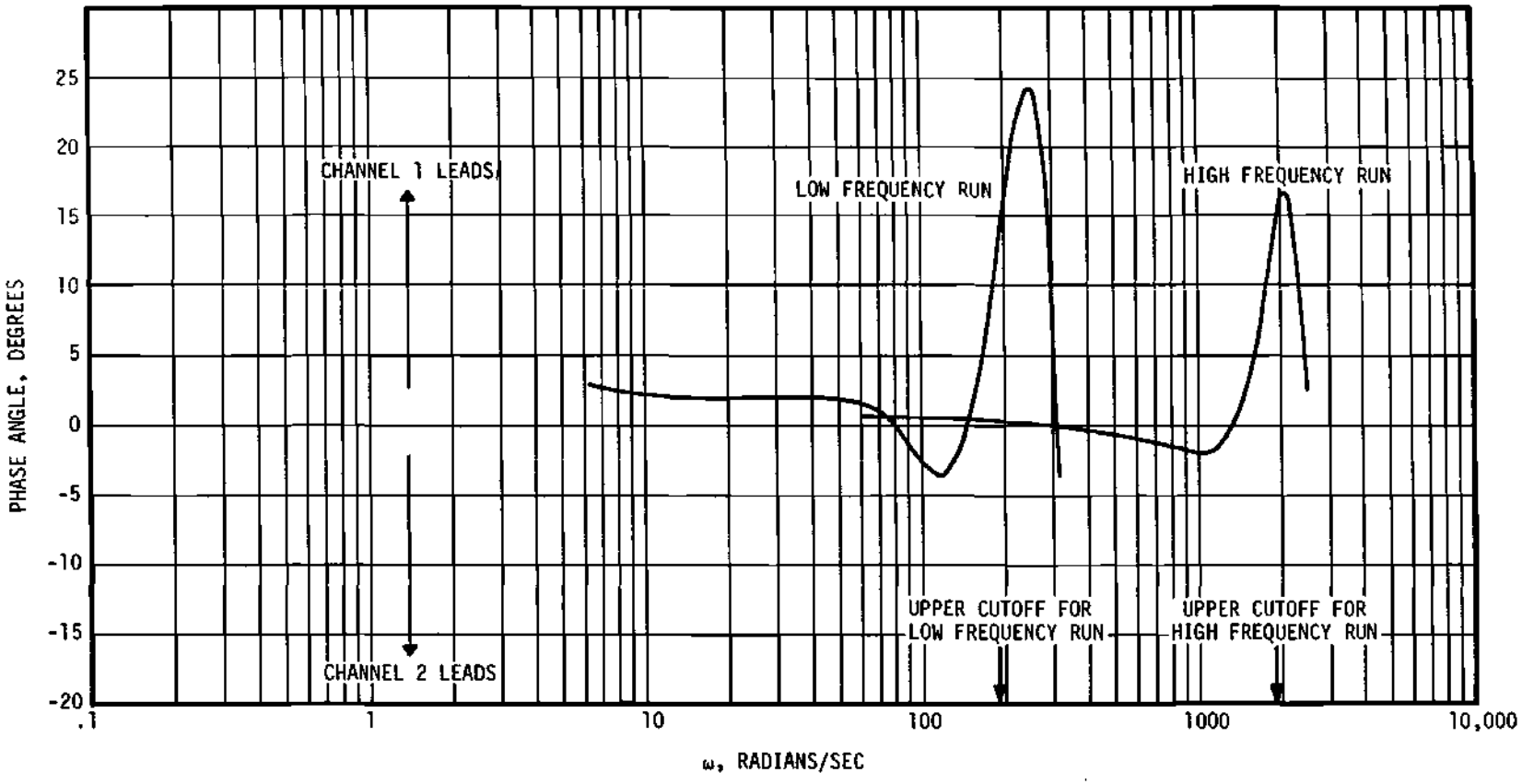

Figure 41. Interchannel Phase Shift for the Complete Noise Analysis System

rad/sec

3. The phase of channel 1 leads channel 2 by 2 degrees at 30 rad/sec and lags by 2 degrees at 1000 rad/sec

4. No difficulties are experienced in analyzing the spectrum in two parts.

Although no data on the response below 30 rad/sec has been presented (due to the lack of a low frequency signal generator), it can be assumed that the response is flat to 6 rad/sec since all equipment with the exception of the band pass filters is directly coupled. These results satisfy the three requirements previously stated.

Experimental Procedure

To collect the data, the following procedure should be used. Note that the frequency spectrum is covered in two steps.

1. All equipment is allowed one hour warm up time.

2. The detectors are positioned in the reactor and the reactor is brought to critical at a predetermined power level (ten watts).

3. Band pass filters are adjusted to pass 0.01 to 300 cps.

4. With no input from the chamber, all components are adjusted to give a zero input to tape recorder.

5. A two minute sample of the zero signal is recorded for reference. Tape speed is 15 inches per second.

6. Connect the chambers and buck out the d.c. component.

7. Adjust electrometer range switch to obtain between 1 and 10 volts output.

8. Record two minutes of data.

9. Reset the upper limit on the filters to 30 cps and tape recorder speed to 7-1/2 inches per second.

10. Repeat from 4, only record data for 15 minutes. Use manual regulating rod control to adjust criticality during the run.

The zero settings are necessary to avoid large d.c. bias which makes the digital analysis less accurate. The two recording speeds are required because the data analysis program used cannot provide sufficient frequency resolution when more than 1.5 decades of frequency are covered. Long data collection times are needed to improve the confidence limits of the analysis.

The analog-to-digital conversion and analysis proceed as follows.

1. Set the tape speed to 3-7/8 inches per second. This cuts the frequency range by a factor of four.

2. Adjust the output of the tape recorder to zero for the zero reference section.

3. Digitize at 200 samples per second. This will resolve up to 400 cps. Collect 60,000 sample points.

4. Set the tape speed to 15 inches per second for the second tape section and adjust for zero.

5. Digitize at 200 samples per second. This will resolve up to 50 cps. Collect 60,000 sample points.

The digital conversion is to be carried out precisely in the manner that Lockheed processes their flight test data. Notice that the sampling rate is so chosen as to resolve frequencies above those present in each data section thus eliminating the possibility of aliasing. Also, the two sections gave an overlapping frequency range.

After the digital tapes are prepared, they are to be taken to the University of Georgia Computer Center at Athens, Georgia for data reduction. The programs used are Lockheed programs 3078 and 3508 with no changes. These are respectively a procedure to reformat the data tape and a standard spectral analysis program for computing power spectra, cross power spectra, and transfer functions. The basic equations included in the spectral analysis program (3508) are:

Autocorrelation:

$$A_j = \frac{1}{N-j} \sum_{i=1}^{N-j} x_i \, x_{i+j} \tag{1}$$

Cross correlation:

$$C_j^{even} = \frac{1}{2(N-j)} \sum_{i=1}^{N-j} x_i \, y_{i+j} + y_i \, x_{i+j} \tag{2}$$

$$C_j^{odd} = \frac{1}{2(N-j)} \sum_{i=1}^{N-j} x_i \, y_{i+j} - y_i \, x_{i+j} \tag{3}$$

Power spectral density:

$$P_k = 4 \, c \, \Delta \, t \left[\frac{1}{2} A_o + \sum_{m=1}^{M} A_m \cos\left(mk \frac{\Pi}{M}\right) \right] \tag{4}$$

Cross power spectral density:

$$P_k^{even} = 4\, c\, \Delta\, t \left[\frac{1}{2} C_o^{even} + \sum_{m=1}^{M} C_m^{even} \cos\left(mk \frac{\Pi}{M}\right) \right] \tag{5}$$

$$P_k^{odd} = 4\, c\, \Delta\, t \sum_{m=o}^{M} C_m^{odd} \sin\left(mk \frac{\Pi}{M}\right) \tag{6}$$

Amplitude of the transfer function:

$$H_k = \frac{\left[(P_k^{even})^2 + (P_k^{odd})^2 \right]^{\frac{1}{2}}}{P_k \text{ (x record)}} \tag{7}$$

Phase of the transfer function:

$$\Psi_k = \tan^{-1}\left(\frac{P_k^{odd}}{P_k^{even}} \right) . \tag{8}$$

In the above equations the following definitions were used:

x_i = time series of the input channel

y_i = time series of the response channel

j = number of lag points

k = number of frequency points

N = total number of time points

c = dimensional constant

Δt = time increment in the digitized record .

The techniques used are described in detail in references 23 or 46 and full information on the programs is available from Lockheed on request. After analysis, the low and high frequency portions of the spectrum are simply pieced together with a possible renormalization of the amplitudes to provide a fit in the overalpping region.

While the upper limit of the frequency spectrum is fixed by the Nyquist frequency (one-half of the sampling rate), the lowest frequency above zero or the bandwidth is an input to the program. For the high frequency case, the lower limit is 10 cps and for the low frequency portion 1 cps. These are chosen as a compromise between desired frequency resolution and computer time necessary.

CHAPTER V

CONCLUSIONS AND RECOMMENDATIONS

The basic objective of this thesis, which was to develop a simple model for the analysis of space dependent modulated neutron experiments, has been accomplished.

A set of space and frequency dependent neutron balance equations has been put into a form suitable for solution with statics techniques. The model, herein called the complex source method, has been successfully tested under a variety of conditions for pile oscillator, wave propagation, and reactor noise experiments. It has also been shown how two existing statics codes, CRAM and EXTERMINATOR, may be used to solve this type of problem. This point is important because the two codes have the ability to handle multidimensional, multigroup systems.

The pile oscillator problem was investigated for two different reactors, NORA and the GTRR. Comparison of the results for NORA with detailed experimental data shows excellent agreement and points out the need to consider spatial effects in pile oscillator experiments. Calculations for the GTRR were not compared directly with experiment but do show a large space dependence and indicate that the method is applicable to a variety of systems. The model is shown to reduce to the static flux equations for the case of zero frequency and to give results that are completely consistent with those of other investigators.

The wave propagation calculations were carried out for very simple

systems for which the solutions were known analytically. For these simple cases, the numerical model was found to reproduce the exact solutions thus showing the correctness of the model. The effects of mesh spacing and the difference between the diffusion and telegrapher's approximations was studied.

Calculation of space dependence of reactor noise was done for the GTRR. The results indicate that spatial effects become significant only at high frequency and show the upper frequency limit for the interpretation of cross correlation measurements with the space independent model. An experimental determination of the noise spectrum was not made; however, the details of a proposed experiment to measure the power spectrum, cross power spectrum, and transfer function between two detectors is discussed.

This thesis has encountered several areas which need further work. A major problem is the convergence rate of the iterative methods used. New techniques are needed which will improve the running times before the complex source method is a practical engineering tool. The method should also be extended to include an arbitrary number of energy groups in the transport approximation. With the inclusion of linear feedback equations, the space-dependence of power reactor transfer functions may be studied. An accurate knowledge of these transfer functions is essential to the development of safe automatic control systems for large power reactors. Using the complex source model, it will be possible to study potential instabilities in a reactor while the design is in progress rather than after the system is operating.

Probably the most useful immediate application of the technique will be in the analysis of neutron wave experiments. The ability of the

method to handle multidimensional or multigroup problems will relieve the experimentalist of the burden of trying to approximate simple systems (plane wave sources) for which analytical solutions exist. He will now be able to do an experiment which is easy to realize in the laboratory, and turn to the numerical solutions for the interpretation of his results. The method should be extremely useful in studying the propagation of a neutron wave across an interface between dissimilar media. This type of experiment has been done by Dr. R. B. Perez at the University of Florida and the results are awaiting analysis.

The noise calculations need the most work. The results discussed herein should be checked with a more accurate set of macroscopic cross sections and compared with experimental data. Assuming that the experiment establishes the validity of the method, the technique can then be extended to power reactors and used as a basis for the synthesis of equations required in a space-dependent control system.

Finally, it should be pointed out that the ability of statics codes to solve a problem for which they were obviously not intended is remarkable. These codes are extremely flexible and should be considered an algorithm for the solution of general sets of differential equations. With this interpretation, the codes can be of great value when applied to fields other than nuclear engineering.

APPENDICES

APPENDIX A

DERIVATION OF THE FINITE DIFFERENCE EQUATIONS

APPENDIX A

DERIVATION OF THE FINITE DIFFERENCE EQUATIONS

The finite difference equations programmed in CHARLIE were derived in the same manner as those in AIM-6 (48). First rewrite the differential equations 23 through 26 in Chapter II using the cross sections defined by equations 27 through 32.

Fast real (group 1):

$$\hat{D}_1\nabla^2\Phi_1 - A_1\Phi_1 + C_{1\rightarrow 1}\Phi_1 + C_{2\rightarrow 1}\Phi_2 + C_{3\rightarrow 1}\Phi_3 + C_{4\rightarrow 1}\Phi_4 = - S_1 \qquad (1)$$

Fast imaginary (group 2):

$$\hat{D}_2\nabla^2\Phi_2 - A_2\Phi_2 - C_{2\rightarrow 1}\Phi_1 + C_{2\rightarrow 2}\Phi_2 - C_{4\rightarrow 1}\Phi_3 + C_{3\rightarrow 1}\Phi_4 = - S_2 \qquad (2)$$

Thermal real (group 3):

$$\hat{D}_3\nabla^2\Phi_3 - A_3\Phi_3 + C_{1\rightarrow 3}\Phi_1 + C_{4\rightarrow 3}\Phi_4 = - S_3 \qquad (3)$$

Thermal imaginary (group 4):

$$\hat{D}_4\nabla^2\Phi_4 - A_4\Phi_4 + C_{1\rightarrow 3}\Phi_2 - C_{4\rightarrow 3}\Phi_3 = - S_4 \qquad (4)$$

In one-dimensional, cylindrical geometry

$$\nabla^2\Phi = \frac{d^2\Phi}{dr^2} + \frac{1}{r}\frac{d\Phi}{dr} . \qquad (5)$$

The central difference approximation at point n is

$$\nabla^2\Phi^n = \left[\frac{\Phi^{n-1} - 2\Phi^n + \Phi^{n+1}}{h^2} + \frac{1}{r_n} \frac{\Phi^{n+1} - \Phi^{n-1}}{2h} \right] \tag{6}$$

where h = mesh spacing.

Substituting equation 6 into 1 through 4 and redefining constants

$$P_1\Phi_1^{n-1} + Q_1\Phi_1^n + R_1\Phi_1^{n+1} + C_{2\rightarrow 1}\Phi_2^n + C_{3\rightarrow 1}\Phi_3^n + C_{4\rightarrow 1}\Phi_4^n = - S_1^n \tag{7}$$

$$P_2\Phi_2^{n-1} + Q_2\Phi_2^n + R_2\Phi_2^{n+1} - C_{2\rightarrow 1}\Phi_1^n + C_{3\rightarrow 1}\Phi_4^n - C_{4\rightarrow 1}\Phi_3^n = - S_2^n \tag{8}$$

$$P_3\Phi_3^{n-1} + Q_3\Phi_3^n + R_3\Phi_3^{n+1} + C_{4\rightarrow 3}\Phi_4^n + C_{1\rightarrow 3}\Phi_1^n = - S_3^n \tag{9}$$

$$P_4\Phi_4^{n-1} + Q_4\Phi_4^n + R_4\Phi_4^{n+1} - C_{4\rightarrow 3}\Phi_3^n + C_{1\rightarrow 3}\Phi_2^n = - S_4^n \tag{10}$$

where

$$P_i \equiv \frac{\hat{D}_i}{h^2} - \frac{\hat{D}_i}{2hr_n} \tag{11}$$

$$R_i \equiv \frac{\hat{D}_i}{h^2} + \frac{\hat{D}_i}{2hr_n} \tag{12}$$

$$Q_i \equiv C_{i\rightarrow i} - A_i - \frac{2\hat{D}_i}{h^2} \tag{13}$$

At the interface I between two regions the neutron current must be continuous.

$$J^-(I) = J^+(I)$$

Using the equations from AIM-6, the currents are

$$J^{-}(I) = - \frac{\hat{D}}{h} \left(1 - \frac{h}{2r_I}\right)(\Phi^I - \Phi^{I-1}) + \frac{h}{2} \left[\text{source - removal}\right]_I \qquad (14)$$

$$J^{+}(I) = + \frac{\hat{D}'}{h'} \left(1 + \frac{h'}{2r_I}\right)(\Phi^I - \Phi^{I-1}) + \frac{h'}{2} \left[\text{source - removal}\right]_I \qquad (15)$$

The primed quantities indicate the region to the right of the boundary. Equating 14 and 15 for each group of neutrons, the interface equations can be put in the same form as equations 7 through 10 except that the coefficients have been modified as indicated by the asterisk. For example, the group one equation would be

$$P_1^* \Phi_1^{I-1} + Q_1^* \Phi_1^I + R_1^* \Phi_1^{I+1} + C_{2\rightarrow 1}^* \Phi_2^I + C_{3\rightarrow 1}^* \Phi_3^I + C_{4\rightarrow 1}^* \Phi_4^I = - S_1^{*I} \qquad (16)$$

where

$$P_i^* \equiv hP_i \qquad (17)$$

$$R_i^* \equiv h'R_i' \qquad (18)$$

$$Q_i^* \equiv \frac{hQ_i}{2} + \frac{h'Q_i'}{2} + \frac{\hat{D}_i - \hat{D}_i'}{2r_I} \qquad (19)$$

$$C_{2\rightarrow 1}^* \equiv \frac{h}{2} C_{2\rightarrow 1} + \frac{h'}{2} C_{2\rightarrow 1}' \qquad (20)$$

$$C_{3\rightarrow 1}^* \equiv \frac{h}{2} C_{3\rightarrow 1} + \frac{h'}{2} C_{3\rightarrow 1}' \qquad (21)$$

$$C^{*}_{4\rightarrow 1} \equiv \frac{h}{2} C_{4\rightarrow 1} + \frac{h'}{2} C'_{4\rightarrow 1} \tag{22}$$

$$S_i^{*I} \equiv \frac{h}{2} S_i^{I} + \frac{h'}{2} S_i'^{I} \tag{23}$$

and for the additional equations

$$C^{*}_{4\rightarrow 3} \equiv \frac{h}{2} C_{4\rightarrow 3} + \frac{h'}{2} C'_{4\rightarrow 3}$$

$$C^{*}_{1\rightarrow 3} \equiv \frac{h}{2} C_{1\rightarrow 3} + \frac{h'}{2} C'_{1\rightarrow 3} \tag{25}$$

At the left hand boundary of the system $r = 0$ and $\frac{d\Phi}{dr} = 0$. Thus $\Phi^{-1} = \Phi^{1}$ for symmetry. The Laplacian at $r = 0$ is

$$\lim_{r\rightarrow 0} \nabla^2 = \lim_{r\rightarrow 0} \frac{d^2}{dr^2} + \frac{1}{r}\frac{d}{dr} = 2\frac{d^2}{dr^2} \tag{26}$$

and

$$^{2}\Phi(0) = 2\left[\frac{\Phi^{-1} - 2\Phi^{o} + \Phi^{1}}{h^2}\right] = \frac{4(\Phi^{1} - \Phi^{o})}{h^2} . \tag{27}$$

At the left hand boundary the constants in equations 7 through 10 become

$$P_i^{o} \equiv 0 \tag{28}$$

$$Q_i^{o} \equiv Q_i^{1} - \frac{2\hat{D}_i}{h^2} \tag{29}$$

$$R_i^{o} \equiv \frac{4\hat{D}_i}{h^2} \tag{30}$$

The other coefficients do not change.

At the right hand boundary B the flux is set to zero at the extrapolated boundary of the system.

$$\Phi_i^B + d_i \left.\frac{d\Phi}{dr}\right|_B = 0 \quad \text{or} \quad \Phi_i^B - \frac{d_i}{\hat{D}_i} J_i^{-B} = 0 \tag{31}$$

where d is the extrapolation distance

$$d_i = 3 \hat{D}_i \left[\frac{0.710466}{1 + 0.710466 \times \frac{3 \hat{D}_i}{2 r_B}} \right] \tag{32}$$

Using this condition simply changes the coefficients to

$$P_i^B \equiv \frac{h d_i}{\hat{D}_i} P_i \tag{33}$$

$$Q_i^B \equiv \frac{h d_i}{2 \hat{D}_i} Q_i + \frac{d_i}{2 r_B} - 1 \tag{34}$$

$$R_i^B \equiv 0 \tag{35}$$

$$C_{2\to 1}^B \equiv \frac{h d_1}{2 \hat{D}_1} C_{2\to 1} \tag{36}$$

$$C_{3\to 1}^B \equiv \frac{h d_1}{2 \hat{D}_1} C_{3\to 1} \tag{37}$$

$$C_{4\to 1}^B \equiv \frac{h d_1}{2 \hat{D}_1} C_{4\to 1} \tag{38}$$

$$S_i^B \equiv \frac{hd_1}{2\hat{D}_1} S_i \tag{39}$$

$$C_{4\rightarrow 3}^B \equiv \frac{hd_2}{2\hat{D}_2} C_{4\rightarrow 3} \tag{40}$$

$$C_{1\rightarrow 3}^B \equiv \frac{h}{2}\frac{d_2}{\hat{D}_2} C_{1\rightarrow 3} \tag{41}$$

These equations completely describe the system and when arranged in matrix form, $[M][\Phi] = [-S]$ the solution vector Φ may be found by matrix inversion or iterative techniques.

APPENDIX B

COMPUTER PROGRAMS

APPENDIX B

COMPUTER PROGRAMS

The two statics codes mentioned in the text, CRAM and EXTERMINATOR, have been modified slightly from the standard versions. These changes have all been incorporated into the working versions of the codes and may be obtained by writing directly to the following persons:

For CRAM write to:

Mr. Gene Volk
Atomic Power Development Associates
1911 First Street
Detroit, Michigan 48226

For EXTERMINATOR write to:

Mr. T. B. Fowler
Oak Ridge National Laboratory
P. O. Box Y
Oak Ridge, Tennessee 37831

The two codes written at Georgia Tech are in ALGOL for the Burrough's B-5500. Listings for CHARLIE and NOISE are given below. The description of the input data should be clear from comments included in the programs.

```
C                                C H A R L I E                                  0
C                                                                               10
C     *     *     *     *     *     *     *     *     *     *     *             20
C                                                                               30
C     A PROGRAM FOR CALCULATING THE SPACE DEPENDENT REACTOR                     40
C     TRANSFER FUNCTION IN THE ONE DIMENSIONAL (CYLINDRICAL)                    50
C     TWO GROUP APPROXIMATION.                                                  60
C     THE EQUATIONS ARE SOLVED BY THE CONGUGATE GRADIENT METHOD                 70
C                                                                               80
C     *     *     *     *     *     *     *     *     *     *     *             90
C                                                                              100
C                                R N MACDONALD                                 110
C                           SCHOOL OF NUCLEAR ENGINEERING                      120
C                         GEORGIA INSTITUTE OF TECHNOLOGY                      130
C                               ATLANTA, GEORGIA                               140
C                               25 FEBRUARY 1966                               150
C                                                                              160
C     *     *     *     *     *     *     *     *     *     *     *             170
C                                                                              180
C     RESTRICTIONS IN THE PROGRAM                                              190
C                                                                              200
C     NOR  =  NUMBER OF REGIONS ≤ 5                                            210
C     NPT  =  NUMBER OF POINTS ≤ 26                                            220
C     NOM  =  NUMBER OF ANGULAR VELOCITIES TO BE CALCULATED ≤ 20               230
C     NPC  =  NUMBER OF PRECURSORS ≤ 15                                        240
C                                                                              250
C     *     *     *     *     *     *     *     *     *     *     *             260
C                                                                              270
C     OPTIONS IN THE PROGRAM                                                   280
C                                                                              290
C     NORM = 0     BUILT IN GAIN NORMALIZATION                                 300
C          = 1     READ IN GAIN NORMALIZATION                                  310
C     NCPS = 0     USE THE DIFFUSION EQUATIONS                                 320
C          = 1     USE THE TELEGRAPHERS EQUATIONS                              330
C     NSLF = 0     DO NOT PUNCH FLUX CARDS                                     340
C          = 1     PUNCH FLUX CARDS                                            350
```

```
%      ID    = 0      OMIT CRAM CROSS SECTIONS                                  360
%            = 1      COMPUTE AND PUNCH CROSS SECTIONS FOR CRAM                 370
%      CRIT  = 0      NO SEARCH FOR CRITICAL HEIGHT                             380
%            = 1      SEARCH FOR CRITICAL HEIGHT BY CHANGING B*2                390
%      DVARY=         DELTA B*2 FOR THE FIRST STEP IN THE SEARCH                 400
%                                                                               410
BEGIN                                                                           420
INTEGER   I, J, K, NOR, NPC, L, M, N, KK, NOS, ITR, NORM;                       430
INTEGER   NPT, NOM, COUNT, CRIT, ITER, ID;                                      440
INTEGER    NCPS, NSLF;                                                          450
ALPHA ARRAY     TITLE[0:12];                                                    460
REAL ARRAY   SIGA, NUSIGF,          D, SIGR[0:2,0:25], SIG1TO2[    0:25],       470
             PHI,S[0:104], H[0:5],          OMEGA[0:20],                        480
             SIGR1, SIGR2[0:5], V[0:2,0:5],                                     490
            NORF, NORT, NGF, NGT,                                               500
             GAINF, GAINT, PHASEF, PHASET[0:26],                                510
             BETA, LAMBDA [0:15],    X[0:25];                                   520
SAVE REAL ARRAY   MTX[0:104,0:104] ;                                            530
REAL ARRAY   EXD[0:2];                                                          540
INTEGER ARRAY   NIF[0:5];                                                       550
REAL   W, Z, BEFF, EPS, DET, DET1, DET2, DVARY,          BSQ ;                  560
REAL     VUL,SXV;                                                               570
DEFINE  VARY=BSQ# ;                                                             580
DEFINE   FORJ = FOR J+1 STEP 1 UNTIL NOR DO # ;                                 590
LABEL   L0, L1, L2, L3, L4, L7, L8 ;                                            600
FILE FTAPE 2(2,10);                                                             610
FILE    CARD  (2,10);                                                           620
FILE OUT PRINT 4(2,15);                                                         630
FILE OUT PUNCH 0(2,10);                                                         640
FORMAT FMT1 (12A6);                                                             650
FORMAT FMT2 (6I12);                                                             660
FORMAT FMT3 (6R12.5);                                                           670
FORMAT FMT4 (1I12,4R12.5);                                                      680
FORMAT FMT5 (1I3,5R15.8);                                                       690
FORMAT FMT6 ("           I        BETA[I]      LAMBDA[I] ", // );               700
FORMAT FMT7 (I12, 2R15.8 / );                                                   710
```

```
FORMAT FMT8 (5R12.5);                                                          720
FORMAT FMT9 ("  I     RADIUS, CM", X5,              "FAST REAL",              730
             "     FAST IMAG.      SLOW REAL     SLOW IMAG." // );           740
FORMAT FMT10(//"REGION",I7,"            GROUP 1       GROUP 2 ",//          750
              "SIGMA REMOVAL    =", 2R15.8,X9,"RADIUS          =",1R15.5//   760
              "NU SIGMA FISSION =", 2R15.8,X9,"INTERFACE NO. =",1I12  //     770
              "SIGMA TRANSFER   =",1R15.8,X24,"HEIGHT          =",1R15.5//   780
              "DIFFUSION COEF.  =", 2R15.8,X9,"BUCKLING        =",1R15.9//   790
              "VELOCITY, CM/SEC =",                                            800
               2E15.5  ////);                                                  810
FORMAT FMT11 (//"   BETA EFFECTIVE  = ", 1R15.8 );                           820
FORMAT FMT12 (X20, "INPUT SOURCE" //);                                         830
FORMAT FMT13 (X20, "CALCULATED FLUX", X10, "OMEGA =", 1R15.5,                  840
             "  RAD/SEC", X10, I3, "  ITERATIONS REQUIRED" //);               850
FORMAT FMT14 (X20,"GAIN AND PHASE SHIFT CALCULATION", X13, "OMEGA =",          860
              1R15.5,"  RAD/SEC"// X38, "FAST", X44, "THERMAL", /             870
              " I   RADIUS, CM", X8, "GAIN", X8, "NORM. GAIN",                 880
              X8, "PHASE", X16, "GAIN", X8, "NORM. GAIN", X8, "PHASE"          890
              // );                                                            900
FORMAT FMT15 (5I12,1R12.5);                                                    910
FORMAT FMT16(1I12," ITERATIONS WERE PERFORMED ON Z TO FIND A ",                920
             "CRITICAL DETERMINANT" //, X20, " HEIGHT =", 1R12.5,              930
             X5, "BUCKLING =" 1E12.5 );                                        940
FORMAT FMT17(////X20,"DATE                =", X6, 1A5, //                      950
                 X20,"PROCESSOR TIME   =",1R15.5,"  SECONDS", //               960
                 X20,"I/O TIME         =",1R15.5,"  SECONDS" );              970
FORMAT FMT18(1I3,2R15.8,1R15.8,1R15.8,X5,1R15.8,1R15.8,1R15.8);                980
FORMAT FMT34 (6E12.5);                                                         990
FORMAT FMT34A("FAST REAL GROUP                OMEGA =", 1R12.5);              1000
FORMAT FMT34B("THERMAL REAL GROUP             OMEGA =", 1R12.5);              1010
FORMAT FMT34C("FAST IMAGINARY GROUP           OMEGA =", 1R12.5);              1020
FORMAT FMT34D("THERMAL IMAGINARY GROUP        OMEGA =", 1R12.5);              1030
LIST LIST1 (FOR I=1 STEP 1 UNTIL 12 DO TITLE[I]);                              1040
LIST LIST2 (NOR, FOR J=1 STEP 1 UNTIL NOR DO NIF[J]);                          1050
LIST LIST3 (FOR J=1 STEP 1 UNTIL NOR DO X[NIF[J]], Z );                        1060
LIST LIST4 (FOR J=1 STEP 1 UNTIL NOR DO [J,SIGA[1,J], SIGA[2,J],               1070
```

```
            X[NIF[J]], NUSIGF[1,J], NUSIGF[2,J], NIF[J],                    1080
            SIG1TO2[J], Z, D[1,J], D[2,J], BSQ, V[1,J], V[2,J] ));          1090
LIST LIST5 (     FOR I+1 STEP 1 UNTIL NOM DO OMEGA[I]);                     1100
LIST LIST6 (NOS);                                                           1110
LIST LIST23 (FOR I+1 STEP 1 UNTIL NOS DO [J, S[4×J+1], S[4×J+2],            1120
             S[4×J+3], S[4×J+4] ] ) ;                                       1130
LIST LIST7 (NPC      );                                                     1140
LIST LIST8 (FOR I+1 STEP 1 UNTIL NPC DO [BETA[I], LAMBDA[I]]);              1150
LIST LIST9 (FOR I+0 STEP 1 UNTIL NPT DO [I, X[I],       PHI[4×I+1],         1160
            PHI[4×I+3], PHI[4×I+2], PHI[4×I+4] ]);                          1170
LIST LIST10 (FOR J+1 STEP 1 UNTIL NOR DO SIGA[1,J]);                        1180
LIST LIST11 (FOR J+1 STEP 1 UNTIL NOR DO SIGA[2,J]);                        1190
LIST LIST12 (FOR J+1 STEP 1 UNTIL NOR DO NUSIGF[1,J]);                      1200
LIST LIST13 (FOR J+1 STEP 1 UNTIL NOR DO NUSIGF[2,J]);                      1210
LIST LIST14 (FOR J+1 STEP 1 UNTIL NOR DO D[1,J]);                           1220
LIST LIST15 (FOR J+1 STEP 1 UNTIL NOR DO D[2,J]);                           1230
LIST LIST16 (FOR J+1 STEP 1 UNTIL NOR DO SIG1TO2[J]);                       1240
LIST LIST17 (FOR J+1 STEP 1 UNTIL NOR DO V[1,J]);                           1250
LIST LIST17A(FOR J+1 STEP 1 UNTIL NOR DO V[2,J]);                           1260
LIST LIST18(FOR I+0 STEP 1 UNTIL NPT DO [I, X[I],       -S[4×I+1],          1270
          -S[4×I+3],-S[4×I+2],-S[4×I+4]]);                                  1280
LIST LIST19 (FOR I+1 STEP 1 UNTIL NPC DO [I, BETA[I], LAMBDA[I]]);          1290
LIST LIST20 (OMEGA[COUNT], ITR);                                            1300
LIST LIST21 (NOM );                                                         1310
LIST LIST22 (FOR I+0 STEP 1 UNTIL NPT DO [I, X[I], GAINF[I  ],              1320
             NGF[I  ], PHASEF[I  ], GAINT[I  ], NGT[I  ], PHASET[I  ]]);    1330
LIST LIST24 (ITER, Z, BSQ);                                                 1340
LIST LIST25 (TIME(0), TIME(2)/60, TIME(3)/60 );                             1350
LIST LIST36 (FOR I+0 STEP 1 UNTIL NPT DO NORF[I]);                          1360
LIST LIST37 (FOR I+0 STEP 1 UNTIL NPT DO NORT[I]);                          1370
LIST LIST38 (NORM,NCPS,NSLF,ID,CRIT,DVARY);                                 1380
LIST LIST39 (FOR J+I STEP 4 UNTIL 4×NPT+I DO PHI[J]);                       1390
%                                                                           1400
%     THE NEXT 4 CARDS CALL A DETERMINATE ROUTINE FROM THE LIBRARY          1410
$$  B T008                                                                 00000000
COMMENT     THE SCALE FACTOR 1.0@+01 HAS BEEN ADDED;                        00006350
```

```
D3:           DIAG ← A[I,I] ;  D ← D × DIAG × 1.0@+01 ;                    00006400
                                                                           99999999
PROCEDURE UTILA (FILID) ; FILE FILID ; %                                       1420
%     THIS PROCEDURE STORES CARDS ON TAPE                                      1430
%                                                                              1440
  BEGIN FILE CARDR   (5,10) ; ARRAY A[0:9] ; LABEL L ; %                       1450
  WHILE TRUE DO BEGIN %                                                        1460
    READ (CARDR,10,A[*])[L] ; %                                                1470
    WRITE(FILID,10,A[*]) ; %                                                   1480
  END ; %                                                                      1490
 L: REWIND (FILID) ; %                                                         1500
  END UTILA ; %                                                                1510
PROCEDURE     ITERATECGM(N,M,A,X,B,ILL);                                     1520
%     SOLVES A SYSTEM OF N EQUATIONS IN M UNKNOWNS BY THE                      1530
%     CONJUGATE GRADIENT METHOD                                                1540
%                                                                              1550
VALUE         N,M ;                                                          1560
INTEGER       N,M, ILL ;                                                     1570
ARRAY         A[0,0], X, B[0] ;                                              1580
        BEGIN                                                                  1590
INTEGER       I,I1,I2 ;                                                      1600
REAL          R1,R2,ALP,BET,C,CHECK,C2,CHECK2;                               1610
ARRAY         P[0:N],R[0:M],ATR[0:N],AP[0:M],XX[0:M] ;                       1620
LABEL   L8;                                                                    1630
              FOR I←1 STEP 1 UNTIL M DO X[I]←1.0;                              1640
              FOR I ← 1 STEP 1 UNTIL M DO                                      1650
        BEGIN                                                                  1660
              R1 ← 0 ;                                                         1670
              IF I≤4 THEN                                                      1680
              FOR I1←1 STEP 1 UNTIL I+4 DO                                     1690
              R1 ← R1 + A[I,I1] × X[I1] ;                                      1700
              IF I≥5 THEN IF I≤M-4 THEN                                        1710
              FOR I1←I-4 STEP 1 UNTIL I+4 DO                                   1720
              R1 ← R1 + A[I,I1] × X[I1] ;                                      1730
              IF I>M-4 THEN                                                    1740
              FOR I1←I-4 STEP 1 UNTIL M DO                                     1750
```

```
     R1 ← R1 + A[I,I1] × X[I1] ;                                    1760
     R[I] ← B[I] - R1 ;                                             1770
END ;                                                               1780
     FOR I ← 1 STEP 1 UNTIL N DO                                    1790
BEGIN                                                               1800
     R1 ← 0 ;                                                       1810
     IF I≤4 THEN                                                    1820
     FOR I1←1 STEP 1 UNTIL I+4 DO                                   1830
     R1 ← R1 + A[I1,I] × R[I1] ;                                    1840
     IF I≥5 THEN IF I≤N-4 THEN                                      1850
     FOR I1←I-4 STEP 1 UNTIL I+4 DO                                 1860
     R1 ← R1 + A[I1,I] × R[I1] ;                                    1870
     IF I>N-4 THEN                                                  1880
     FOR I1←I-4 STEP 1 UNTIL N DO                                   1890
     R1 ← R1 + A[I1,I] × R[I1] ;                                    1900
     P[I] ← R1 ;                                                    1910
     ATR[I] ← R1 ;                                                  1920
END ;                                                               1930
     FOR ILL ← 1 STEP 1 UNTIL 9×N DO                                1940
BEGIN                                                               1950
     FOR I ← 1 STEP 1 UNTIL M DO                                    1960
BEGIN                                                               1970
     R1 ← 0 ;                                                       1980
     IF I≤4 THEN                                                    1990
     FOR I1←1 STEP 1 UNTIL I+4 DO                                   2000
     R1 ← R1 + A[I,I1] × P[I1] ;                                    2010
     IF I≥5 THEN IF I≤M-4 THEN                                      2020
     FOR I1←I-4 STEP 1 UNTIL I+4 DO                                 2030
     R1 ← R1 + A[I,I1] × P[I1] ;                                    2040
     IF I>M-4 THEN                                                  2050
     FOR I1←I-4 STEP 1 UNTIL M DO                                   2060
     R1 ← R1 + A[I,I1] × P[I1] ;                                    2070
     AP[I] ← R1 ;                                                   2080
END ;                                                               2090
     R1 ← R2 ← 0 ;                                                  2100
     FOR I ← 1 STEP 1 UNTIL N DO                                    2110
```

```
      R2 ← R2 + ATR[I] × ATR[I] ;                                          2120
      FOR I ← 1 STEP 1 UNTIL M DO                                          2130
      R1 ← R1 + AP[I] × AP[I] ;                                            2140
      ALP ← R2 / R1 ;                                                      2150
      CHECK←0;                                                             2160
      CHECK2←0;                                                            2170
      FOR I ← 1 STEP 1 UNTIL N DO                                          2180
BEGIN                                                                      2190
      XX[I] ← X[I] ;                                                       2200
      X[I] ← X[I] + ALP ×  P[I] ;                                          2210
      C ← ABS(XX[I]/X[I] -1.0);                                            2220
      C2←ABS(XX[I]-X[I]);                                                  2230
      IF C>CHECK THEN CHECK ← C ;                                          2240
      IF C2>CHECK2 THEN CHECK2←C2;                                         2250
END ;                                                                      2260
      IF CHECK≤1.0@-05 THEN IF CHECK2≤1.0@-07 THEN GO TO L8;               2270
      FOR I ← 1 STEP 1 UNTIL M DO                                          2280
      R[I] ← R[I] - ALP × AP[I] ;                                          2290
      FOR I ← 1 STEP 1 UNTIL N DO                                          2300
BEGIN                                                                      2310
      R1 ← 0 ;                                                             2320
      IF I≤4 THEN                                                          2330
      FOR I1←1 STEP 1 UNTIL I+4 DO                                         2340
      R1 ← R1 + A[I1,I] × R[I1] ;                                          2350
      IF I≥5 THEN IF I≤N-4 THEN                                            2360
      FOR I1←I-4 STEP 1 UNTIL I+4 DO                                       2370
      R1 ← R1 + A[I1,I] × R[I1] ;                                          2380
      IF I>N-4 THEN                                                        2390
      FOR I1←I-4 STEP 1 UNTIL N DO                                         2400
      R1 ← R1 + A[I1,I] × R[I1] ;                                          2410
      ATR[I] ← R1 ;                                                        2420
END ;                                                                      2430
      R1 ← 0 ;                                                             2440
      FOR I ← 1 STEP 1 UNTIL N DO                                          2450
      R1 ← R1 + ATR[I] × ATR[I] ;                                          2460
      BET ← R1 / R2 ;                                                      2470
```

```
            FOR I ← 1 STEP 1 UNTIL N DO                                    2480
            P[I] ← BET × P[I] + ATR[I] ;                                   2490
         END ;                                                             2500
L8:      END ITERATECGM ;                                                  2510
%     ****    START OF THE PROGRAM    ****                                2520
%                                                                         2530
%                                                                         2540
      UTILA(CARD);                                                        2550
COMMENT READ INPUT DATA;                                                  2560
                                                                          2570
L0:   READ(CARD,FMT1,LIST1)(L3);  % TITLE                                 2580
      READ(CARD,FMT15,LIST38);    % OPTIONS                              2590
      READ(CARD,FMT2,LIST2);      % REGIONS AND INTERFACE NUMBERS        2600
      NPT ← NIF[NOR];                                                     2610
      READ(CARD,FMT3,LIST3);      % RADII AND HEIGHT                     2620
      READ(CARD,FMT8,LIST17);     % VELOCITY FOR GROUP 1                 2630
      READ(CARD,FMT8,LIST17A);    % VELOCITY FOR GROUP 2                 2640
      READ(CARD,FMT8,LIST10);     % SIGMA REMOVAL FOR GROUP 1            2650
      READ(CARD,FMT8,LIST11);     % SIGMA REMOVAL FOR GROUP 2            2660
      READ(CARD,FMT8,LIST12);     % NU SIGMA FISSION FOR GROUP 1         2670
      READ(CARD,FMT8,LIST13);     % NU SIGMA FISSION FOR GROUP 2         2680
      READ(CARD,FMT8,LIST14);     % DIFFUSION COEFFICIENT FOR GROUP 1    2690
      READ(CARD,FMT8,LIST15);     % DIFFUSION COEFFICIENT FOR GROUP 2    2700
      READ(CARD,FMT8,LIST16);     % SIGMA SCATTER GROUP 1 TO 2           2710
      READ(CARD,FMT2,LIST7);      % NUMBER OF PRECURSORS                 2720
      READ(CARD,FMT3,LIST8);      % BETAS AND LAMBDAS                    2730
      READ(CARD,FMT2 ,LIST21);    % NUMBER OF FREQUENCIES                2740
      READ(CARD,FMT3,LIST5);      % FREQUENCIES                          2750
      IF NORM=1 THEN BEGIN                                                2760
         READ(CARD,FMT3,LIST36);  % NORMALIZATION FOR GROUP 1            2770
         READ(CARD,FMT3,LIST37);  % NORMALIZATION FOR GROUP 2            2780
      END;                                                                2790
      BEFF←0;                                                             2800
      FOR I←1 STEP 1 UNTIL NPC DO  BEFF←BEFF+BETA[I];                     2810
      X[0]←0; NIF[0]←0;                                                   2820
      FOR J←1 STEP 1 UNTIL NOR DO                                         2830
```

```
      BEGIN                                                                    2840
      H[J] ←(X[NIF[J]]-X[NIF[J-1]])/(NIF[J]-NIF[J-1]);                         2850
         FOR N←NIF[J-1]+1 STEP 1 UNTIL NIF[J] DO                               2860
            X[N] ← X[N-1] + H[J];                                              2870
      END;                                                                     2880
      ITER←1;                                                                  2890
      BSQ ← (3.14159265/Z)↑2;                                                  2900
%        PRINT THE INPUT                                                       2910
      WRITE(PRINT[PAGE]);                                                      2920
      WRITE(PRINT,FMT1 ,LIST1 );                                               2930
      WRITE(PRINT,FMT10,LIST4);                                                2940
      WRITE(PRINT,FMT6);                                                       2950
      WRITE(PRINT,FMT7,LIST19);                                                2960
      WRITE(PRINT,FMT11,BEFF);                                                 2970
      COUNT←1;                                                                 2980
%     READ SOURCES                                                             2990
L8:   IF COUNT=1 THEN BEGIN                                                    3000
      FOR I←1 STEP 1 UNTIL 4×NIF[NOR]+4 DO S[I] ← 0 ;                          3010
      READ(CARD,FMT2,LIST6);       % NUMBER OF SOURCES                       3020
      READ(CARD,FMT4,LIST23);      % SOURCES                                 3030
      FOR I←1 STEP 1 UNTIL 4×NIF[NOR]+4 DO S[I] ← -S[I] ;                      3040
      WRITE(PRINT[PAGE]);                                                      3050
      WRITE(PRINT      ,FMT12);                                                3060
      WRITE(PRINT,FMT9);                                                       3070
      WRITE(PRINT,FMT5 ,LIST18);                                               3080
      END;                                                                     3090
%     INTEGRAL OF THE SOURCE TIMES VOLUME                                      3100
      SXV ← 0;                                                                 3110
      VOL ← 0.785398 × X[1]↑2 ;                                                3120
      FOR J←1 STEP 1 UNTIL 2 DO                                                3130
      SXV ← SQRT(S[J]↑2 + S[J+2]↑2) × VOL + SXV;                               3140
      FOR N←1 STEP 1 UNTIL NPT-1 DO                                            3150
      BEGIN                                                                    3160
      VOL ← 0.785398×( (X[N]+X[N+1] )↑2 - (X[N-1]+X[N])↑2 ) ;                  3170
      FOR J←4×N+1 STEP 1 UNTIL 4×N+2 DO                                        3180
      SXV ← SQRT(S[J]↑2 + S[J+2]↑2) × VOL + SXV;                               3190
```

```
      END;
      VOL ← 3.141592 × ( (X[NPT]*2) - (X[NPT-1] + X[NPT] )*2 / 4 ) ;
      FOR J←4×NPT+1 STEP 1 UNTIL 4×NPT+2 DO
      SXV ← SQRT(S[J]*2 + S[J+2]*2) × VOL + SXV;
L2:   FOR J←1 STEP 1 UNTIL NGR DO BEGIN
      SIGR[1,J] ← SIGA[1,J] + D[1,J] × BSQ ;
      SIGR[2,J] ← SIGA[2,J] + D[2,J] × BSQ ;
      END;
L1:   ;
BEGIN
REAL ARRAY   AA,CC[0:5], BB,DD,SIGTF[0:25], P,Q,R,T[0:2,0:25];
REAL   SUM1, SUM2, TEMP, W   ;
LABEL   L5;
ALPHA ARRAY   CHAR[0:80];
FILE   PTAPE 2(2,10);
FORMAT FMT19(X12,5("REGION"I2,X4) // ) ;
FORMAT FMT20("         D1 ="3R12.9 / "         D2 =" 3R12.9 /
             "     SIGR1 ="3R12.9 / "     SIGR2 =" 3R12.9 /
             "        AA ="3R12.9 / "        BB =" 3R12.9 /
             "        DD ="3R12.9 / "        T1 =" 3R12.9 /
             "        T2 ="3R12.9 / "   SIG1T02 =" 3R12.9 /
             "        Q1 ="3R12.9 / "        Q2 =" 3R12.9 /
             "        P1 ="3R12.9 / "        P2 =" 3R12.9 /
             "        R1 ="3R12.9 / "        R2 =" 3R12.9 ) ;
FORMAT FMT21( / "     EXD1 ="R12.9, "     EXD2 ="R12.9 //);
FORMAT FMT22("MODIFIED CROSS SECTIONS FOR CRAM", X10,"OMEGA ="R12.5//);
FORMAT FMT23("I"1I1,"D  1E-9          ",4E13.5);
FORMAT FMT24(X5," 1.0          ",4E13.5);
FORMAT FMT25(X5," 0.0          0.0          0.0          0.0          0"
            ,",0",X11);
FORMAT FMT26(X5," 1.0          0            0            0            0"
            ,X13);
FORMAT FMT27(X5," 0            ",3E13.5," 0",X13);
FORMAT FMT28(X5," 0            ",2E13.5," 0            ",1E13.5 );
FORMAT FMT29("*  REGION"113,"  NEXT 8CARDS ");
FORMAT FMT30("*  CROSS SECTIONS FOR CRAM ",X10,"OMEGA ="R12.5);
```

```
FORMAT FMT31("*  SOURCE ON NEXT 8 CARDS" / "I"1I1,"D  ",                    3560
            "1E-9          1E+9          1E+9          1E+9          1E+9"/  3570
        "      0.0           0.0           0.0           0.0           0.0"/  3580
        "      0.0           0.0           0.0           0.0           0.0"/  3590
        "      0.0           0.0           0.0           1.0           0.0"/  3600
        "      0.0           0.0           0.0           0.0           0.0"/  3610
        "      0.0           0.0           0.0           0.0           0.0"/  3620
        "      0.0           0.0           0.0           0.0           0.0"/  3630
        "      0.0           0.0           0.0           0.0           0.0"); 3640
FORMAT FMT32("*  HEIGHT="1R12.5,X9,"BUCKLING   ="1R12.9 );                   3650
FORMAT FMT33(80A1);                                                         3660
LIST LIST26(FOR J=1 STEP 1 UNTIL NOR  DO J ) ;                              3670
LIST LIST27(FORJ D[1,J],FORJ D[2,J],FORJ SIGR1[J] , FORJ SIGR2[J] ,         3680
            FORJ AA[J] , FORJ BB[NIF[J-1]+1] , FORJ DD[NIF[J-1]+1] ,        3690
            FORJ T[1,NIF[J-1]+1] , FORJ T[2,NIF[J-1]+1] ,                   3700
            FORJ SIG1TO2[J] ,                                               3710
            FORJ Q[1,NIF[J-1]+1], FORJ Q[2,NIF[J-1]+1],                     3720
            FORJ P[1,NIF[J-1]+1], FORJ P[2,NIF[J-1]+1],                     3730
            FORJ R[1,NIF[J-1]+1], FORJ R[2,NIF[J-1]+1] ) ;                  3740
LIST LIST28(J,D[1,J],D[1,J],D[2,J],D[2,J]);                                 3750
LIST LIST29(SIGR1[J],SIGR1[J],SIGR2[J],SIGR2[J]);                           3760
LIST LIST30(AA[J],-T[1,NIF[J-1]+1],SIG1TO2[J]);                             3770
LIST LIST31(T[1,NIF[J-1]+1],AA[J],SIG1TO2[J]);                              3780
LIST LIST32(BB[NIF[J-1]+1],-DD[NIF[J-1]+1],-T[2,NIF[J-1]+1]);               3790
LIST LIST33(DD[NIF[J-1]+1],BB[NIF[J-1]+1],T[2,NIF[J-1]+1]);                 3800
LIST LIST34(Z,BSQ);                                                         3810
LIST LIST35(FOR I=1 STEP 1 UNTIL 72 DO CHAR[I]);                            3820
COMMENT    COMPUTE CONSTANTS ;                                              3830
                                                                            3840
      W=OMEGA[COUNT];                                                       3850
      IF CRIT=1 THEN W=0;                                                   3860
      SUM1=0;                                                               3870
      IF BEFF#0 THEN                                                        3880
      FOR I=1 STEP 1 UNTIL NPC DO                                           3890
         SUM1= SUM1+ LAMBDA[I]*2 * BETA[I] / (W*2 + LAMBDA[I]*2 );          3900
      FOR J=1 STEP 1 UNTIL NOR DO                                           3910
```

```
      AA[J] ← (1 - BEFF + SUM1)×NUSIGF[1,J];                                    3920
   SUM2←0;                                                                      3930
   IF BEFF≠0 THEN                                                               3940
   FOR I←1 STEP 1 UNTIL NPC DO                                                  3950
      SUM2← SUM2+ W×LAMBDA[I]×BETA[I] / (W↑2 + LAMBDA[I]↑2);                    3960
   FOR J←1 STEP 1 UNTIL NOR DO                                                  3970
      CC[J] ← NUSIGF[1,J] × SUM2;                                               3980
                                                                                3990
COMMENT     INTERIOR POINTS;                                                    4000
   FOR J←1 STEP 1 UNTIL NOR DO                                                  4010
      FOR N←NIF[J-1]+1 STEP 1 UNTIL NIF[J] DO BEGIN                             4020
         TEMP ← 1.0/H[J] - 0.5/X[N];                                            4030
         P[1,N] ← D[1,J]×TEMP / H[J];                                           4040
         P[2,N] ← D[2,J]×TEMP / H[J];                                           4050
         TEMP ← 1.0/H[J] + 0.5/X[N];                                            4060
         R[1,N] ← D[1,J]×TEMP / H[J];                                           4070
         R[2,N] ← D[2,J]×TEMP / H[J];                                           4080
         BB[N] ← (1-BEFF+SUM1)×NUSIGF[2,J];                                     4090
         DD[N] ← NUSIGF[2,J]×SUM2;                                              4100
         Q[1,N]←AA[J]- SIGR[1,J] -   2×D[1,J]/H[J]↑2  ;                         4110
         Q[2,N]←-SIGR[2,J] -2×D[2,J]/H[J]↑2  ;                                  4120
         T[1,N] ← CC[J ] + W/V[1,J];                                            4130
         T[2,N] ← W/V[2,J];                                                     4140
         IF NCPS=1 THEN BEGIN                                                   4150
         Q[1,N] ← Q[1,N]    + 3 × D[1,J] × W↑2 / V[1,J]↑2;                      4160
         Q[2,N] ← Q[2,N]    + 3× D[2,J] × W↑2 / V[2,J]↑2;                       4170
         T[1,N] ← T[1,N] + W/V[1,J] × 3 × D[1,J] × SIGR[1,J];                   4180
         T[2,N] ← T[2,N] + W/V[2,J] × 3 × D[2,J] × SIGR[2,J];                   4190
         END;                                                                   4200
         SIGTF[N] ← SIG1TO2[J];                        END;                     4210
COMMENT     INTERFACE POINTS;                                                   4220
   FOR J←1 STEP 1 UNTIL NOR-1 DO BEGIN                                          4230
      N←NIF[J];                                                                 4240
      P[1,N] ← H[J] × P[1,N];                                                   4250
      P[2,N] ← H[J] × P[2,N];                                                   4260
      Q[1,N] ← H[J]×Q[1,N]/2+H[J+1]×Q[1,N+1]/2+(D[1,J]-D[1,J+1])                4270
```

```
                / (2×X[N]) ;                                                    4280
      Q[2,N] ← H[J]×Q[2,N]/2 + H[J+1]×Q[2,N+1]/2 +                              4290
                (D[2,J]-D[2,J+1])/ (2×X[N]) ;                                   4300
      R[1,N] ← D[1,J+1]×(1.0/H[J+1]+0.5/X[N]);                                  4310
      R[2,N] ← D[2,J+1]×(1.0/H[J+1]+0.5/X[N]);                                  4320
      T[1,N] ← (H[J]×T[1,N] + H[J+1]×T[1,N+1])/2;                               4330
      T[2,N] ← (H[J]×T[2,N] + H[J+1]×T[2,N+1])/2;                               4340
      BB[N]   ← (H[J]×BB[N]   + H[J+1]×BB[N+1]  )/2;                            4350
      DD[N]   ← (H[J]×DD[N]   + H[J+1]×DD[N+1]  )/2;                            4360
      SIGTF[N] ←(H[J]×SIGTF[N] + H[J+1]×SIGTF[N+1])/2;                          4370
      IF COUNT=1 THEN                                                           4380
      FOR I←4×N+1 STEP 1 UNTIL 4×N+4 DO                                         4390
      S[I] ← (H[J] + H[J+1]) × S[I] / 2;                                        4400
   END;                                                                         4410
COMMENT    RIGHT HAND BOUNDRY;                                                  4420
   N←NIF[NOR];                                                                  4430
   FOR I←1 STEP 1 UNTIL 2 DO                                                    4440
      EXD[I] ←  3×D[I,NOR]×(0.710466/(1+0.710466×                               4450
            (3×D[I,NOR]/(2×X[N]))));                                            4460
   Q[1,N] ← Q[1,N]×EXD[1]×H[NOR]/(2×D[1,NOR])+EXD[1]/(2×X[N])-1;                4470
   Q[2,N] ← Q[2,N]×EXD[2]×H[NOR]/(2×D[2,NOR])+EXD[2]/(2×X[N])-1;                4480
   P[1,N] ← P[1,N]×EXD[1]×H[NOR]/D[1,NOR];                                      4490
   P[2,N] ← P[2,N]×EXD[2]×H[NOR]/D[2,NOR];                                      4500
   T[1,N] ← T[1,N]×EXD[1]×H[NOR]/(2×D[1,NOR]);                                  4510
   T[2,N] ← T[2,N]×EXD[2]×H[NOR]/(2×D[2,NOR]);                                  4520
   BB[  N] ← BB[  N]×EXD[2]×H[NOR]/(2×D[2,NOR]);                                4530
   DD[  N] ← DD[  N]×EXD[2]×H[NOR]/(2×D[2,NOR]);                                4540
   SIGTF[N] ← SIGTF[N]×EXD[2]×H[NOR]/(2×D[2,NOR]);                              4550
      IF COUNT=1 THEN                                                           4560
   FOR I←4×N+1 STEP 2 UNTIL 4×N+3 DO BEGIN                                      4570
      S[I] ← S[I] × EXD[1] × H[NOR] / (2 × D[1,NOR]);                           4580
      S[I+1] ← S[I+1] × EXD[2] × H[NOR] / (2 × D[2,NOR]);                       4590
   END;                                                                         4600
%                                                                               4610
%     COMPUTE MODIFIED CROSS SECTIONS FOR CRAM                                  4620
%                                                                               4630
```

```
IF ID=1 THEN BEGIN                                                          4640
FOR J←1 STEP 1 UNTIL NOR DO BEGIN                                           4650
   SIGR1[J] ← SIGR[1,J] ;                                                   4660
   SIGR2[J] ← SIGR[2,J] ;                                                   4670
IF NCPS=1 THEN BEGIN                                                        4680
   SIGR1[J] ← SIGR1[ J] - 3×D[1,J]×W↑2/V[1,J]↑2 ;                           4690
   SIGR2[J] ← SIGR2[ J] - 3×D[2,J]×W↑2/V[2,J]↑2 ;                           4700
END;                                                                        4710
END ;                                                                       4720
WRITE (PRINT[PAGE]) ;                                                       4730
WRITE (PRINT,FMT1,LIST1);                                                   4740
WRITE (PRINT,FMT22,W) ;                                                     4750
WRITE (PRINT,FMT19,LIST26) ;                                                4760
WRITE (PRINT,FMT32,LIST34);                                                 4770
WRITE (PRINT,FMT20,LIST27) ;                                                4780
WRITE (PRINT,FMT21,EXD[1],EXD[2]) ;                                         4790
WRITE (PUNCH,FMT30,W);                                                      4800
WRITE (PUNCH,FMT32,LIST34);                                                 4810
FOR J←1 STEP 1 UNTIL NOR DO BEGIN                                           4820
   WRITE (PUNCH,FMT29,J);                                                   4830
   WRITE (PRINT,FMT29,J);                                                   4840
   WRITE (PTAPE,FMT23,LIST28);                                              4850
   WRITE (PTAPE,FMT24,LIST29);                                              4860
   WRITE (PTAPE,FMT25       );                                              4870
   WRITE (PTAPE,FMT26       );                                              4880
   WRITE (PTAPE,FMT27,LIST30);                                              4890
   WRITE (PTAPE,FMT28,LIST31);                                              4900
   WRITE (PTAPE,FMT28,LIST32);                                              4910
   WRITE (PTAPE,FMT27,LIST33);                                              4920
REWIND(PTAPE);                                                              4930
FOR K←1 STEP 1 UNTIL 8 DO BEGIN                                             4940
   READ (PTAPE,FMT33,LIST35);                                               4950
   FOR I←1 STEP 1 UNTIL 80 DO                                               4960
   IF CHAR[I] = "@" THEN  CHAR[I] ← "E" ;                                   4970
   WRITE (PRINT,FMT33,LIST35);                                              4980
   WRITE (PUNCH,FMT33,LIST35);                                              4990
```

```
        END;                                                                    5000
      REWIND(PTAPE);                                                            5010
      END;                                                                      5020
      WRITE (PUNCH,FMT31,J);                                                    5030
      WRITE (PRINT,FMT31,J);                                                    5040
      GO TO L7 ;                                                                5050
      END;                                                                      5060
COMMENT    LEFT HAND BOUNDRY;                                                   5070
      Q[1,0] ← Q[1,1] - 2×D[1,1]/H[1]↑2;                                        5080
      Q[2,0] ← Q[2,1] - 2×D[2,1]/H[1]↑2;                                        5090
      R[1,0] ← 4×D[1,1]/H[1]↑2;                                                 5100
      R[2,0] ← 4×D[2,1]/H[1]↑2;                                                 5110
      T[1,0] ← T[1,1];                                                          5120
      T[2,0] ← T[2,1];                                                          5130
      BB[0] ← BB[1];                                                            5140
      DD[0] ← DD[1];                                                            5150
      SIGTF[0] ← SIGTF[1];                                                      5160
                                                                                5170
COMMENT    LOAD COEFICIENT  MATRIX;                                             5180
      KK←(NPT+1)×4   ;                                                          5190
L5:   FOR I←1 STEP 1 UNTIL KK DO FOR J←1 STEP 1 UNTIL KK DO MTX[I,J]←0;         5200
      FOR M←0 STEP 1 UNTIL NPT DO BEGIN                                         5210
         N←4×M+1;                                                               5220
         MTX[N,N]      ← Q[1,M];                                                5230
         MTX[N,N+1]    ← BB[M];                                                 5240
         MTX[N,N+2]    ← T[1,M];                                                5250
         MTX[N,N+3]    ← DD[M];                                                 5260
         MTX[N+1,N]    ← SIGTF[M];                                              5270
         MTX[N+1,N+1] ← Q[2,M];                                                 5280
         MTX[N+1,N+3] ← T[2,M];                                                 5290
         MTX[N+2,N]    ← -T[1,M];                                               5300
         MTX[N+2,N+1] ← -DD[M];                                                 5310
         MTX[N+2,N+2] ← Q[1,M];                                                 5320
         MTX[N+2,N+3] ← BB[M];                                                  5330
         MTX[N+3,N+1] ← -T[2,M];                                                5340
         MTX[N+3,N+2] ← SIGTF[M];                                               5350
```

```
            MTX[N+3,N+3] ← Q[2,M];                                          5360
        END;                                                                5370
        FOR M←1 STEP 1 UNTIL NPT DO BEGIN                                   5380
            N←4×M+1;                                                        5390
            MTX[N,N-4]   ← P[1,M];                                          5400
            MTX[N+1,N-3] ← P[2,M];                                          5410
            MTX[N+2,N-2] ← P[1,M];                                          5420
            MTX[N+3,N-1] ← P[2,M];                                          5430
        END;                                                                5440
        FOR M←0 STEP 1 UNTIL NPT-1 DO BEGIN                                 5450
            N←4×M+1;                                                        5460
            MTX[N,N+4]   ← R[1,M];                                          5470
            MTX[N+1,N+5] ← R[2,M];                                          5480
            MTX[N+2,N+6] ← R[1,M];                                          5490
            MTX[N+3,N+7] ← R[2,M];                                          5500
        END;                                                                5510
                                                                            5520
COMMENT      SEARCH FOR CRITICAL DETERMINANT;                               5530
        IF CRIT=1 THEN BEGIN                                                5540
LABEL   L6;                                                                 5550
MONITOR PRINT(DET,ITER,VARY,Z);                                             5560
        EPS ←(KK+1)×10-10;                                                  5570
        DET ← DETERMINANT(KK,MTX,EPS) ;                                     5580
        IF DET=0 THEN BEGIN                                                 5590
L6;         CRIT←0;                                                         5600
            WRITE(PRINT,FMT16,LIST24);                                      5610
            GO TO L1;                                                       5620
        END;                                                                5630
        IF ITER=1 THEN BEGIN                                                5640
            ITER ←ITER + 1;                                                 5650
            VARY ← VARY + DVARY;                                            5660
            DET1 ← DET;                                                     5670
            GO TO L2;                                                       5680
        END;                                                                5690
        ITER ←ITER+1;                                                       5700
        DET2 ← DET ;                                                        5710
```

```
      DVARY ← -DET2 × DVARY/(DET2-DET1);                                    5720
      IF ABS(DVARY)≤1.0@-09 THEN GO TO L6 ;                                 5730
      VARY ← VARY + DVARY        ;                                          5740
         Z ← 3.14159265 × SQRT(1.0/VARY);                                   5750
      DET1 ← DET2;                                                          5760
      GO TO L2;                                                             5770
      END;                                                                  5780
END;                                                                        5790
                                                                            5800
%        SOLVE FOR THE FLUXS                                                5810
      FOR I←1 STEP 1 UNTIL KK DO PHI[I]←0 ;                                 5820
L4:   ITERATECGM(KK,KK,MTX,PHI,S,ITR);                                      5830
      FOR I←1 STEP 1 UNTIL KK DO PHI[I]←PHI[I]/SXV;                         5840
%     PUNCH FLUX CARDS                                                      5850
      IF NSLF=1 THEN                                                        5860
      BEGIN                                                                 5870
      WRITE(PUNCH,FMT1,LIST1);                                              5880
      I←1;                                                                  5890
      WRITE(PUNCH,FMT34A,OMEGA[COUNT]);                                     5900
      WRITE(PUNCH,FMT34,LIST39);                                            5910
      I←2;                                                                  5920
      WRITE(PUNCH,FMT34B,OMEGA[COUNT]);                                     5930
      WRITE(PUNCH,FMT34,LIST39);                                            5940
      I←3;                                                                  5950
      WRITE(PUNCH,FMT34C,OMEGA[COUNT]);                                     5960
      WRITE(PUNCH,FMT34,LIST39);                                            5970
      I←4;                                                                  5980
      WRITE(PUNCH,FMT34D,OMEGA[COUNT]);                                     5990
      WRITE(PUNCH,FMT34,LIST39);                                            6000
      END;                                                                  6010
%     GAIN AND PHASE CALCULATION                                            6020
      L←COUNT;                                                              6030
      FOR J←0 STEP 1 UNTIL NPT   DO BEGIN                                   6040
         N←4×J+1;                                                           6050
         GAINF[J] ← SQRT(PHI[N]↑2 + PHI[N+2]↑2);                            6060
         GAINT[J] ← SQRT(PHI[N+1]↑2 + PHI[N+3]↑2);                          6070
```

```
          IF NORM=0 THEN                                                          6080
          IF COUNT = 1 THEN BEGIN                                                 6090
          NORF[J] ← GAINF[J];                                                     6100
          NORT[J] ← GAINT[J];                                                     6110
          END;                                                                    6120
        NGF[J] ← GAINF[J] / NORF[J] ;                                             6130
        NGT[J] ← GAINT[J] / NORT[J] ;                                             6140
         PHASEF[J] ← ARCTAN(PHI[N+2     ] / PHI[N]) × 57.29578;                   6150
         IF PHI[N]<0 THEN PHASEF[J] ← PHASEF[J] - 180;                            6160
         IF PHASEF[J]>0 THEN PHASEF[J]←PHASEF[J]-360 ;                            6170
         PHASET[J] ← ARCTAN(PHI[N+3       ] / PHI[N+1       ])×57.29578;         6180
         IF PHI[N+1       ]<0 THEN PHASET[J] ← PHASET[J] - 180;                   6190
         IF PHASET[J]>0 THEN PHASET[J]←PHASET[J]-360 ;                            6200
      END;                                                                        6210
%     PRINT GAIN AND PHASE                                                        6220
      WRITE(PRINT[PAGE]);                                                         6230
      WRITE(PRINT,FMT13,LIST20);                                                  6240
      WRITE(PRINT,FMT9);                                                          6250
      WRITE(PRINT,FMT5,LIST9);                                                    6260
      WRITE(PRINT[PAGE]);                                                         6270
      WRITE(PRINT,FMT14,OMEGA[COUNT]);                                            6280
      WRITE(PRINT,FMT18,LIST22);                                                  6290
                                                                                  6300
L7:   IF COUNT<NOM THEN BEGIN                                                     6310
         COUNT←COUNT+1;                                                           6320
         GO TO L1 END;                                                            6330
      GO TO L0;                                                                   6340
L3:   WRITE(PRINT[PAGE]);                                                         6350
      WRITE(PRINT,FMT17,LIST25);
END.                                                                              6370
```

```
%                                   N O I S E                                    0
%                                                                               10
%      A PROGRAM TO CALCULATE THE SPACE DEPENDENT POWER SPECTRUM, CROSS         20
%      POWER SPECTRUM AND TRANSFER FUNCTION OF A NUCLEAR REACTOR AS             30
%      MEASURED IN TWO DETECTOR NOISE EXPERIMENTS                               40
%                                                                               50
%                              R N MACDONALD                                    60
%                         SCHOOL OF NUCLEAR ENGINEERING                         70
%                         GEORGIA INSTITUTE OF TECHNOLOGY                       80
%                              ATLANTA, GEORGIA                                 90
%                                MARCH 3, 1966                                 100
%                                                                              110
BEGIN                                                                          120
FILE IN CARD  0(2,10);                                                         130
FILE OUT PRINT 4(2,15);                                                        140
SAVE                                                                           150
ALPHA ARRAY   TITLE[0:12], SKIP[0:12];                                         160
SAVE                                                                           170
REAL  ARRAY    HFRE, HTRE, HFIM, HTIM[0:2,0:6,1:14,0:25 ], S[0:11,0:6 ];       180
SAVE                                                                           190
REAL ARRAY    FREAL,FIMAG,TREAL,TIMAG[0:25,0:20];                              200
INTEGER       I,J,K,L,NOM,NSL,NPT,NXPP,M,N;                                    210
SAVE                                                                           220
INTEGER ARRAY XPP[0:40], PINP,PRES[0:20];                                      230
SAVE                                                                           240
REAL  ARRAY   X[0:25], VOL,AREA[0:6 ], GRAD1,GRAD2[0:6 ];                      250
SAVE                                                                           260
REAL  ARRAY   SIGA1,SIGA2,SIGF1,SIGF2,SIGIT02, D1R,D2R,D1L,D2L[0:6 ];          270
SAVE                                                                           280
REAL ARRAY    PHI01,PHI02[0:6 ], OMEGA[0:20], PHI1,PHI2[0:6 ];                 290
SAVE                                                                           300
REAL ARRAY  GAINF,GAINT,PHASEF,PHASET[0:20,0:20], FPS,TPS[0:25,0:20];          310
SAVE                                                                           320
DEFINE   FORJ = FOR J←1 STEP 1 UNTIL NSL DO # ;                                350
DEFINE   FORI = FOR I←0 STEP 1 UNTIL NPT DO # ;                                360
DEFINE   FORL = FOR L←1 STEP 1 UNTIL NOM DO # ;                                370
```

```
FORMAT FMT1 (12A6);                                                          380
FORMAT FMT2 (6I12);                                                          390
FORMAT FMT3 (6E12.5);                                                        400
FORMAT FMT4 (X36,1R12.5);                                                    410
FORMAT FMT5(/ 40I5);                                                         420
FORMAT FMT6(/ 6R15.8);                                                       430
FORMAT FMT21 (X35,"NOISE SOURCE AMPLITUDE IN EACH REGION",///X5,             440
              "SOURCE",X46,"REGION",/X6,"TYPE              0          ",     450
              "     1                2                3              4",     460
              "                5                6" // );                      470
FORMAT FMT22 (/I8, 7R15.8);                                                  480
FORMAT FMT35(X35,"CROSS POWER SPECTRUM CALCULATION" ///, "      INPUT",      490
             "   RESPONSE          FAST              FAST           ",       500
             "THERMAL           THERMAL",/ "      POINT    POINT       ",    510
             "    REAL             IMAG.             REAL            ",     520
             " IMAG." /  );                                                  530
FORMAT FMT36(//X5, "OMEGA ="1R12.5);                                         540
FORMAT FMT37(X35,"TRANSFER FUNCTION CALCULATION" ///,    "      INPUT",      550
             "   RESPONSE          FAST              FAST           ",       560
             "THERMAL           THERMAL",/ "      POINT    POINT       ",    570
             "    GAIN             PHASE             GAIN            ",     580
             " PHASE"  /  );                                                 590
FORMAT FMT38(X20, "AUTO POWER SPECTRUM CALCULATION", X20,                    600
             "OMEGA =",1R12.5,///                                            610
             "         I    RADIUS            FAST             THERMAL" //);  620
FORMAT FMT39(I10,1R12.5,X5,1R15.8,X5,1R15.8);                                630
FORMAT FMT40(2I10,4(X5,1R15.8));                                             640
LIST LIST1 (FOR I=1 STEP 1 UNTIL 12 DO TITLE[I]);                            650
LIST LIST2 (NOM,NSL,NPT,NXPP);                                               660
LIST LIST3 (FORI  HFRE[K,J,L,I]);                                            670
LIST LIST4 (FORI  HTRE[K,J,L,I]);                                            680
LIST LIST5 (FORI  HFIM[K,J,L,I]);                                            690
LIST LIST6 (FORI  HTIM[K,J,L,I]);                                            700
LIST LIST7 (FORI X[I]);                                                      710
LIST LIST8 (FOR J=1 STEP 1 UNTIL NSL DO PHI1[J]);                            720
LIST LIST9 (FOR J=1 STEP 1 UNTIL NSL DO PHI2[J]);                            730
```

```
LIST LIST10 (FORJ VOL[J]);                                                    740
LIST LIST11 (AREA[0], FORJ AREA[J]);                                          750
LIST LIST12 (FORJ SIGA1[J]);                                                  760
LIST LIST13 (FORJ SIGA2[J]);                                                  770
LIST LIST14 (FORJ SIGF1[J]);                                                  780
LIST LIST15 (FORJ SIGF2[J]);                                                  790
LIST LIST16 (FORJ SIG1TO2[J]);                                                800
LIST LIST17 (D1L[0], FORJ D1L[J]);                                            810
LIST LIST18 (D2L[0], FORJ D2L[J]);                                            820
LIST LIST19 (GRAD1[0], FORJ GRAD1[J]);                                        830
LIST LIST20 (GRAD2[0], FORJ GRAD2[J]);                                        840
LIST LIST21 (PHI01[0], FORJ PHI01[J]);                                        850
LIST LIST22 (PHI02[0], FORJ PHI02[J]);                                        860
LIST LIST23 (D1R[0], FORJ D1R[J]);                                            870
LIST LIST24 (D2R[0], FORJ D2R[J]);                                            880
LIST LIST25 (FOR K←1 STEP 1 UNTIL NXPP DO [PINP[K],PRES[K]]);                 890
LIST LIST26 (FOR I←1 STEP 1 UNTIL 12 DO SKIP[I]);                             900
LIST LIST30 (FOR K←1 STEP 1 UNTIL 11 DO [K,FOR J←0 STEP 1 UNTIL 6             910
             DO [S[K,J]]] );                                                  920
LIST LIST42 (FORI [I,X[I],FPS[I,L],TPS[I,L] ]);                               930
LIST LIST40 (FOR I←1 STEP 1 UNTIL NXPP DO [PINP[I],PRES[I],                   940
             FREAL[I,L],FIMAG[I,L],TREAL[I,L],TIMAG[I,L] ]);                  950
LIST LIST41 (FOR I←1 STEP 1 UNTIL NXPP DO [PINP[I],PRES[I],                   960
             GAINF[I,L],PHASEF[I,L],GAINT[I,L],PHASET[I,L] ]);                970
      READ (CARD,FMT1,LIST1);      %    TITLE                                980
      READ (CARD, / ,LIST2);       %    NOM, NSL, NPT, NXPP                  990
%             NOM  =  NUMBER OF FREQUENCIES                                  1000
%             NSL  =  NUMBER OF SOURCE LOCATIONS                             1010
%             NPT  =  NUMBER OF SPACE POINTS                                 1020
%             NXPP =  NUMBER OF CROSS POWER POINTS                           1030
      READ (CARD, / ,LIST7);       %    RADIAL MESH IN CM                    1040
      READ (CARD, / ,LIST25);      %    POINTS FOR CROSS POWER SPECTRUM      1050
      READ (CARD, / ,LIST8);       %    STATIC FLUX, FAST GROUP              1060
      READ (CARD, / ,LIST9);       %    STATIC FLUX, THERMAL GROUP           1070
      READ (CARD, / ,LIST10);      %    SOURCE VOLUMES                       1080
      READ (CARD, / ,LIST11);      %    SOURCE REGION SURFACE AREAS          1090
```

```
FORJ BEGIN                                                                    1460
S[1,J] ← SQRT(2×PHI1[J]×SIGA1[J]×VOL[J]);                                     1470
S[2,J] ← SQRT(2×PHI2[J]×SIGA2[J]×VOL[J]);                                     1480
S[3,J] ← SQRT(2×PHI1[J]×SIG1TO2[J]×VOL[J]);                                   1490
S[4,J] ← S[3,J];                                                              1500
S[5,J] ← SQRT(2×PHI1[J]×SIGF1[J]×VOL[J]×(N2PN-2×NPN+PN) );                    1510
S[6,J] ← SQRT(2×PHI2[J]×SIGF2[J]×VOL[J]×N2PN);                                1520
S[7,J] ← SQRT(2×PHI2[J]×SIGF2[J]×VOL[J]);                                     1530
S[8,J] ← SQRT(ABS((PHI01[J]/2-D1L[J]  × GRAD1[J])×AREA[J]));                  1540
S[9,J] ← SQRT(ABS((PHI01[J]/2+D1R[J]  × GRAD1[J])×AREA[J]));                  1550
S[10,J] ← SQRT(ABS((PHI02[J]/2-D2L[J]  × GRAD2[J])×AREA[J]));                 1560
S[11,J] ← SQRT(ABS((PHI02[J]/2+D2R[J]  × GRAD2[J])×AREA[J]));                 1570
END;                                                                          1580
S[8,0] ←  SQRT((PHI01[0]/2 - D1L[0]×GRAD1[0])×AREA[0]);                       1590
S[9,0] ←  SQRT((PHI01[0]/2 + D1R[0]×GRAD1[0])×AREA[0]);                       1600
S[10,0] ← SQRT((PHI02[0]/2 - D2L[0]×GRAD2[0])×AREA[0]);                       1610
S[11,0] ← SQRT((PHI02[0]/2 + D2R[0]×GRAD2[0])×AREA[0]);                       1620
WRITE (PRINT[PAGE]);                                                          1630
WRITE (PRINT,FMT21);                                                          1640
WRITE (PRINT,FMT22,LIST30);                                                   1650
FOR J←1 STEP 1 UNTIL NSL DO                                                   1660
FOR K←1 STEP 1 UNTIL 2 DO                                                     1670
FORL                                                                          1680
BEGIN                                                                         1690
READ (CARD,FMT1,LIST26);     %     SKIPS AN ID CARD                           1700
READ (CARD,FMT4,OMEGA[L]);                                                    1710
READ (CARD,FMT3,LIST3);                                                       1720
READ (CARD,FMT4,OMEGA[L]);                                                    1730
READ (CARD,FMT3,LIST4);                                                       1740
READ (CARD,FMT4,OMEGA[L]);                                                    1750
READ (CARD,FMT3,LIST5);                                                       1760
READ (CARD,FMT4,OMEGA[L]);                                                    1770
READ (CARD,FMT3,LIST6);                                                       1780
END;                                                                          1790
FOR J←1 STEP 1 UNTIL NSL DO                                                   1800
FOR L←1 STEP 1 UNTIL NOM DO                                                   1810
```

```
      READ (CARD, / ,LIST12);      %    SIGMA ABSORPTION FAST                    1100
      READ (CARD, / ,LIST13);      %    SIGMA ABSORPTION THERMAL                 1110
      READ (CARD, / ,LIST14);      %    SIGMA FISSION FAST                       1120
      READ (CARD, / ,LIST15);      %    SIGMA FISSION THERMAL                    1130
      READ (CARD, / ,LIST16);      %    SIGMA DOWNSCATTER                        1140
      READ (CARD, / ,LIST17);      %    DIFFUSION COEFFICIENT FAST LEFT          1150
      READ (CARD, / ,LIST24);      %    DIFFUSION COEFFICIENT FAST RIGHT         1160
      READ (CARD, / ,LIST18);      %    DIFFUSION COEFFICIENT THERMAL LEF        1170
      READ (CARD, / ,LIST23);      %    DIFFUSION COEFFICIENT THERMAL RT.        1180
      READ (CARD, / ,LIST19);      %    FAST FLUX GRADIENT                       1190
      READ (CARD, / ,LIST20);      %    THERMAL FLUX GRADIENT                    1200
      READ (CARD, / ,LIST21);      %    INTERFACE FLUX FAST GROUP                1210
      READ (CARD, / ,LIST22);      %    INTERFACE FLUX THERMAL GROUP             1220
WRITE (PRINT,FMT1 ,LIST1 );                                                     1230
WRITE (PRINT,FMT5 ,LIST2 );                                                     1240
WRITE (PRINT,FMT6 ,LIST7 );                                                     1250
WRITE (PRINT,FMT5 ,LIST25);                                                     1260
WRITE (PRINT,FMT6 ,LIST8 );                                                     1270
WRITE (PRINT,FMT6 ,LIST9 );                                                     1280
WRITE (PRINT,FMT6 ,LIST10);                                                     1290
WRITE (PRINT,FMT6 ,LIST11);                                                     1300
WRITE (PRINT,FMT6 ,LIST12);                                                     1310
WRITE (PRINT,FMT6 ,LIST13);                                                     1320
WRITE (PRINT,FMT6 ,LIST14);                                                     1330
WRITE (PRINT,FMT6 ,LIST15);                                                     1340
WRITE (PRINT,FMT6 ,LIST16);                                                     1350
WRITE (PRINT,FMT6 ,LIST17);                                                     1360
WRITE (PRINT,FMT6 ,LIST24);                                                     1370
WRITE (PRINT,FMT6 ,LIST18);                                                     1380
WRITE (PRINT,FMT6 ,LIST23);                                                     1390
WRITE (PRINT,FMT6 ,LIST19);                                                     1400
WRITE (PRINT,FMT6 ,LIST20);                                                     1410
WRITE (PRINT,FMT6 ,LIST21);                                                     1420
WRITE (PRINT,FMT6 ,LIST22);                                                     1430
%     FOR U235 USE THE FOLLOWING FISSION PARAMETERS                             1440
      PN=1;   NPN=2.43;   N2PN=4.36;                                            1450
```

```
      BEGIN                                                                    1820
INTEGER     I;                                                                 1830
PROCEDURE POWERSPEC;                                                           1840
BEGIN                                                                          1850
      FOR I←1 STEP 1 UNTIL NXPP DO                                             1860
      BEGIN                                                                    1870
      M ← PINP[I];                                                             1880
      N ← PRES[I];                                                             1890
      FREAL[I,L] ← RESFR[M]×RESFR[N] + RESFI[M]×RESFI[N] + FREAL[I,L];         1900
      FIMAG[I,L] ← RESFR[M]×RESFI[N] - RESFI[M]×RESFR[N] + FIMAG[I,L];         1910
      TREAL[I,L] ← RESTR[M]×RESTR[N] + RESTI[M]×RESTI[N] + TREAL[I,L];         1920
      TIMAG[I,L] ← RESTR[M]×RESTI[N] - RESTI[M]×RESTR[N] + TIMAG[I,L];         1930
      END;                                                                     1940
      FORI                                                                     1950
      BEGIN                                                                    1960
      FPS[I,L] ← RESFR[I]↑2 + RESFI[I]↑2 + FPS[I,L];                           1970
      TPS[I,L] ← RESTR[I]↑2 + RESTI[I]↑2 + TPS[I,L];                           1980
      END;                                                                     1990
END POWERSPEC;                                                                 2000
% 1.  FAST ABSORPTION                                                          2010
      FORI BEGIN                                                               2020
      RESFR[I] ← HFRE[1,J,L,I]×S[1,J];                                         2030
      RESTR[I] ← HTRE[1,J,L,I]×S[1,J];                                         2040
      RESFI[I] ← HFIM[1,J,L,I]×S[1,J];                                         2050
      RESTI[I] ← HTIM[1,J,L,I]×S[1,J];                                         2060
      END;                                                                     2070
                                                                               2080
      POWERSPEC;                                                               2090
% 2.  THERMAL ABSORPTION                                                       2100
      FORI BEGIN                                                               2110
      RESFR[I] ← HFRE[2,J,L,I] × S[2,J];                                       2120
      RESTR[I] ← HTRE[2,J,L,I] × S[2,J];                                       2130
      RESFI[I] ← HFIM[2,J,L,I] × S[2,J];                                       2140
      RESTI[I] ← HTIM[2,J,L,I] × S[2,J];                                       2150
      END;                                                                     2160
      POWERSPEC;                                                               2170
```

```
% 3.  DOWNSCATTERING                                                          2180
     FORI BEGIN                                                              2190
     RESFR[I] ← ( -HFRE[1,J,L,I]    + HFRE[2,J,L,I])×S[3,J];                 2200
     RESTR[I] ← ( -HTRE[1,J,L,I]    + HTRE[2,J,L,I])×S[3,J];                 2210
     RESFI[I] ← ( -HFIM[1,J,L,I]    + HFIM[2,J,L,I])×S[3,J];                 2220
     RESTI[I] ← ( -HTIM[1,J,L,I]    + HTIM[2,J,L,I])×S[3,J];                 2230
     END;                                                                    2240
     POWERSPEC;                                                              2250
% 4.  FAST FISSION                                                           2260
     FORI BEGIN                                                              2270
     RESFR[I] ← HFRE[1,J,L,I] × S[5,J];                                      2280
     RESTR[I] ← HTRE[1,J,L,I] × S[5,J];                                      2290
     RESFI[I] ← HFIM[1,J,L,I] × S[5,J];                                      2300
     RESTI[I] ← HTIM[1,J,L,I] × S[5,J];                                      2310
     END;                                                                    2320
     POWERSPEC;                                                              2330
% 5.  THERMAL FISSION                                                        2340
     FORI BEGIN                                                              2350
     RESFR[I] ← HFRE[1,J,L,I]×S[6,J]-HFRE[2,J,L,I]×S[7,J];                   2360
     RESTR[I] ← HTRE[1,J,L,I]×S[6,J]-HTRE[2,J,L,I]×S[7,J];                   2370
     RESFI[I] ← HFIM[1,J,L,I]×S[6,J]-HFIM[2,J,L,I]×S[7,J];                   2380
     RESTI[I] ← HTIM[1,J,L,I]×S[6,J]-HTIM[2,J,L,I]×S[7,J];                   2390
     END;                                                                    2400
     POWERSPEC;                                                              2410
% 6.  FAST CURRENT IN FROM THE LEFT                                          2420
     FORI BEGIN                                                              2430
     RESFR[I] ←(HFRE[1,J,L,I] - HFRE[1,J-1,L,I]) × S[8,J-1];                 2440
     RESTR[I] ←(HTRE[1,J,L,I] - HTRE[1,J-1,L,I]) × S[8,J-1];                 2450
     RESFI[I] ←(HFIM[1,J,L,I] - HFIM[1,J-1,L,I]) × S[8,J-1];                 2460
     RESTI[I] ←(HTIM[1,J,L,I] - HTIM[1,J-1,L,I]) × S[8,J-1];                 2470
     END;                                                                    2480
     POWERSPEC;                                                              2490
% 7.  FAST CURRENT IN FROM THE RIGHT                                         2500
     FORI BEGIN                                                              2510
     RESFR[I] ← (HFRE[1,J,L,I] - HFRE[1,J+1,L,I]) × S[9,J];                  2520
     RESTR[I] ← (HTRE[1,J,L,I] - HTRE[1,J+1,L,I]) × S[9,J];                  2530
```

```
      RESFI[I] ← (HFIM[1,J,L,I] - HFIM[1,J+1,L,I]) × S[9,J];                    2540
      REST I[I] ← (HTIM[1,J,L,I] - HTIM[1,J+1,L,I]) × S[9,J];                   2550
      END;                                                                      2560
      POWERSPEC;                                                                2570
% 8.  FAST CURRENT OUT TO THE LEFT                                             2580
      FORI BEGIN                                                                2590
      RESFR[I] ← (-HFRE[1,J,L,I] + HFRE[1,J-1,L,I])× S[9,J-1];                  2600
      REST R[I] ← (-HTRE[1,J,L,I] + HTRE[1,J-1,L,I])× S[9,J-1];                 2610
      RESFI[I] ← (-HFIM[1,J,L,I] + HFIM[1,J-1,L,I])× S[9,J-1];                  2620
      REST I[I] ← (-HTIM[1,J,L,I] + HTIM[1,J-1,L,I])× S[9,J-1];                 2630
      END;                                                                      2640
      POWERSPEC;                                                                2650
% 9.  FAST CURRENT OUT TO THE RIGHT                                            2660
      FORI BEGIN                                                                2670
      RESFR[I] ← (-HFRE[1,J,L,I] + HFRE[1,J+1,L,I]) × S[8,J];                   2680
      REST R[I] ← (-HTRE[1,J,L,I] + HTRE[1,J+1,L,I]) × S[8,J];                  2690
      RESFI[I] ← (-HFIM[1,J,L,I] + HFIM[1,J+1,L,I]) × S[8,J];                   2700
      REST I[I] ← (-HTIM[1,J,L,I] + HTIM[1,J+1,L,I]) × S[8,J];                  2710
      END;                                                                      2720
      POWERSPEC;                                                                2730
% 10. THERMAL CURRENT IN FROM THE LEFT                                         2740
      FORI BEGIN                                                                2750
      RESFR[I] ← (HFRE[2,J,L,I] - HFRE[2,J-1,L,I]) ×S[10,J-1];                  2760
      REST R[I] ← (HTRE[2,J,L,I] - HTRE[2,J-1,L,I]) ×S[10,J-1];                 2770
      RESFI[I] ← (HFIM[2,J,L,I] - HFIM[2,J-1,L,I]) ×S[10,J-1];                  2780
      REST I[I] ← (HTIM[2,J,L,I] - HTIM[2,J-1,L,I]) ×S[10,J-1];                 2790
      END;                                                                      2800
      POWERSPEC;                                                                2810
% 11. THERMAL CURRENT IN FROM THE RIGHT                                        2820
      FORI BEGIN                                                                2830
      RESFR[I] ← (HFRE[2,J,L,I] - HFRE[2,J+1,L,I]) ×S[11,J];                    2840
      REST R[I] ← (HTRE[2,J,L,I] - HTRE[2,J+1,L,I]) ×S[11,J];                   2850
      RESFI[I] ← (HFIM[2,J,L,I] - HFIM[2,J+1,L,I]) ×S[11,J];                    2860
      REST I[I] ← (HTIM[2,J,L,I] - HTIM[2,J+1,L,I]) ×S[11,J];                   2870
      END;                                                                      2880
      POWERSPEC;                                                                2890
```

```
% 12. THERMAL CURRENT OUT TO THE LEFT                                    2900
      FORI BEGIN                                                        2910
      RESFR[I] ← (-HFRE[2,J,L,I] + HFRE[2,J-1,L,I]) ×S[11,J-1];         2920
      RESTR[I] ← (-HTRE[2,J,L,I] + HTRE[2,J-1,L,I]) ×S[11,J-1];         2930
      RESFI[I] ← (-HFIM[2,J,L,I] + HFIM[2,J-1,L,I]) ×S[11,J-1];         2940
      RESTI[I] ← (-HTIM[2,J,L,I] + HTIM[2,J-1,L,I]) ×S[11,J-1]          2950
      END;                                                              2960
      POWERSPEC;                                                        2970
% 13. THERMAL CURRENT OUT TO THE RIGHT                                  2980
      FORI BEGIN                                                        2990
      RESFR[I] ← (-HFRE[2,J,L,I] + HFRE[2,J+1,L,I]) ×S[10,J];           3000
      RESTR[I] ← (-HTRE[2,J,L,I] + HTRE[2,J+1,L,I]) ×S[10,J];           3010
      RESFI[I] ← (-HFIM[2,J,L,I] + HFIM[2,J+1,L,I]) ×S[10,J];           3020
      RESTI[I] ← (-HTIM[2,J,L,I] + HTIM[2,J+1,L,I]) ×S[10,J]            3030
      END;                                                              3040
      POWERSPEC;                                                        3050
      END;                                                              3060
%     CALCULATE GAIN AND PHASE OF THE TRANSFER FUNCTION                 3070
      FOR L←1 STEP 1 UNTIL NOM DO                                       3080
      FOR I←1 STEP 1 UNTIL NXPP DO                                      3090
      BEGIN                                                             3100
      J ← PINP[I];                                                      3110
      GAINF[I,L] ← SQRT(FREAL[I,L]*2 + FIMAG[I,L]*2) / FPS[J,L];        3120
      GAINT[I,L] ← SQRT(TREAL[I,L]*2 + TIMAG[I,L]*2) / TPS[J,L];        3130
      PHASEF[I,L] ← ARCTAN(FIMAG[I,L]/FREAL[I,L]) × 57.29578;           3140
      PHASET[I,L] ← ARCTAN(TIMAG[I,L]/TREAL[I,L]) × 57.29578;           3150
      IF FREAL[I,L]<0 THEN PHASEF[I,L]←PHASEF[I,L]-180;                 3160
      IF TREAL[I,L]<0 THEN PHASET[I,L]←PHASET[I,L]-180;                 3170
      END;                                                              3180
%     CALCULATE THE AMPLITUDE OF THE AUTO POWER SPECTRA                 3190
      FORI                                                              3200
      FORL                                                              3210
      BEGIN                                                             3220
      FPS[I,L] ← SQRT(FPS[I,L]);                                        3230
      TPS[I,L] ← SQRT(TPS[I,L]);                                        3240
      END;                                                              3250
```

```
%     PRINT THE RESULTS                                                    3260
      WRITE (PRINT[PAGE])};                                                3270
      FOR L←1 STEP 1 UNTIL NOM DO                                          3280
      BEGIN                                                                3290
      WRITE (PRINT,FMT38,OMEGA[L])};                                       3300
      WRITE (PRINT,FMT39,LIST42)};                                         3310
      WRITE (PRINT[PAGE])};                                                3320
      END};                                                                3330
                                                                           3340
      WRITE (PRINT,FMT35)};                                                3350
      FOR L←1 STEP 1 UNTIL NOM DO                                          3360
      BEGIN                                                                3370
      WRITE (PRINT,FMT36,OMEGA[L])};                                       3380
      WRITE (PRINT,FMT40,LIST40)};                                         3390
      END};                                                                3400
      WRITE (PRINT[PAGE])};                                                3410
      WRITE (PRINT,FMT37)};                                                3420
      FOR L←1 STEP 1 UNTIL NOM DO                                          3430
      BEGIN                                                                3440
      WRITE (PRINT,FMT36,OMEGA[L])};                                       3450
      WRITE (PRINT,FMT40,LIST41)};                                         3460
      END};                                                                3470
END.                                                                       3480
```

APPENDIX C

DESCRIPTION OF THE REACTORS STUDIED

APPENDIX C

DESCRIPTION OF THE REACTORS STUDIED

The NORA Reactor

NORA is a critical assembly used for studies in reactor physics and kinetics. The fuel is of natural and enriched uranium in D_2O and mixed D_2O/H_2O moderators. In the experiments analyzed, the reactor had the following characteristics:

Fuel: UO_2, three percent enriched, 112 stringers with diameter $\approx$ 12 mm.

Moderator: D_2O, 99.605 percent.

Lattice: Square, pitch 10 cm.

Core dimensions: Diameter, 119.4 cm; height 109.6 cm.

Side reflector: D_2O, 52.8 cm; Graphite, 50 cm.

Bottom reflector: D_2O, 10 cm; Graphite, 70 cm.

The pile oscillator consisted of three sets of cadmium disks rotating past each other, giving a reactivity signal very close to a sine wave. The oscillator was placed 7.1 cm off the centerline of the core and the flux response was measured by detectors placed at 7.9, 17.7, 37.6, 62.5, and 114.2 cm from the core centerline.

The cross sections used for the analysis were obtained from Dr. P. T. Hansson (43) and are the same set used for the original analog studies (25). The macroscopic cross sections, mesh spacing, and dimensions of the system are given in Table 3. The delayed neutron fractions and

Table 3. Macroscopic Cross Sections for NORA

	Group 1	Group 2		
Region 1				
Sigma removal	= 0.00991400	0.00365400	Radius	= 59.70000
Nu sigma fission	= 0.00000000	0.00556020	Interface No.	= 15
Sigma transfer	= 0.00967580		Height	= 133.52113
Diffusion coef.	= 1.29196700	0.81795700	Buckling	= 0.000553605
Velocity, cm/sec	= 2.00000@+06	2.20000@+05		
Region 2				
Sigma removal	= 0.01090000	0.00011100	Radius	= 112.50000
Nu sigma fission	= 0.00000000	0.00000000	Interface No.	= 21
Sigma transfer	= 0.01090000		Height	= 133.52113
Diffusion coef.	= 1.30500000	0.82550000	Buckling	= 0.000553605
Velocity, cm/sec	= 2.00000@+06	2.20000@+05		
Region 3				
Sigma removal	= 0.00282000	0.00082500	Radius	= 162.50000
Nu sigma fission	= 0.00000000	0.00000000	Interface No.	= 25
Sigma transfer	= 0.00282000		Height	= 133.52113
Diffusion coef.	= 1.19200000	1.05000000	Buckling	= 0.000553605
Velocity, cm/sec	= 2.00000@+06	2.20000@+05		

Table 4. Delayed Neutron Constants for NORA

I	Beta[I]	Lambda [I]
1	0.00025	0.01270
2	0.00140	0.03170
3	0.00125	0.11500
4	0.00270	0.31100
5	0.00087	1.40000
6	0.00018	3.87000
7	0.00048	0.27800
8	0.00015	0.01690
9	0.00005	0.00490
10	0.00003	0.00152
11	0.00002	0.00043
12	0.00002	0.00012
13	2.00000@-06	0.00004
14	7.00000@-07	3.70000@-06

Beta effective = 0.00739

precursor decay constants are given in Table 4.

The Georgia Tech Research Reactor

The GTRR is a heterogeneous, heavy water moderated and cooled reactor, fueled with highly enriched plates of uranium-aluminum alloy. A plan view of the reactor is shown in Figure 42. A complete description may be found in reference 49.

The reactor core is approximately two feet in diameter, two feet high, and when fully loaded contains 19 fuel elements on a six inch triangular pitch. Each assembly is of the MTR type and contains ten plates. The total uranium content is 2.7 kg. The fuel is centrally located in a six foot diameter aluminum tank which provides a two foot thick D_2O reflector on all sides of the core. The tank is suspended in a graphite cup which provides an additional two feet of reflector radially and beneath the vessel.

For the reactor noise measurements, the core loading was twelve elements. The elements were arranged symmetrically about the center as shown in Figure 42. The central position was left vacant to make room for one of the ionization chambers. The second detector was placed in the H-1 beam port just outside the core (radius = 53.2 cm) or at the D_2O-graphite interface (radius = 91.44 cm).

In order to obtain one-dimensional symmetry, the reactor was homogenized into five regions:

1. Central D_2O, 11.43 cm, 4 mesh intervals
2. First fuel ring, 7.62 cm, 3 mesh intervals
3. Second fuel ring, 11.176 cm, 4 mesh intervals

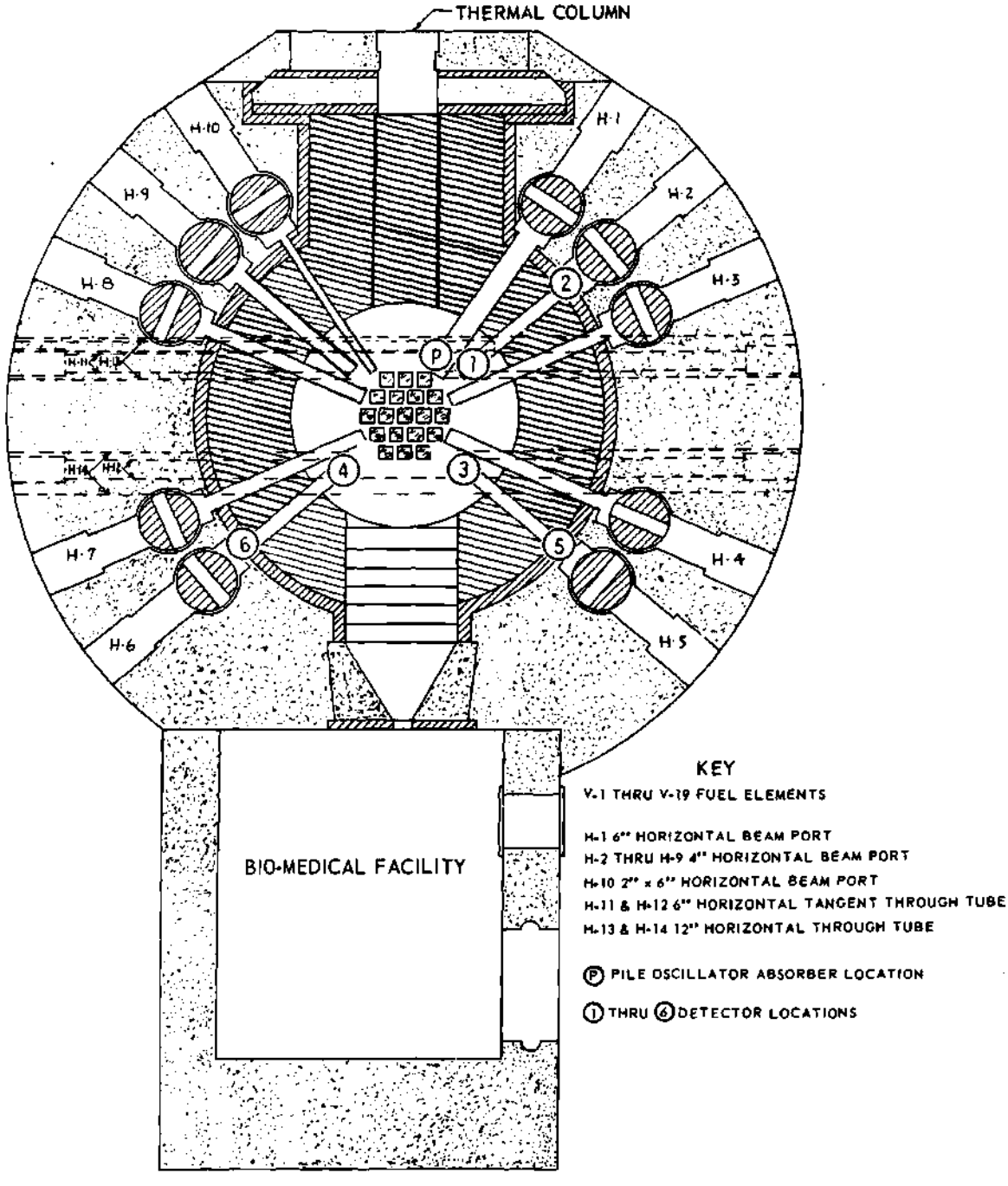

Figure 42. Horizontal Section of the GTRR at the Core Midplane

4. D_2O reflector, 61.214 cm, 8 mesh intervals

5. Graphite reflector, 60.96 cm, 6 mesh intervals.

The macroscopic cross sections for these regions are given in Table 5. They were obtained by volume weighting a set of macroscopic cross sections prepared for the GTRR by Dr. Don Roy of the Babcock-Wilcox Company, Lynchburg, Virginia. A complete description of the procedure for obtaining the cross sections may be found in reference 35. Delayed neutron data are those measured by Graham (50) for the GTRR and are given in Table 6.

Table 5. Macroscopic Cross Sections for the GTRR

	Group 1	Group 2		
Region 1				
Sigma removal	= 0.01198224	0.00007510	Radius	= 11.43000
Nu sigma fission	= 0.00000000	0.00000000	Interface No.	= 4
Sigma transfer	= 0.01198000		Height	= 75.96500
Diffusion coef.	= 1.87700000	0.84000000	Buckling	= 0.001710301
Velocity, cm/sec	= 2.00000@+06	2.86880@+05		
Region 2				
Sigma removal	= 0.01068040	0.02454600	Radius	= 19.05000
Nu sigma fission	= 0.00186230	0.04740000	Interface No.	= 7
Sigma transfer	= 0.00931754		Height	= 75.96500
Diffusion coef.	= 1.71997700	0.91738400	Buckling	= 0.001710301
Velocity, cm/sec	= 2.00000@+06	2.98870@+05		
Region 3				
Sigma removal	= 0.01143300	0.01039100	Radius	= 30.22600
Nu sigma fission	= 0.00078500	0.01998100	Interface No.	= 11
Sigma transfer	= 0.01085765		Height	= 75.96500
Diffusion coef.	= 1.80744100	0.87097100	Buckling	= 0.001710301
Velocity, cm/sec	= 2.00000@+06	2.91930@+05		
Region 4				
Sigma removal	= 0.01883684	0.00008540	Radius	= 91.44000
Nu sigma fission	= 0.00000000	0.00000000	Interface No.	= 19
Sigma transfer	= 0.01880000		Height	= 75.96500
Diffusion coef.	= 1.27400000	0.79400000	Buckling	= 0.001710301
Velocity, cm/sec	= 2.00000@+06	2.48160@+05		

Table 5. Macroscopic Cross Sections for the GTRR (Concluded)

	Group 1	Group 2		
Region 5				
Sigma removal	= 0.00656123	0.00025500	Radius	= 152.40000
Nu sigma fission	= 0.00000000	0.00000000	Interface No.	= 25
Sigma transfer	= 0.00655000		Height	= 75.96500
Diffusion coef.	= 0.96940000	0.83100000	Buckling	= 0.001710301
Velocity, cm/sec	= 2.00000@+06	2.48160@+05		

Table 6. Delayed Neutron Constants for the GTRR

I	Beta[I]	Lambda [I]
1	0.00185000	1.96000000
2	0.00061200	0.44100000
3	0.00206000	0.28800000
4	0.00121000	0.11700000
5	0.00150000	0.03050000
6	0.00025400	0.00925000
7	0.00002330	0.00227000
8	0.00001510	0.00077300
9	0.00001070	0.00031500
10	0.00001700	0.00011800
11	0.00000379	0.00005850
12	0.00000021	0.00001370

Beta effective = 0.00755610

APPENDIX D

SAMPLE PROBLEMS FOR THE NORA REACTOR

APPENDIX D

SAMPLE PROBLEMS FOR THE NORA REACTOR

Two sample problems for the NORA reactor having the critical height and frequency of 100 radians per second. The first problem was done with CHARLIE using the option to punch the modified cross sections for CRAM. The second is the CRAM problem with the special subroutine TEMPB 3 which computes gain and phase angle.

SAMPLE PROBLEM FOR CHARLIE
NORA REACTOR CRITICAL HEIGHT (USING THE DIFFUSION EQN.)

REGION 1	GROUP 1	GROUP 2		
SIGMA REMOVAL =	0.00991400	0.00365400	RADIUS =	59.70000
NU SIGMA FISSION =	0.00000000	0.00556020	INTERFACE NO. =	15
SIGMA TRANSFER =	0.00967580		HEIGHT =	133.52113
DIFFUSION COEF. =	1.29196700	0.81795700	BUCKLING =	0.000553605
VELOCITY, CM/SEC =	2.00000E+06	2.20000E+05		

REGION 2	GROUP 1	GROUP 2		
SIGMA REMOVAL =	0.01090000	0.00011100	RADIUS =	112.50000
NU SIGMA FISSION =	0.00000000	0.00000000	INTERFACE NO. =	21
SIGMA TRANSFER =	0.01090000		HEIGHT =	133.52113
DIFFUSION COEF. =	1.30500000	0.82550000	BUCKLING =	0.000553605
VELOCITY, CM/SEC =	2.00000E+06	2.20000E+05		

REGION 3	GROUP 1	GROUP 2		
SIGMA REMOVAL =	0.00282000	0.00002500	RADIUS =	162.50000
NU SIGMA FISSION =	0.00000000	0.00000000	INTERFACE NO. =	25
SIGMA TRANSFER =	0.00282000		HEIGHT =	133.52113
DIFFUSION COEF. =	1.19200000	1.05000000	BUCKLING =	0.000553605
VELOCITY, CM/SEC =	2.00000E+06	2.20000E+05		

I	BETA[I]	LAMBDA[I]
1	0.00025	0.01270
2	0.00140	0.03170
3	0.00125	0.11500
4	0.00270	0.31100
5	0.00087	1.40000
6	0.00018	3.87000
7	0.00048	0.27800
8	0.00015	0.01690
9	0.00005	0.00490
10	0.00003	0.00152
11	0.00002	0.00043
12	0.00002	0.00012
13	2.00000E-06	0.00004
14	7.00000E-07	3.70000E-06

BETA EFFECTIVE = 0.00739

INPUT SOURCE

I	RADIUS, CM	FAST REAL	FAST IMAG.	SLOW REAL	SLOW IMAG.
0	0.00000000	0.00000000	0.00000000	1.00000000	0.00000000
1	3.98000000	0.00000000	0.00000000	0.00000000	0.00000000
2	7.96000000	0.00000000	0.00000000	0.00000000	0.00000000
3	11.94000000	0.00000000	0.00000000	0.00000000	0.00000000
4	15.92000000	0.00000000	0.00000000	0.00000000	0.00000000
5	19.90000000	0.00000000	0.00000000	0.00000000	0.00000000
6	23.88000000	0.00000000	0.00000000	0.00000000	0.00000000
7	27.86000000	0.00000000	0.00000000	0.00000000	0.00000000
8	31.84000000	0.00000000	0.00000000	0.00000000	0.00000000
9	35.82000000	0.00000000	0.00000000	0.00000000	0.00000000
10	39.80000000	0.00000000	0.00000000	0.00000000	0.00000000
11	43.78000000	0.00000000	0.00000000	0.00000000	0.00000000
12	47.76000000	0.00000000	0.00000000	0.00000000	0.00000000
13	51.74000000	0.00000000	0.00000000	0.00000000	0.00000000
14	55.72000000	0.00000000	0.00000000	0.00000000	0.00000000
15	59.70000000	0.00000000	0.00000000	0.00000000	0.00000000
16	63.50000000	0.00000000	0.00000000	0.00000000	0.00000000
17	77.30000000	0.00000000	0.00000000	0.00000000	0.00000000
18	86.10000000	0.00000000	0.00000000	0.00000000	0.00000000
19	94.90000000	0.00000000	0.00000000	0.00000000	0.00000000
20	103.70000000	0.00000000	0.00000000	0.00000000	0.00000000
21	112.50000000	0.00000000	0.00000000	0.00000000	0.00000000
22	125.00000000	0.00000000	0.00000000	0.00000000	0.00000000
23	137.50000000	0.00000000	0.00000000	0.00000000	0.00000000
24	150.00000000	0.00000000	0.00000000	0.00000000	0.00000000
25	162.50000000	0.00000000	0.00000000	0.00000000	0.00000000

CALCULATED FLUX OMEGA = 100.00000 RAD/SEC 256 ITERATIONS REQUIRED

I	RADIUS, CM	FAST REAL	FAST IMAG.	SLOW REAL	SLOW IMAG.
0	0.00000	1.11429	-1.59999	8.90820	-3.43923
1	3.98000	1.00015	-1.59375	4.19930	-3.41265
2	7.96000	0.86025	-1.57575	2.74758	-3.36100
3	11.94000	0.71806	-1.54664	1.94629	-3.28796
4	15.92000	0.58447	-1.50788	1.41634	-3.19663
5	19.90000	0.46433	-1.45964	1.03215	-3.08920
6	23.88000	0.35824	-1.40279	0.73830	-2.96765
7	27.86000	0.26627	-1.33786	0.50625	-2.83395
8	31.84000	0.18779	-1.26517	0.31967	-2.69024
9	35.82000	0.12198	-1.18477	0.16835	-2.53898
10	39.80000	0.06809	-1.09627	0.04538	-2.38319
11	43.78000	0.02553	-0.99863	-0.05441	-2.22670
12	47.76000	-0.00602	-0.88983	-0.13531	-2.07467
13	51.74000	-0.02665	-0.76628	-0.20126	-1.93428
14	55.72000	-0.03510	-0.62203	-0.25642	-1.81586
15	59.70000	-0.03043	-0.44738	-0.30551	-1.73470
16	63.50000	-0.01302	-0.18671	-0.36418	-1.46864
17	77.30000	-0.00542	-0.07854	-0.36254	-1.18338
18	86.10000	-0.00248	-0.03329	-0.32771	-0.84941
19	98.90000	-0.00107	-0.01430	-0.27599	-0.60797
20	103.70000	-0.00050	-0.00662	-0.21703	-0.41614
21	112.50000	-0.00027	-0.00362	-0.15642	-0.26379
22	125.00000	-0.00014	-0.00166	-0.10006	-0.14850
23	137.50000	-0.00007	-0.00078	-0.05934	-0.07959
24	150.00000	-0.00003	-0.00033	-0.02882	-0.03614
25	162.50000	-8.71604E-06	-0.00005	-0.00817	-0.00518

GAIN AND PHASE SHIFT CALCULATION OMEGA = 100.00000 RAD/SEC

I	RADIUS, CM	FAST GAIN	FAST NORM. GAIN	FAST PHASE	THERMAL GAIN	THERMAL NORM. GAIN	THERMAL PHASE
0	0.00000	3.80141	0.00432476	-55.14517	91.18434	0.01974259	-21.11028
1	3.98000	3.54036	0.00407803	-57.88981	29.28160	0.00727539	-39.10141
2	7.96000	3.22301	0.00380648	-61.36861	18.84550	0.00496187	-50.73445
3	11.94000	2.90833	0.00356233	-65.09874	14.59873	0.00404137	-59.37681
4	15.92000	2.61554	0.00336018	-68.80636	12.22444	0.00356940	-66.10320
5	19.90000	2.34615	0.00319828	-72.35347	10.60851	0.00329018	-71.52479
6	23.88000	2.09616	0.00307017	-75.67438	9.35206	0.00310827	-76.02942
7	27.86000	1.86078	0.00296893	-78.74355	8.28757	0.00298109	-79.87164
8	31.84000	1.63593	0.00288857	-81.55718	7.33955	0.00288720	-83.22364
9	35.82000	1.41856	0.00282435	-84.12165	6.47475	0.00281481	-86.20648
10	39.80000	1.20644	0.00277267	-86.44593	5.68163	0.00275693	-88.90914
11	43.78000	0.99791	0.00273088	-88.53574	4.96116	0.00270922	-91.39985
12	47.76000	0.79183	0.00269715	-90.38738	4.32257	0.00266890	-93.73143
13	51.74000	0.58789	0.00267037	-91.97688	3.78194	0.00263424	-95.94034
14	55.72000	0.38815	0.00265049	-93.22956	3.36310	0.00260430	-98.03756
15	59.70000	0.20107	0.00264039	-93.89094	3.10251	0.00257879	-99.98846
16	63.50000	0.03503	0.00264038	-93.99007	2.28952	0.00253184	-103.92678
17	77.30000	0.00620	0.00264037	-94.08951	1.43875	0.00249360	-107.59268
18	86.10000	0.00111	0.00264038	-94.19055	0.82889	0.00246179	-111.09725
19	94.90000	0.00021	0.00264040	-94.29742	0.44579	0.00243588	-114.41584
20	103.70000	0.00004	0.00264036	-94.42293	0.22028	0.00241507	-117.54322
21	112.50000	0.00001	0.00264018	-94.58600	0.09405	0.00239868	-120.66738
22	125.00000	2.76594E-06	0.00263906	-94.83762	0.03207	0.00238540	-123.97197
23	137.50000	6.16071E-07	0.00263816	-95.06392	0.00986	0.00237775	-126.70353
24	150.00000	1.07936E-07	0.00263622	-95.23530	0.00214	0.00237465	-128.57033
25	162.50000	2.64011E-09	0.00263623	-95.26624	0.00004	0.00237449	-128.85343

MODIFIED CROSS SECTIONS FOR CRAM OMEGA = 100.00000

	REGION 1	REGION 2	REGION 3	REGION
D1 =	1.291967000	1.305000000	1.192000000	
D2 =	0.817957000	0.825500000	1.050000000	
STGR1 =	0.010629229	0.011622444	0.003479888	
STGR2 =	0.004106318	0.000567489	0.001405634	
AA =	0.000000000	0.000000000	0.000000000	
BB =	0.005519109	0.000000000	0.000000000	
DD =	0.000000172	0.000000000	0.000000000	
T1 =	0.000052060	0.000052275	0.000050622	
T2 =	0.000459126	0.000455185	0.000456559	
SIGITO2 =	0.009675800	0.010900000	0.002820000	
Q1 =	-0.173752257	-0.045325957	-0.010737488	
Q2 =	-0.107381109	-0.021887220	-0.014845638	
P1 =	0.040780757	0.015769308	0.007247360	
P2 =	0.025818698	0.009975144	0.006384000	
R1 =	0.122342270	0.017934205	0.008010240	
R2 =	0.077456093	0.011344587	0.007056000	

EXD1 = 2.520919401 EXD2 = 2.222462523

```
*  REGION  1  NEXT 8CARDS
I1D  1E-9          1.291967000  1.291967000  0.817957000  0.817957000
      1.0          0.010629229  0.010629229  0.004106318  0.004106318
      0.0        0.0          0.0          0.0          0.0
      1.0        0            0            0            0
       0          0.000000000 -0.000052060  0.009675800  0
       0          0.000052060  0.000000000  0                0.009675800
       0          0.005519109 -0.000000172  0               -0.000459126
       0          0.000000172  0.005519109  0.000459126  0
*  REGION  2  NEXT 8CARDS
I2D  1E-9          1.305000000  1.305000000  0.825500000  0.825500000
      1.0          0.011622444  0.011622444  0.000567489  0.000567489
      0.0        0.0          0.0          0.0          0.0
      1.0        0            0            0            0
       0          0.000000000 -0.000052275  0.010900000  0
       0          0.000052275  0.000000000  0                0.010900000
       0                       0.000000000  0               -0.000455185
       0          0.000000000                0.000455185  0
*  REGION  3  NEXT 8CARDS
I3D  1E-9          1.192000000  1.192000000  1.050000000  1.050000000
      1.0          0.003479888  0.003479888  0.001405634  0.001405634
      0.0        0.0          0.0          0.0          0.0
      1.0        0            0            0            0
       0          0.000000000 -0.000050622  0.002820000  0
       0          0.000050522  0.000000000  0                0.002820000
       0                       0.000000000  0               -0.000456559
       0          0.000000000                0.000456559  0
*  SOURCE ON NEXT 8 CARDS
I4D  1E-9          1E+9         1E+9         1E+9         1E+9
      0.0        0.0          0.0          0.0          0.0
      0.0        0.0          0.0          0.0          0.0
      0.0        0.0          0.0          1.0          0.0
      0.0        0.0          0.0          0.0          0.0
      0.0        0.0          0.0          0.0          0.0
      0.0        0.0          0.0          0.0          0.0
      0.0        0.0          0.0          0.0          0.0
```

```
SAMPLE PROBLEM FOR CRAM
= RUN 138 OF 01/01/66 BY LIAISON APDA CHAMF  JOB G89 CHARGE  1515   981  ID
= 32K CORE,     15 MINUTES,     50 PAGES,   1000 CARDS,     50 FRAMES       (MAXIMUM NEEDS AT EXECUTION TIME)
    (32)          (15)            (50)        (1000)          (50)          (GUARANTEED DAYSHIFT ALLOTMENTS)

$F SYSTEM                                  0000.0 0 CLOCK  01/01/66  138

*LOAD(UB1),EXECUTE,DUMP,MAP,DATA

                                                                          0000.0 0 CLOCK  01/01/66  138
```

```
PROBLEM     1
     PROBLEM 138      OMEGA=100
     0C   5   0   1   6    2000 GEOMETRY CYL
     ACCURACY       0.0005          0.0005          0.0005      -1.0        0.05
     NM 0(1.99)  1(1.99)  2(3.98)  16(8.8)  22(12.5)  26
     *  CROSS SECTIONS FOR CRAM          OMEGA     100.00000
     110  1E-9          1.291967        1.291967        .817957         .817957
          1             .010629229      .010629229      .004106318      .004106318
          0             0               0               0               0
          1             0               0               0               0
          0             0               -.00005206      .0096758        0
          0             .00005206       0               0               .0096758
          0             .005519101      -.165E-6        0               -.000459126
          0             .165E-6         .005519101      .000459126      0
     120  1E-9          1.305           1.305           .8255           .8255
          1             .011622444      .011622444      .000567489      .000567489
          0             0               0               0               0
          1             0               0               0               0
          0             0               -.000052275     .0109           0
          0             .000052275      0               0               .0109
          0             0               0               0               -.000455185
          0             0               0               .000455185      0
     130  1E-9          1.192           1.192           1.05            1.05
          1             .003479888      .003479888      .001405634      .001405634
          0             0               0               0               0
          1             0               0               0               0
          0             0               -.000050622     .00282          0
          0             .000050622      0               0               .00282
          0             0               0               0               -.000456559
          0             0               0               .000456559      0
     140  1E-9          1E+9            1E+9            1E+9            1E+9
          0.0           0.0             0.0             0.0             0.0
          0.0           0.0             0.0             0.0             0.0
          0.0           0.0             0.0             1.0             0.0
          0.0           0.0             0.0             0.0             0.0
          0.0           0.0             0.0             0.0             0.0
          0.0           0.0             0.0             0.0             0.0
          0.0           0.0             0.0             0.0             0.0
     M1 11 1 14 1   M2 11 1   M3 12 1   M4 13 1
     Z1  M1  1   Z2  M2  1   Z3  M3  1   Z4  M4  1
     C1  0  Z1  1  Z2 16  Z3  22  Z4  26        0   1E9
     SP 0 0 0 0 0 0
     PROBLEM 138      OMEGA=100

FLUXS ETC ARE STORED IN        1 TO    432
CROSS SECTIONS IN            432 TO    604
MATERIAL DATA IN             604 TO    630
ZONE DATA IN                 630 TO    646
SPECTRUM DATA IN             646 TO    657
F. DIFF. COEFFICIENTS IN     657 TO   2087

    5 GROUPS, CONTROL TYPE   6, R  MESH WITH   1* 26 POINTS

ACCURACY      0.000500       0.000500       0.000500      -1.000000      0.050000

B.C.
  0  0.              26

MESH 1
  0  0.100000E 01     1
```

MESH 2

0 0.199000E 01 2 0.398000E 01 16 0.880000E 01 22 0.125000E 02 26

ISOTOPE 1

33333.0000000	0.2580045	0.2580045	0.4075194	0.4075194
1.0000000	0.0106292	0.0106292	0.0041063	0.0041063
0.	0.	0.	0.	0.
1.0000000	0.	0.	0.	0.
0.	0.	-0.0000521	0.0096758	0.
0.	0.0000521	0.	0.	0.0096758
0.	0.0055191	-0.0000002	0.	-0.0004591
0.	0.0000002	0.0055191	0.0004591	0.

ISOTOPE 2

33333.0000000	0.2554278	0.2554278	0.4037957	0.4037957
1.0000000	0.0116224	0.0116224	0.0005675	0.0005675
0.	0.	0.	0.	0.
1.0000000	0.	0.	0.	0.
0.	0.	-0.0000523	0.0109000	0.
0.	0.0000523	0.	0.	0.0109000
0.	0.	0.	0.	-0.0004552
0.	0.	0.	0.0004552	0.

ISOTOPE 3

```
33333.0000000   0.2716421   0.2716421   0.3174603   0.3174603
    1.0000000   0.0034799   0.0034799   0.0014056   0.0014056
    0.          0.          0.          0.          0.
    1.0000000   0.          0.          0.          0.
    0.          0.         -0.0000506   0.0028200   0.
    0.          0.0000506   0.          0.          0.0028200
    0.          0.          0.          0.         -0.0004566
    0.          0.          0.          0.0004566   0.
ISOTOPE     4
```

```
33333.0000000   0.0000000   0.0000000   0.0000000   0.0000000
    0.          0.          0.          0.          0.
    0.          0.          0.          0.          0.
    0.          0.          0.          1.0000000   0.
    0.          0.          0.          0.          0.
    0.          0.          0.          0.          0.
    0.          0.          0.          0.          0.
    0.          0.          0.          0.          0.
MATERIAL     1
I   1 DENSITY      1.0000000    4        1.0000000
MATERIAL     2
I   1 DENSITY      1.0000000
MATERIAL     3
I   2 DENSITY      1.0000000
MATERIAL     4
I   3 DENSITY      1.0000000

ZONE     1
M   1 V.F.         1.0000000
ZONE     2
M   2 V.F.         1.0000000
ZONE     3
M   3 V.F.         1.0000000
ZONE     4
M   4 V.F.         1.0000000

     FLUXREAD
WILL READ FLUXS ONLY FROM BINARY CARDS
     PRINT
```

FLUXES PRINTED WITH THE SAME NORMALIZATION AS THOSE ON COMPILER DUMP TAPE

CHANNEL 1 R= 0.5000 H.C. 0. 0.100000E 10

PT	Z	ZONE	G= 1	2	3	4	5	AVG. FLUX
1	3.9950	1	5.83213E-02	6.20077E-02	-9.38500E-02	4.32894E-01	-2.01312E-01	5.16122E-02
2	7.9850	2	5.83213E-02	5.93637E-02	-9.36710E-02	2.94789E-01	-2.00634E-01	2.36339E-02
3	5.9700	2	5.83213E-02	5.39632E-02	-9.31408E-02	1.95177E-01	-1.98933E-01	3.07634E-03
4	9.9500	2	5.83194E-02	4.57758E-02	-9.17686E-02	1.34152E-01	-1.95283E-01	-9.76059E-03
5	11.9300	2	5.83186E-02	3.77750E-02	-8.97034E-02	9.66578E-02	-1.90463E-01	-1.74989E-02
6	17.9100	2	5.83101E-02	3.04086E-02	-8.72342E-02	7.05511E-02	-1.84628E-01	-2.25168E-02
7	21.8900	2	5.83160E-02	2.38369E-02	-8.41647E-02	5.10643E-02	-1.77898E-01	-2.57693E-02
8	25.8700	2	5.83138E-02	1.80883E-02	-8.06125E-02	3.69034E-02	-1.70385E-01	-2.77383E-02
9	27.8500	2	5.83122E-02	1.31427E-02	-7.66060E-02	2.38191E-02	-1.62204E-01	-2.87072E-02
10	31.8300	2	5.83099E-02	8.95623E-03	-7.21618E-02	1.40643E-02	-1.53482E-01	-2.88628E-02
11	37.8100	2	5.83080E-02	5.48221E-03	-6.72789E-02	6.15361E-03	-1.44369E-01	-2.83408E-02
12	41.7900	2	5.83064E-02	2.67982E-03	-6.19297E-02	-2.57600E-04	-1.35045E-01	-2.72491E-02
13	45.7700	2	5.83049E-02	9.20181E-04	-5.60463E-02	-5.43869E-03	-1.25744E-01	-2.56406E-02
14	47.7500	2	5.83056E-02	-1.00730E-03	-4.94983E-02	-9.62446E-03	-1.16784E-01	-2.37216E-02
15	51.7300	2	5.83039E-02	-1.88667E-03	-4.20586E-02	-1.30443E-02	-1.08606E-01	-2.14583E-02
16	57.7100	2	5.83024E-02	-2.06308E-03	-3.33503E-02	-1.59480E-02	-1.01853E-01	-1.89824E-02
17	64.1000	3	5.83213E-02	-1.04352E-03	-1.64685E-02	-2.02348E-02	-9.48699E-02	-1.48591E-02
18	72.9000	3	5.83204E-02	-4.49307E-04	-6.90145E-03	-2.15840E-02	-7.62894E-02	-9.38075E-03
19	81.7000	3	5.83178E-02	-1.94795E-04	-2.91376E-03	-2.03578E-02	-5.78683E-02	-4.60335E-03
20	90.5000	3	5.83166E-02	-8.52008E-05	-1.24110E-03	-1.77515E-02	-4.22508E-02	-6.02403E-04
21	99.3000	3	5.83143E-02	-3.81354E-05	-5.40088E-04	-1.44845E-02	-2.97392E-02	2.70245E-03
22	108.1000	3	5.83122E-02	-1.86451E-05	-2.55362E-04	-1.09798E-02	-1.98688E-02	5.43791E-03
23	118.7500	4	5.83213E-02	-1.05065E-05	-1.36336E-04	-7.27293E-03	-1.15264E-02	7.87502E-03
24	131.2500	4	5.83198E-02	-5.28385E-06	-6.50661E-05	-4.44980E-03	-6.30956E-03	9.49802E-03
25	143.7500	4	5.83173E-02	-2.42441E-06	-2.86864E-05	-2.36047E-03	-3.08929E-03	1.05673E-02
26	156.2500	4	5.83151E-02	-6.80662E-07	-7.87565E-06	-7.16306E-04	-8.98801E-04	1.13383E-02

ENTER

PROGRAM ENDS AT LOCATION 12159 DATA STARTS 28732

1.000000 1.000035 0.999608

SOURCE TYPE PROBLEM. NO CONTROL

1.000000 1.000080 0.999719

1.000000 1.000054 0.999878

1.000000 1.000080 0.999991

1.000000 1.000312 0.999977

1.000000 1.000385 0.999901

1.000000 1.000248 0.999923

1.000000 1.000070 0.999953

1.000000 1.000007 0.999857

RESTART 1 26 0.100000E 01 0. RESTART

PRINT

FLUXES PRINTED WITH THE SAME NORMALIZATION AS THOSE ON COMPILER DUMP TAPE

CHANNEL 1 R= 0.5000 B.C. 0. 0.100000E 10

PT	Z	ZONE	G= 1	2	3	4	5	AVG. FLUX
1	0.9950	1	5.83212E-02	6.20000E-02	-9.38499E-02	4.32895E-01	-2.01312E-01	5.16129E-02
2	2.9850	2	5.83212E-02	5.93640E-02	-9.36709E-02	2.94790E-01	-2.00634E-01	2.36341E-02
3	4.9700	2	5.83212E-02	5.39636E-02	-9.31407E-02	1.95177E-01	-1.98939E-01	3.07657E-03
4	9.9500	2	5.83194E-02	4.57772E-02	-9.17685E-02	1.34153E-01	-1.95282E-01	-9.76037E-03
5	14.9300	2	5.83185E-02	3.77753E-02	-8.97033E-02	9.66584E-02	-1.90463E-01	-1.74987E-02
6	17.9100	2	5.83180E-02	3.04089E-02	-8.72341E-02	7.05517E-02	-1.84628E-01	-2.25166E-02
7	21.8900	2	5.83159E-02	2.38362E-02	-8.41647E-02	5.10649E-02	-1.77898E-01	-2.57691E-02
8	25.8700	2	5.83137E-02	1.80885E-02	-8.06124E-02	3.59040E-02	-1.70305E-01	-2.77382E-02
9	29.8500	2	5.83120E-02	1.31430E-02	-7.66099E-02	2.38197E-02	-1.62204E-01	-2.87070E-02
10	33.8300	2	5.83096E-02	8.95649E-03	-7.21617E-02	1.40649E-02	-1.53482E-01	-2.88626E-02
11	37.8100	2	5.83077E-02	5.48246E-03	-6.72788E-02	6.15415E-03	-1.44369E-01	-2.83406E-02
12	41.7900	2	5.83061E-02	2.68005E-03	-6.19297E-02	-2.57088E-04	-1.35044E-01	-2.72490E-02
13	45.7700	2	5.83056E-02	5.20333E-04	-5.60463E-02	-5.43821E-03	-1.25744E-01	-2.56805E-02
14	49.7500	2	5.83053E-02	-1.00711E-03	-4.94983E-02	-9.62400E-03	-1.16784E-01	-2.37215E-02
15	53.7300	2	5.83036E-02	-1.88651E-03	-4.20586E-02	-1.30438E-02	-1.08606E-01	-2.14583E-02
16	57.7100	2	5.83020E-02	-2.06295E-03	-3.33502E-02	-1.59476E-02	-1.01853E-01	-1.89823E-02
17	64.1000	3	5.83212E-02	-1.04345E-03	-1.64685E-02	-2.02344E-02	-9.48699E-02	-1.48590E-02
18	72.9000	3	5.83204E-02	-4.49280E-04	-6.90144E-03	-2.15837E-02	-7.62894E-02	-9.38069E-03
19	81.7000	3	5.83177E-02	-1.94783E-04	-2.91376E-03	-2.03575E-02	-5.78683E-02	-4.60333E-03
20	90.5000	3	5.83165E-02	-8.51960E-05	-1.24110E-03	-1.77513E-02	-4.22509E-02	-6.02398E-04
21	99.3000	3	5.83141E-02	-3.81333E-05	-5.40068E-04	-1.44844E-02	-2.97393E-02	2.70244E-03
22	108.1000	3	5.83120E-02	-1.86441E-05	-2.55362E-04	-1.09797E-02	-1.98689E-02	5.43789E-03
23	118.7500	4	5.83212E-02	-1.05060E-05	-1.36336E-04	-7.27288E-03	-1.15264E-02	7.87502E-03
24	131.2500	4	5.83198E-02	-5.28359E-06	-6.50860E-05	-4.44977E-03	-6.30957E-03	9.49801E-03
25	143.7500	4	5.83172E-02	-2.42430E-06	-2.86864E-05	-2.36045E-03	-3.08930E-03	1.05673E-02
26	156.2500	4	5.83149E-02	-6.80631E-07	-7.87564E-06	-7.16302E-04	-8.98803E-04	1.13382E-02

FLUXPUNCH NABKZZ

FLUX DUMP ONLY WILL BE PUT ON CARDS LABELLED NABK
DUMP

FLUX DUMP WILL BE PUT ON TAPE 3
COMPILE

ALL DATA WILL BE READ FROM TAPE 3 EXCEPT FLUXES AND ZONE NUMBERS

PROBLEM 138 OMEGA=100
ZONEXN

CROSS SECTIONS ZONES 1 TO 4

*** OVERFLOW ON +,-,OR * OPERATION AT CORE LOCATION 10027

*** UNDERFLOW ON +,-,OR * OPERATION AT CORE LOCATION 10027

ZONE 1

0.666667E 09	0.258005E-00	0.258005E-00	0.407519E-00	0.407519E-00	0.100000E 01	0.106292E-01	0.106292E-01
0.410632E-02	0.410632E-02	0.	0.	0.	0.	0.	0.100000E 01
0.	0.	0.100000E 01	0.	0.	0.	-0.520600E-04	0.967580E-02
0.	0.	0.520600E-04	0.	0.	0.967580E-02	0.	0.551910E-02
-0.165000E-06	0.	-0.459126E-03	0.	0.165000E-06	0.551910E-02	0.459126E-03	0.
-0.170141E 39	0.333333E 09	0.255428E-00	0.255428E-00	0.403796E-00	0.403796E-00	0.100000E 01	0.116224E-01
0.116224E-01	0.567489E-03	0.100057E 01	0.	0.100000E 01	0.305629E-36	0.100000E 01	

ZONE 2

0.333333E 09	0.258005E-00	0.258005E-00	0.407519E-00	0.407519E-00	0.100000E 01	0.106292E-01	0.106292E-01
0.410632E-02	0.410632E-02	0.	0.	0.	0.	0.	0.100000E 01
0.	0.	0.	0.	0.	0.	-0.520600E-04	0.967580E-02
0.	0.	0.520600E-04	0.	0.	0.967580E-02	0.	0.551910E-02
-0.165000E-06	0.	-0.459126E-03	0.	0.165000E-06	0.551910E-02	0.459126E-03	0.
-0.170141E 39	0.333333E 09	0.255428E-00	0.255428E-00	0.403796E-00	0.403796E-00	0.100000E 01	0.116224E-01
0.116224E-01	0.567489E-03	0.567489E-03	0.	0.	0.	0.	

ZONE 3

0.333333E 09	0.255428E-00	0.255428E-00	0.403796E-00	0.403796E-00	0.100000E 01	0.116224E-01	0.116224E-01
0.567489E-03	0.567489E-03	0.	0.	0.	0.	0.	0.100000E 01
0.	0.	0.	0.	0.	0.	-0.522750E-04	0.109000E-01
0.	0.	0.522750E-04	0.	0.	0.109000E-01	0.	0.
0.	0.	-0.455185E-03	0.	0.	0.	0.455185E-03	0.
-0.170141E 39	0.333333E 09	0.279542E-00	0.279542E-00	0.317460E-00	0.317460E-00	0.100000E 01	0.347989E-02
0.347989E-02	0.140563E-02	0.140563E-02	0.	0.	0.	0.	

ZONE 4

0.333333E 09	0.279642E-00	0.279642E-00	0.317460E-00	0.317460E-00	0.100000E 01	0.347989E-02	0.347989E-02
0.140563E-02	0.140563E-02	0.	0.	0.	0.	0.	0.100000E 01
0.	0.	0.	0.	0.	0.	-0.506220E-04	0.282000E-02
0.	0.	0.506220E-04	0.	0.	0.282000E-02	0.	0.
0.	0.	-0.456559E-03	0.	0.	0.	0.456559E-03	0.
-0.170141E 39	0.333333E 09	0.333333E-09	0.333333E-09	0.333333E-09	0.333333E-09	0.	0.
0.	0.	0.	0.	0.	0.	0.	

PROBLEM 138 OMEGA=100
TEMP 3

PHASE ANGLE FOR CHANNEL 1 FAST GROUP

-56.54667 -57.63547 -59.91300 -63.48846 -67.18142 -70.78196 -74.18739 -77.35294 -80.26479 -82.92480

-85.34134 -87.52203 -89.46802 -91.18560 -92.68824 -93.99964 -95.12946 -96.09467 -96.90451 -97.56693

-98.08871 -98.47579 -98.73647 -98.88102 -98.91061 -98.82936

GAIN FOR CHANNEL 1 FAST GROUP

0.1923E 01 0.1902E 01 0.1846E 01 0.1758E 01 0.1670E 01 0.1584E 01 0.1500E 01 0.1417E 01 0.1338E 01 0.1247E 01

0.1153E 01 0.1063E 01 0.9613E 00 0.8491E 00 0.7221E 00 0.5731E 00 0.2829E-00 0.1186E-00 0.5008E-01 0.2133E-01

0.9285E-02 0.4391E-02 0.2345E-02 0.1120E-02 0.4937E-03 0.1356E-03

PHASE ANGLE FOR CHANNEL 1 THERMAL GROUP

-24.94014 -34.23916 -45.54678 -55.51222 -63.09252 -69.08667 -73.98406 -78.10052 -81.64581 -84.76412

-87.55907 -90.10908 -92.47540 -94.71104 -96.84855 -98.89879 -102.03998 -105.79719 -109.38130 -112.78927

-115.96823 -118.92550 -122.25093 -125.19306 -127.38253 -128.55312

GAIN FOR CHANNEL 1 THERMAL GROUP

0.8186E 01 0.6114E 01 0.4779E 01 0.4062E 01 0.3662E 01 0.3389E 01 0.3174E 01 0.2966E 01 0.2811E 01 0.2643E 01

0.2478E 01 0.2316E 01 0.2139E 01 0.2010E 01 0.1876E 01 0.1760E 01 0.1663E 01 0.1557E 01 0.1452E 01 0.7859E 00

0.5673E 00 0.3693E-00 0.2337E-00 0.1324E-00 0.6667E-01 0.1971E-01

```
PROBLEM 138       OMEGA=100
:STOP
THIS JOH COMPLETED

*** PROGRAM SIZE LIMITS I/O BUFFERING. THIS COULD BE AN ECONOMIC
  * ERROR
```

LITERATURE CITED

1. T. W. Kerlin, "Status of Space-Time Analysis," Nuclear Safety, 6 (4), 395-398 (1965).

2. A. F. Henry and N. J. Curlee, "Verification of a Method for Treating Neutron Space-Time Problems," Nuclear Science and Engineering, 4, 727-744 (1958).

3. A. Radkowsky (Ed.), Selected Basic Techniques, Naval Reactor Physics Handbook, Vol. 1, U. S. Atomic Energy Commission, 1964.

4. H. Nishihara, "Application of Adiabatic Approximation to the Space-Dependent Boiling-Water Reactor Kinetics," Transactions of the American Nuclear Society, 7 (2), 222-223 (1964).

5. Y. B. Yasinsky, A. F. Henry, and W. G. Clarke, "Some Numerical Experiments Comparing Approximate Methods for Reactor Kinetics Analysis," Trans. Am. Nucl. Soc., 7 (2), 224-225 (1964).

6. R. L. Crowther and W. H. Wolf, "Numerical Method for Analysis of Non-Linear Axial Dynamics of Large Boiling Water Reactors," Trans. Am. Nucl. Soc., 6 (2), 210-211 (1963).

7. W. R. Cadwell, A. F. Henry and A. J. Vigilotti, "WIGLE-A Program for the Solution of the Two-Group Space-Time Diffusion Equations in Slab Geometry," USAEC Report WAPD-TM-416, Bettis Atomic Power Laboratory (1964).

8. H. L. Garabedian and C. B. Leffert, "A Time-Dependent Analysis of Spatial Flux Distributions," Nuclear Science and Engineering, 6, 26-32 (1959).

9. E. R. Cohen, "Some Topics in Reactor Kinetics," Proceedings of the Second United Nations International Conference on the Peaceful Uses of Atomic Energy, Geneva, 1958, Vol. 11, pp. 302-309, United Nations, New York, N. Y., 1958.

10. J. N. Grace, "Analysis of a Reactivity Instability Experiment with Boiling and Nonlinear Analysis of Spatial Stability and Flux Tilt Transients," Proceedings of the Conference on Transfer Function Measurements and Reactor Stability Analysis, USAEC Report ANL-6205, pp. 174-184 (1960).

11. S. Kaplan, "The Property of Finality and the Analysis of Problems in Reactor Space-Time Kinetics by Various Modal Expansions," Nuclear Science and Engineering, 9, 357-361 (1961).

12. S. Kaplan et al., "Space-Time Reactor Dynamics," Third United Nations International Conference on the Peaceful Uses of Atomic Energy, Geneva, 1964, Paper A/Conf. 28/P/271.

13. D. E. Daugherty and C. M. Shen, "The Space-Time Neutron Kinetic Equations Obtained by the Semidirect Variational Method," Nuclear Science and Engineering, 13, 141-148 (1962).

14. S. Kaplan, O. J. Marlowe, and J. Bewick, "Application of Synthesis Techniques to Problems Involving Time Dependence," Nuclear Science and Engineering, 18, 163-176 (1964).

15. M. N. Moore, "Role of the Dispersion Law in Space-Dependent Kinetics," Reactor Kinetics and Control, TID-7662, pp. 169-178 (1964).

16. M. N. Moore, "Noise Field of a Reactor," Noise Analysis in Nuclear Systems, TID-7679, pp. 13-28 (1964).

17. M. N. Moore, "The Determination of Reactor Dispersion Laws From Modulated-Neutron Experiments," Nuclear Science and Engineering, 21, 565-574 (1965).

18. A. M. Weinberg and H. C. Schweinler, "Theory of Oscillating Absorber in a Chain Reactor," Physical Review, 74, 851-863 (1948).

19. V. Raievski and J. Horowitz, "Determination of the Mean Transfer Free Path of Thermal Neutrons by Measurement of the Complex Diffusion Length," Proceedings of the First United Nations Conference on the Peaceful Uses of Atomic Energy, Vol. 5, p. 42, (1955).

20. M. N. Moore, "The Determination of Reactor Transfer Functions From Measurements at Steady State," Nuclear Science and Engineering, 3, 387-394 (1958).

21. C. E. Cohn, "Determination of Reactor Kinetics Parameters by Pile Noise Analysis," Nuclear Science and Engineering, 5, 331-335 (1959).

22. C. E. Cohn, "A Simplified Theory of Pile Noise," Nuclear Science and Engineering, 7, 472-475 (1960).

23. J. A. Thie, Reactor Noise, Rowman and Littlefield, New York, N. Y., 1963.

24. Noise Analysis in Nuclear Systems, TID-7679 (1963).

25. P. T. Hansson and L. R. Foulke, "Investigations in Spatial Reactor Kinetics," Nucl. Sci. and Eng., 17, 528-533 (1963).

26. R. E. Uhrig, "Oscillatory Techniques in a Subcritical Assembly," Proceedings of the University Subcritical Assemblies Conference, TID-7619 (1962).

27. R. B. Perez, R. S. Booth, and R. H. Hartley, Trans. Am. Nucl. Soc., 6 (2), (1963).

28. R. S. Booth, R. H. Hartley, and R. B. Perez, Trans. Am. Nucl. Soc., 8 (1), (1965).

29. R. S. Denning, R. S. Booth, and R. B. Perez, Trans. Am. Nucl. Soc., 7 (2), (1964).

30. J. Dunlap and R. B. Perez, "The Dispersion Law for a Natural Uranium, Heavy Water, Subcritical Assembly," Proceedings of the Symposium on Neutron Noise, Waves, and Pulse Propagation, University of Florida, Gainesville, Florida, February, 1966.

31. T. Nomura, S. Gotoh, K. Yamaki, "Reactivity Measurements by Neutron Noise Analysis Using Two-Detector Correlation Method and Supercritical Reactor Noise Analysis," Proceedings of the Symposium on Neutron Noise, Waves, and Pulse Propagation, University of Florida, Gainesville, Florida, February, 1966.

32. K. Saito and M. Otsuka, "Power Spectral Density and Reactor Transfer Function in a Zero Power Reactor," Proceedings of the Symposium on Neutron Noise, Waves, and Pulse Propagation, University of Florida, Gainesville, Florida, February, 1966.

33. W. Seifritz, D. Stegemann, and W. Väth, "Two-Detector Cross Correlation Experiments in the Fast-Thermal Argonant Reactor STARK," Proceedings of the Symposium on Neutron Noise, Waves, and Pulse Propagation, University of Florida, Gainesville, Florida, February, 1966.

34. A. Hassitt, "A Computer Program to Solve the Multigroup Diffusion Equations, CRAM," TRG Report 229(R), United Kingdom Atomic Energy Authority, Risley, Warrington, Lancashire, 1962.

35. R. J. Johnson, Investigation of the Space Dependent, Zero Power, Reactor Source Transfer Function, PhD. Thesis, Georgia Institute of Technology, Atlanta, Georgia, (in process).

36. T. B. Fowler, M. L. Tobias, and D. R. Vandy, "EXTERMINATOR-A Multigroup Code for Solving Neutron Diffusion Equations in One and Two Dimensions," USAEC Report ORNL-TM-842, Oak Ridge National Laboratory, 1965.

37. M. Clark, Jr. and K. F. Hansen, Numerical Methods of Reactor Analysis, Academic Press, New York, p. 121, 1964.

38. F. S. Beckman, "The Solution of Linear Equations by the Conjugate Gradient Method," Mathematical Methods for Digital Computers, John Wiley and Sons, Inc., New York, pp. 62-72, 1965.

39. J. C. Carter, D. W. Sparks, and J. H. Tessier, "The Period Effect in Reactor Dynamics," ANL 6852, 1964.

40. G. R. Keepin, Physics of Nuclear Kinetics, Addison-Wesley, Reading, Mass., p. 161-166, 1965.

41. R. L. Brehm, "The Analysis of Neutron Wave-Type Experiments," Proceedings of the Symposium on Neutron Noise, Waves, and Pulse Propagation, University of Florida, Gainesville, Florida, February, 1966.

42. T. Hoshino, J. Wakabayashi, and S. Hayashi, "New Approximate Solution of Space- and Energy-Dependent Reactor Kinetics," Nucl. Sci. and Eng., 23, 170-182 (1965).

43. P. T. Hansson, Aktiebolaget Atomenergi, Stockholm, Sweden (personal communication).

44. R. J. Johnson and R. N. Macdonald, "Calculation of Space Dependent Effects in Pile Oscillator and Reactor Noise Measurements," Proceedings of the Symposium on Neutron Noise, Waves, and Pulse Propagation, University of Florida, Gainesville, Florida, February, 1966.

45. A. Travelli, "The Complex Relaxation Length of Neutron Waves in Multigroup Transport Theory," Proceedings of the Symposium on Neutron Noise, Waves, and Pulse Propagation, University of Florida, Gainesville, Florida, February, 1966.

46. R. B. Blackmon and J. W. Tukey, The Measurement of Power Spectra, Dover Publications, Inc., New York, 1958.

47. W. K. Brookshier, "Electrometer Circuit Design for Extended Band Widths," Nuclear Instruments and Methods, 35 (22), 317-327 (1964).

48. H. P. Flatt, "Finite Difference Approximation to the Neutron Diffusion Equation," Atomics International TDR 5889, December 8, 1960.

49. Final Safeguards Report for the Georgia Tech Research Reactor, Georgia Institute of Technology, Atlanta, Georgia, February, 1963.

50. W. W. Graham, III, The Determination of Effective Delayed Neutron and Photoneutron Kinetics Parameters in a Highly Enriched Heavy-Water Reactor, PhD. Thesis, Georgia Institute of Technology, Atlanta, Georgia, August, 1965.

51. C. E. Cohn, R. J. Johnson, and R. N. Macdonald, "Calculation of Space Dependent Reactor Transfer Functions," Nucl. Sci. and Eng., (in press).

VITA

Robert Neill Macdonald was born in Syracuse, New York, December 29, 1935. In 1944 his family moved to Decatur, Georgia where he was graduated from Decatur High School in 1953. He entered Georgia Institute of Technology that fall and received the degree Bachelor of Science in Chemical Engineering in 1957.

After graduation, Mr. Macdonald moved to Los Angeles, California where he was a research engineer with North American Aviation. His duties involved the analysis and design of heating and ventilating systems for the F-100 fighter-bombers.

After leaving North American Aviation and spending six months on active duty with the U. S. Air Force Reserves, he returned to Georgia Tech in 1959 to begin work on a degree of Master of Science in Nuclear Engineering. Upon graduation in 1961 he returned to Los Angeles with the Rocketdyne Division of North American Aviation on a temporary basis. During the next six months he was involved with heat transfer and thermodynamics studies of advanced rocket engine concepts. As a result of this work, he was co-inventor of a rocket engine based on the principle of non-regenerative cooling.

Transferring to the Atomics International Division of North American Aviation enabled Mr. Macdonald to gain experience in analysis and core design of the SNAP nuclear reactors. His primary activities were to develop computer programs to solve problems in reactor physics. In 1963 he left

Gordon Inman Bloom to return to Georgia Tech to finish his formal education.

While working on his Ph.D. Mr. Macdonald taught an undergraduate course entitled "Introduction to Nuclear Engineering." He was also a co-author of two papers, "Calculating Space Dependent Reactor Transfer Functions by Statics Techniques" and "Calculation of Space Dependent Effects in Pile Oscillator and Reactor Noise Measurements." These papers form the basis for his thesis research.

Mr. Macdonald was married to Melinda Cowan of Atlanta, Georgia in 1963. He is a member of the American Nuclear Society and Sigma Xi. After receiving his degree he plans to accept a position with International Business Machines Corporation in Atlanta.